NUREG/CR-2482
BNL-NUREG-51494
Vol. 7

# Review of DOE Waste Package Program

Subtask 1.1 - National Waste Package Program
April 1984 - September 1984

Prepared by P. Soo, Ed.

**Brookhaven National Laboratory**

**Prepared for**
**U.S. Nuclear Regulatory**
**Commission**

GPO Printed copy price: $4.50

NUREG/CR-2482
BNL-NUREG-51494
Vol. 7

# REVIEW OF DOE WASTE PACKAGE PROGRAM
## Subtask 1.1 - National Waste Package Program
## April 1984 - September 1984

P. Soo, Editor

Contributors:

E. Gause
P. Soo

Manuscript Completed: September 1984
Date Published: March 1985

Prepared by the Nuclear Waste Management Division
D. G. Schweitzer, Head
Department of Nuclear Energy, Brookhaven National Laboratory
Associated Universities, Inc.
Upton, New York 11973

Prepared for the Division of Waste Management
Office of Nuclear Material Safety and Safeguards
U.S. Nuclear Regulatory Commission
Washington, D.C. 20555
NRC FIN A3164

## ABSTRACT

The present effort is part of an ongoing task to review the national high level waste package effort. It includes evaluations of reference waste form, container, and packing material components with respect to determining how they may contribute to the containment and controlled release of radionuclides after waste packages have been emplaced in salt, basalt, tuff, and granite repositories. In the current Biannual Report a review was carried out to determine the ability of spent fuel cladding to provide additional radionuclide containment capability should the container/overpack system fail prematurely.

CONTENTS

CONTENTS (Continued)

FIGURES

TABLES

TABLES (Continued)

ACKNOWLEDGEMENT

The authors gratefully acknowledge the skills and patience of Mrs. G. Sayes in the typing and preparation of this report.

## EXECUTIVE SUMMARY

Based on published information, an evaluation has been made of the radionuclide containment capability of Zircaloy and stainless steel spent fuel cladding in repository environments. In order to assess mechanisms that could cause breach of containment, it was necessary to first outline the anticipated environments in salt, basalt and tuff repositories, based on available data from testing and modeling sources. Near-field conditions include groundwater chemistry, hydrology, thermal environments and stress conditions around the waste package. Estimates of the changing temperature and radiation dose with time were based on current package designs and are design-dependent. An inventory of the radionuclides to be contained by the cladding was obtained. It has been estimated that up to 10% of the fission gases may be present in the fuel-cladding gap. Rods release Xe and Kr and other gaseous/volatile radionuclides present in the fuel-cladding gap to the repository environment.

The characteristics of the cladding material in a repository will be influenced by the handling that the fuel rods have received during reactor operation and storage in a spent fuel pool. It is believed that less than 0.01% of fuel rods currently fail in-reactor. Various waterside and fuelside processes enhanced by neutron irradiation are responsible for the failures. In-reactor, oxide layers/crud deposits form on the rods and are sources of fission and activation products and transuranics. There is measurable radioactivity in spent fuel pools due to spallation and/or leaching of the deposits. The fractional release of activity from spent fuel while it is in pool storage is estimated to be in the range of $7.6 \times 10^{-11}$ to $1.9 \times 10^{-9}$ of the radionuclide inventory (at discharge), not including gaseous fission products that are released. However, based on the examination of cladding in pool storage for 20 years, it was concluded that the storage pool conditions are not significantly corrosive for Zircaloy and stainless steel.

Possible corrosion failure modes for Zircaloy in a repository include uniform corrosion, fuelside and waterside stress-corrosion cracking, and hydride formation. Possible corrosion failure modes for stainless steels in a repository include uniform, pitting, and crevice corrosion, waterside stress-corrosion cracking, and hydrogen/helium embrittlement. The most likely mechanism for breach of containment in Zircaloy cladding is fuelside stress-corrosion cracking believed to be caused by aggressive gases in the fuel-cladding gap. Uniform corrosion processes of Zircaloy may be enhanced by the presence of silicate ion. The most likely corrosion mechanism for breach of containment in stainless steel cladding is cracking in chloride and caustic solutions.

Preliminary static leach tests at 25-30°C on defected and undefected fuel rods and bare fuel in deionized water indicate that the undefected cladding (1) releases measurable radioactivity to the leachant and (2) decreases by several orders of magnitude the release rates of U, Pu and Cs. A conclusion about the containment capability of the cladding cannot be made until (1) there is a quantitative definition of containment in terms of the maximum acceptable release rates and (2) the release rates of the predominant radionuclides during the containment period from non-failed and failed rods under repository conditions have been determined.

## 1. INTRODUCTION

In the licensing procedure for a high level waste geologic repository two NRC criteria are of major importance with respect to the performance objectives for the engineered system. These are detailed in Final Rule 10 CFR 60 (Disposal of High Level Waste in Geologic Repositories) dated June 1983. The first objective specifies that:

> "Containment of HLW within the waste packages will be substantially complete for a period to be determined by the Commission taking into account the factors specified in subsection 60.113(b) (of 10 CFR 60) provided, that such period shall be not less than 300 years nor more than 1,000 years after permanent closure of the geologic repository; and
>
> "The release rate of any radionuclide from the engineered barrier system following the containment period shall not exceed one part in 100,000 per year of the inventory of that radionuclide calculated to be present at 1000 years following permanent closure, or such other fraction of the inventory as may be approved or specified by the Commission; provided, that this requirement does not apply to any radionuclide which is released at a rate less than 0.1% of the calculated total release rate limit. The calculated total relese rate limit shall be taken to be one part in 100,000 per year of the inventory of radioactive waste, originally emplaced in the underground facility, that remains after 1,000 years of radioactive decay."

To meaningfully address these performance objectives it will be necessary for the license applicant to consider:

a. How and when groundwater enters the engineered repository system
b. How and when groundwater penetrates the geologic packing material (discrete backfill)
c. How and when groundwater penetrates the container system and causes corrosion failure
d. How and when groundwater leaches radionuclides from the waste form
e. How and when the radionuclides are transported through the failed container system, packing material and disturbed host rock to the near field environment.

For these scenarios, in which the individual engineered barriers are breached, probable chemical (corrosion) failure/degradation modes and mechanical failure/degradation modes need to be identified and quantified. These will depend on the specific design of the engineered system including selection of materials, local temperatures, local repository water conditions, radiation effects, water flow rates, and lithostatic/hydrostatic pressures, etc. It is only through a comprehensive knowledge of these factors that the performance of the individual engineered barriers can be determined and compliance with the above-mentioned NRC criteria demonstrated.

The purpose of the current study is to outline in logical sequence the important performance assessments for barrier components which may need to be addressed for licensing with respect to demonstrating compliance with the containment and controlled radionuclide release performance objectives. Figures 1.1 and 1.2 are schematics outlining the logic for performance assessment. They specify those failure/degradation modes which are considered to be important for the materials and host rocks currently being considered in the national high level waste terminal storage program. By accumulating a comprehensive data base on these failure modes, those which will ultimately be controlling can be identified.

Although Figure 1.1 describes a plan for the comprehensive performance assessment of the individual engineered barrier components it is not mandatory for each component to be fully characterized. If the license applicant can demonstrate that one component alone can meet an NRC performance objective then a detailed characterization of the other engineered barriers is unnecessary. It would suffice to show that the other barriers are redundant and do not compromise the ability of the primary barrier to meet the objective. For example, if it can be shown that a container system alone can remain unbreached for 300-1000 years under anticipated waste package conditions, then a comprehensive data base on the performance of the secondary barriers would not be needed to address the containment time. Similarly, if the waste form has a radionuclide release rate which will meet the controlled release criterion under anticipated repository conditions a detailed knowledge of the radionuclide retardation capabilities of packing materials is also not needed. Thus, a licensing strategy based on full compliance with an NRC performance objective by a single barrier would be a cost saving endeavor. On the other hand, if compliance requires the conjoint action of more than one barrier, so that each barrier contributes partial compliance, the data base to characterize performance will necessarily involve single-component and multi-component tests to quantify interaction effects. Strategies which may be used to demonstrate compliance are discussed in a separate report (NUREG/CR-2951, 1982).

## 1.1 Reference

NUREG/CR-2951, BNL-NUREG-51588, "Draft Staff Technical Position, Subtask 1.1: Waste Package Performance After Repository Closure," M. S. Davis and D. G. Schweitzer, Brookhaven National Laboratory, September 1982.

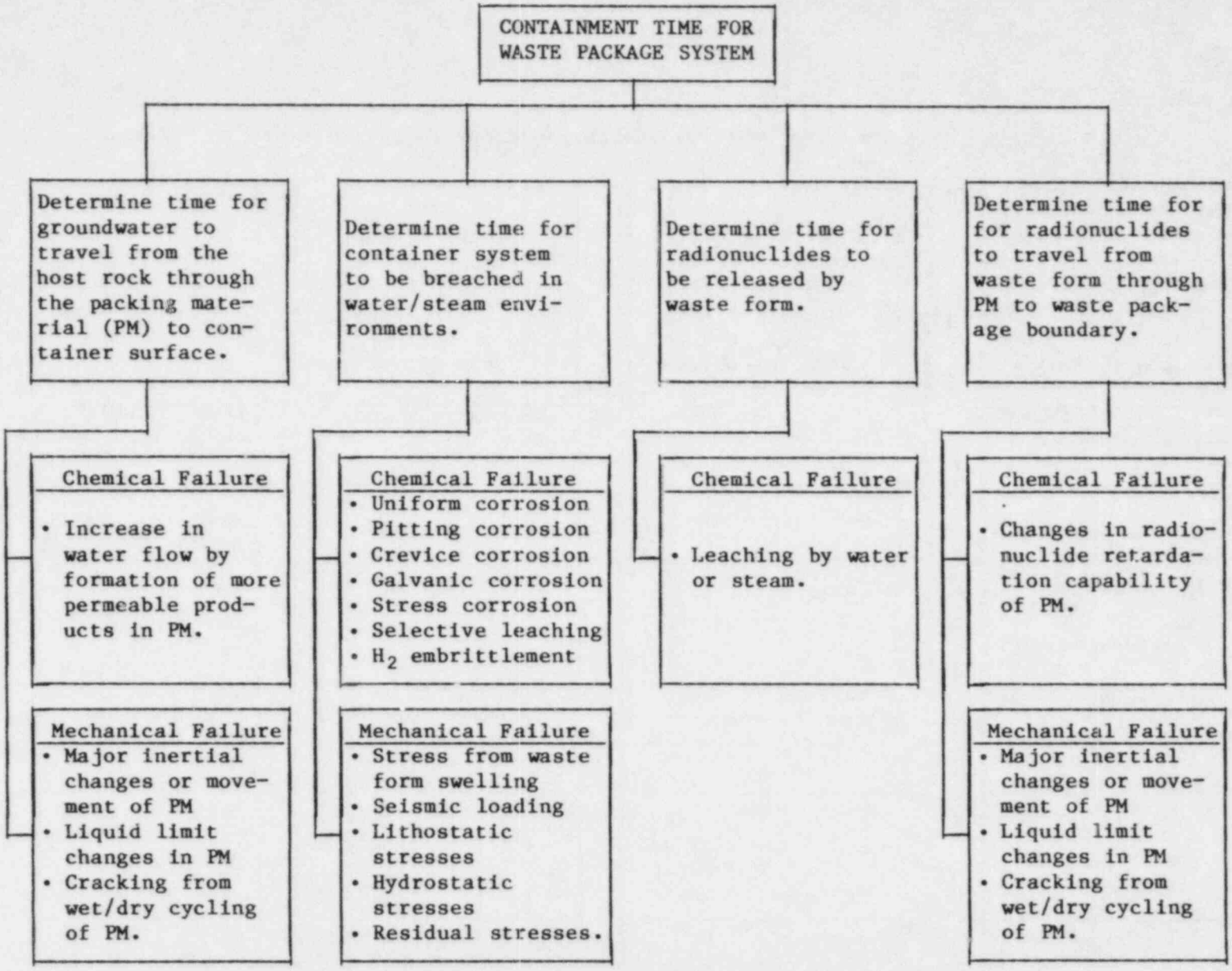


Figure 1.1 Chemical and mechanical failure/degradation modes affecting containment of radionuclides by the waste package system.

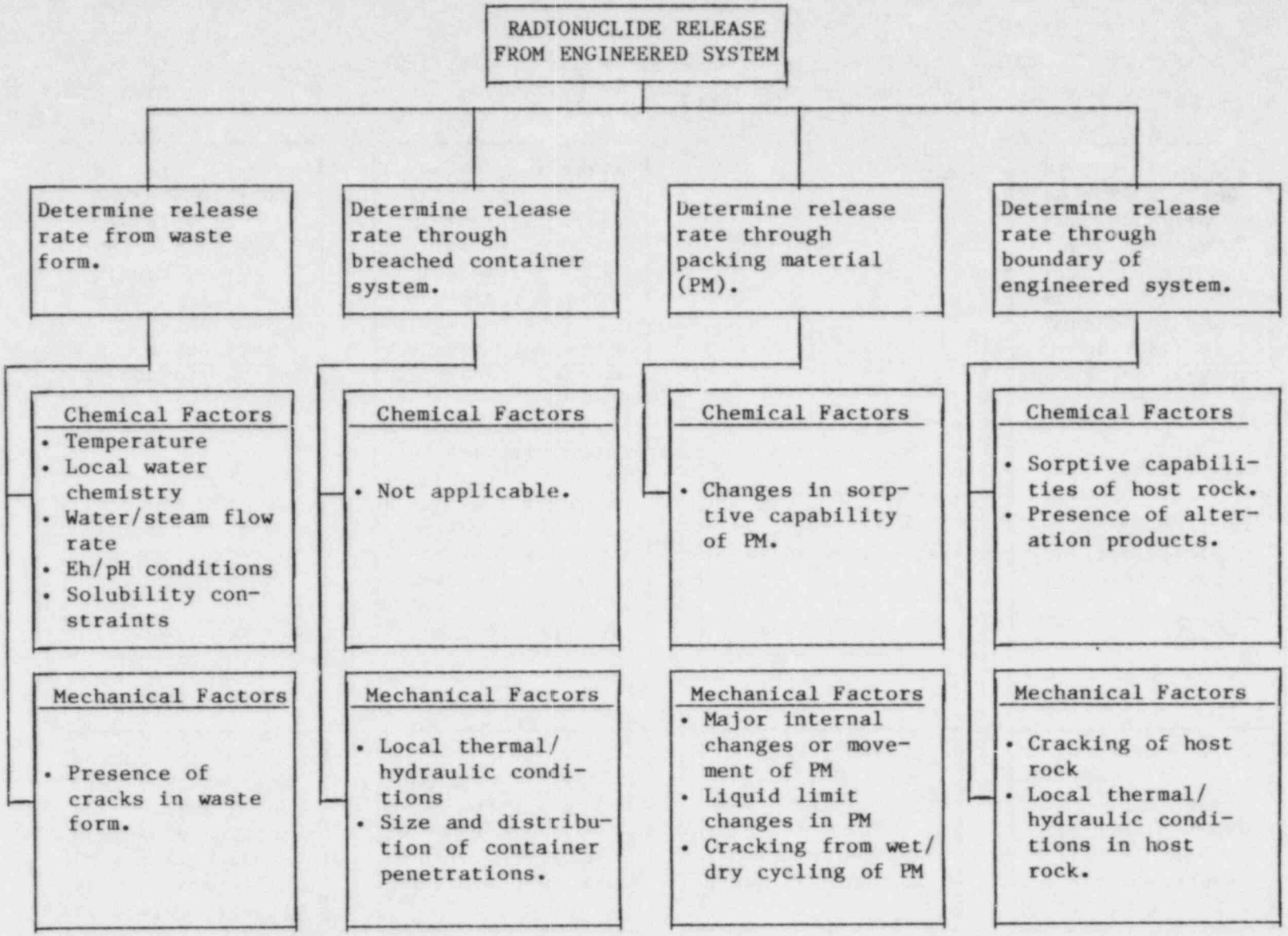


Figure 1.2 Factors affecting radionuclide release from the engineered barrier system.

## 2. NEAR-FIELD REPOSITORY CONDITIONS

### 2.1 Basalt

This section of the program has been completed and is reported in a previous Biannual Report (NUREG/CR-2482, Vol. 3, 1983).

### 2.2 Salt

This section of the program has been completed and is reported in a previous Biannual Report (NUREG/CR-2482, Vol. 3, 1983).

### 2.3 Tuff

This section of the program has been completed and is reported in a previous Biannual Report (NUREG/CR-2482, Vol. 4, 1983).

### 2.4 Granite

This section of the program has been completed and is reported in a previous Biannual Report (NUREG/CR-2482, Vol. 6, 1984).

# 3. WASTE FORM FAILURE AND DEGRADATION MODES

## 3.1 Borosilicate Glass

This part of the program has been completed and is reported elsewhere (NUREG/CR-2482, Vol. 4, 1983).

## 3.2 Spent Fuel Cladding Failure

Earlier work in the Brookhaven National Laboratory (BNL) program has addressed in detail the anticipated environments around emplaced waste packages in salt, basalt, and tuff repositories (NUREG/CR-2482, Vol. 3, 1983, Vol. 4, 1983, and Vol. 6, 1984). Since new data have become available after the publication of these reports, a brief summary will be given below to specify the anticipated environments to be expected around spent fuel waste packages. A knowledge of such conditions will enable an evaluation to be made of the most likely corrosion failure modes for spent fuel containers and fuel cladding. At this time, the aqueous environment expected while the fuel is being stored in pools at the reactor site will not be addressed. They are, however, likely to be far less aggressive than conditions expected in a repository system. This conclusion is supported by work done at Pacific Northwest Laboratories (PNL-3921, 1981), which entailed the examination of Zircaloy-clad spent fuel after 10-20 years of pool storage.

### 3.2.1 Waste Package Environment in a Salt Repository

#### 3.2.1.1 Salt Brine Chemistry

Molecke (SAND83-0516, 1983) has cataloged various brine chemistries of relevance to the salt repository effort including test solutions being used in supporting research programs. They fall into two categories, including high NaCl or high Na-Mg-K-Cl content. These are given in Tables 3.1 and 3.2. Brine A is representative of the chemistry of brine inclusions in the salt, whereas Brine B chemistries are typical of water in contact with halite at the repository level.

Under the hydrothermal[1] conditions present during the repository post-closure period, changes in the brine chemistry will result. Some laboratory tests carried out by Pacific Northwest Laboratories (PNL) and Sandia National Laboratory (SNL) (Molecke, M. A., 1982) show that, in simulated waste package tests, the pH of Brine B fell from 6.8 to 3.8 (Table 3.2). This was attributed to hydrolysis effects. However, another possible contributing factor could be connected with the thermal release of gaseous constituents from the salt. Uerpmann (1982) and Pan[illegible] and Soo (NUREG/CR-3091, Vol. 3, Appendix A, 1984) have demonstrated that gases released include HCl, $SO_2$, $CO_2$, $H_2S$, and $H_2O$. Some of these will dissolve in the brine to give acidic solutions. Later

---

[1]The term "hydrothermal" is used here to denote reactions involving superheated water; i.e. reactions at any temperature above 100°C where pressure is sufficient to maintain water in the liquid phase. Note that, in strict earth sciences nomenclature, such conditions involving temperatures between 100 and 373°C are "mesothermal."

Table 3.1. Brine "A-like" and other brine composition comparisons (mg/L).

| Ion | (WIPP/ Generic) Brine A (±3%) | WIPP Inclusion No.1 (Preliminary) | WIPP Inclusion No.2 (Preliminary) | MCC Brine | Quinare Brine Q (±10%) (55°C) | USGS WRT-6a (±10%)* | OTHER Saturated NaCl (20°C) | OTHER Saturated NaCl (100°C) | Seawater |
|---|---|---|---|---|---|---|---|---|---|
| $Na^+$ | 42,000 | 63,000 ± 5000 | 32,000 ± 1,100 | 35,400 | 6,500 | 27,000 | 142,000 | 154,000 | 10,651 |
| $K^+$ | 30,000 | 8700 ± 500 | 6800 ± 200 | 25,300 | 29,000 | 35,000 | | | 380 |
| $Mg^{++}$ | 35,000 | 23,000 ± 2000 | 40,000 ± 1400 | 29,600 | 85,000 | 33,000 | | | 1,272 |
| $Ca^{++}$ | 600 | 210 ± 20 | 150 ± 10 | | | 47,000 | | | 400 |
| $Sr^{++}$ | 5 | | | | | | | | 13 |
| $Zn^{++}$ | | | | | | | | | |
| $Li^+$ | 20 | | | | | | | | |
| $Rb^+$ | 20 | | | | | | | | |
| $Cs^+$ | 1 | | | | | | | | |
| $Fe^{+++}$ | 2 | | | | | | | | |
| $Cl^-$ | 190,000 | 160,000 ± 9,000 | 160,000 ± 5000 | 164,000 | 270,000 | 250,000 | 218,000 | 237,000 | 18,980 |
| $SO_4^{--}$ | 3,500 | 13,200 ± 2600 | 13,200 ± 2600 | | 13,000 | | | | 884 |
| B(as $BO_3^{---}$) | 1,200 | | | | | | | | |
| $HCO_3^-$ | 700 | | | | | | | | 146 |
| $Br^-$ | 400 | | | | | | | | 65 |
| $I^-$ | 10 | | | | | | | | 0.05 |
| $F^-$ | | | | | | | | | |
| pH: | 6.5 | | | 6.5 | | | | | 8.1 |

Table 3.2. Brine "B-like" brine composition comparisons (mg/L).

| Ion | (WIPP/ Generic) Brine B (±3%) | ONWI Composite Permian P | Equilibrated Permian P no. 2 | Pretest PNL-SNL | Brine-Backfill PNL-SNL | Posttest PNL-SNL | Flow WIPP-12 | Downhole WIPP-12 | Flow ERDA-6 | Downhole ERDA-6 |
|---|---|---|---|---|---|---|---|---|---|---|
| $Na^+$ | 115,000 | 123,460 | 123,000 | 159,000 | 155,000 | 119,000 | 114,000 | 140,000 | 112,000 | 140,000 |
| $K^+$ | 15 | 39 | 39 | 2,550 | 2,370 | 5,000 | 3,100 | 3,200 | 3,800 | 4,800 |
| $Mg^{++}$ | 10 | 134 | 122 | 409 | 463 | 158 | 1,700 | 1,400 | 450 | 270 |
| $Ca^{++}$ | 900 | 1,560 | 1,100 | 370 | 695 | 267 | 410 | 380 | 490 | 360 |
| $Sr^{++}$ | 15 | 35 | 35 | 18 | 43 | 34 | 15 | -- | 18 | -- |
| $Zn^{++}$ | | 7.8 | 8 | <2.5 | -- | 199 | 0.5 | -- | 0.6 | -- |
| $Li^+$ | 20 | | | | | | 220 | 210 | 240 | 205 |
| $Rb^+$ | 20 | | | | | | | | | |
| $Cs^+$ | 1 | | | -- | -- | 64 | | | | |
| $Fe^{+++}$ | 2 | | | <5 | -- | 55 | 3.6 | 6.3 | 3.6 | 5.7 |
| $Cl^-$ | 175,000 | 191,380 | 191,000 | 190,000 | 231,000 | 197,000 | 160,000 | 180,000 | 170,000 | 180,000 |
| $SO_4^{--}$ | 3,500 | 3,197 | 1,910 | 2,086 | 3,237 | 16,300 | 17,000 | 18,000 | 16,000 | 14,000 |
| B(as $BO_3^{---}$) | 1,200 | | | 16 | 11 | 1,280 | 1,200* | 960* | 680* | 740* |
| $HCO_3^-$ | 700 | 30 | 23 | 7.8 | 15 | 0 | 2,600 | 2,400 | 2,600 | 1,800 |
| $Br^-$ | 400 | 32 | 24 | | | | 430 | 460 | 880 | 720 |
| $I^-$ | 10 | | | | | | | | | |
| $F^-$ | | 1.1 | 1.0 | 37 | 37 | 0 | 4.3 | -- | 1.7 | -- |
| pH: | 6.5 | 7.055 | | 6.9 | 6.8 | 3.8 | 7.17 | 7.76 | 6.42 | 7.02 |
| Field Eh: (mV) | | | | | | | -211 | | -152 | |

*Values reported as B, but assumed to actually be $BO_3^{---}$

-- = below measureable detection limits

during the post-closure period, it is likely that brine pH will be increased to give an alkaline solution, as a result of the radiation-induced formation of colloidal sodium and the subsequent formation of sodium hydroxide. The tests carried out by PNL and SNL also show that, under high temperatures, the $SO_4^{2-}$ concentrations increased from 3,237 to 16,300 mg/L. These $SO_4^{2-}$ levels combined with the high $Cl^-$ concentrations will cause the brine to be relatively corrosive compared to other repository groundwaters. Thus, a detailed evaluation of corrosion failure modes of container/overpack materials will be required for such brine chemistries. Also, spent fuel cladding corrosion data will be needed if DOE intends to give credit to this component for radionuclide containment.

3.2.1.2 Hydrology

Salt is considered to be an ideal host rock for nuclear waste because of its low water content. However, it has been shown in several studies (for example, Roedder and Belkin, 1978) that brine inclusions migrate up a thermal gradient and eventually reach a waste package. Extrapolation of test data indicates that, for a waste container with a thermal load of 2.16 kW and an overall areal thermal load of 100 kW/acre, the total brine inflow with a waste package borehole will be about 8 L after 300 years, after accounting for the decreasing thermal load in that period. For an areal load of 150 kW/acre, the amount would be about 11.5 L (ORNL/TM-7201, 1980). Unless this brine collects in an area not in contact with the waste container, it is expected to cause corrosion. Corrosive species in the brine will not be depleted since it will be in contact with adjacent salt, and oxygen and hydrogen will be generated by gamma radiolysis effects (see below). It should be noted that some workers (Roedder, E. 1982) consider that the brine inflow rate mentioned above could be up to two orders of magnitude too low.

3.2.1.3 Thermal Environment

Recent calculations for the reference spent fuel package are given in Figure 3.1 for an areal loading of 49 kW/acre (12 $W/m^2$) (ONWI-438, 1983). The maximum design temperature for the fuel rod centerline is ≈375°C. It should be noted that the calculated temperature is design-dependent and that current conceptual designs do not specifically include the use of a packing material (ONWI-438, 1983).

One important point needs to be made regarding thermal effects in rock salt. Roedder and Belkin (1978) have shown that Carlsbad, New Mexico, salt suffers decrepitation within days at atmospheric pressure. If large brine inclusions are present, the decrepitation temperature may be as low as 60°C. The resultant fracture of the salt releases moisture and the cracks could provide easier pathways for brine migration unless the fractures are sealed by salt creep.

In other work by Levy and others (1981), it was shown that for salt, specimens electron-irradiated to a dose of $5 \times 10^9$ rads fractured along crystallographic planes without any externally applied stress. The effect appears to be associated with a radiation-enhanced decrease in the decrepitation temperature and is possibly associated with the generation of radiolytic hydrogen and

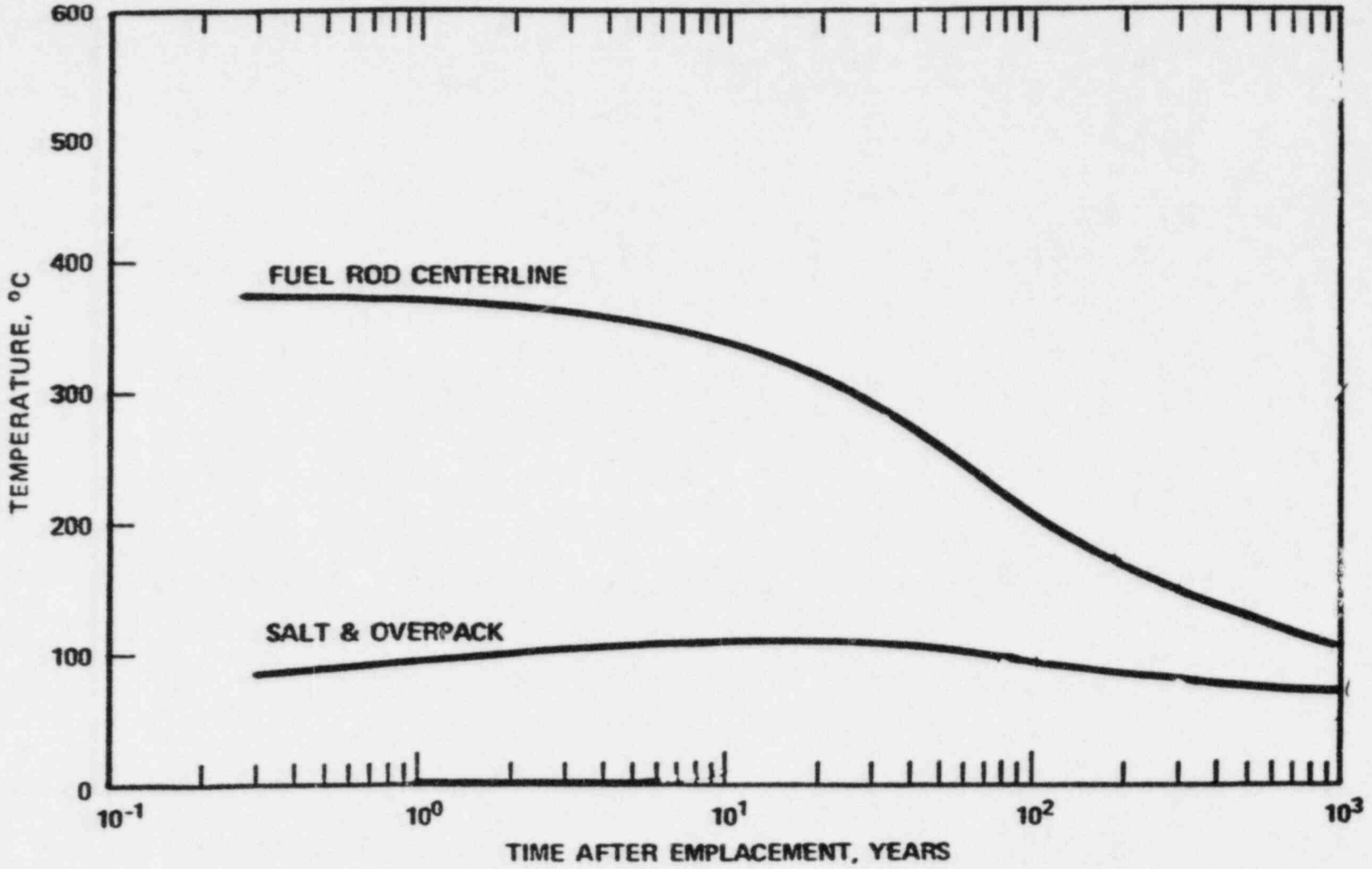


Figure 3.1. Reference spent fuel borehole package thermal performance in a salt repository (ONWI-438, 1983).

oxygen in the brine inclusions. These gas pressures would be additive to the vapor pressures within the inclusions and lead to earlier decrepitation.

3.2.1.4 Irradiation Environment

During the 300-1000 years radionuclide containment period, significant doses of gamma irradiation will be administered to crushed salt packing and nearby host rock. The anticipated total dose, however, will be dependent on the types and thicknesses of the package components and the waste loading. An upper gamma dose level of $10^9$ to $10^{10}$ rads, however, is estimated for a spent fuel package from recent work (ONWI-438, 1983). As mentioned above, Levy and his co-workers have demonstrated in electron irradiation tests (used to simulate gamma irradiation effects) that large quantities of F-centers and colloidal sodium will be expected adjacent to the container/overpack system as a consequence of irradiation. Compressive deformation creates internal defects in salt which are shown to accelerate colloidal sodium generation rates.

More recent work at Brookhaven National Laboratory (BNL) (NUREG/CR-3091, Vol. 3, Appendix A, 1984) focused on the implications of F-center and colloidal sodium generation around non-shielded salt waste packages. Salt samples were gamma irradiated at 40 and 125°C with and without saturated brine being present. Dry granulated Carlsbad (New Mexico) salt irradiated at 40°C to doses up to $10^{10}$ rads gave highly alkaline solutions upon dissolving to the solubility limit in deionized water. The pH reached a maximum value of about 9.3 after a dose of $2.9 \times 10^9$ rads and thereafter remained constant. During irradiation, decrepitation occurred resulting in spallation of the rock salt samples. During dissolution, there was audible popping and gas (probably hydrogen) was generated. Dry salt, and salt in the presence of saturated brine, irradiated at 125°C gave similar increases in pH and in the measured total base concentration in solution. It is believed that the increases in alkalinity of the brine are closely associated with colloidal sodium interactions with water to give NaOH and $H_2$.

An important feature of this work is that the brine adjacent to the salt being irradiated at 125°C became acidic with time, reaching a value of about 3.5 after approximately 300 hours. This is thought to be attributable to the thermal release of HCl, $SO_2$ and $CO_2$ as described above. However, hydrolysis effects involving $MgCl_2$ may be a contributing factor.

To separate irradiation and thermal effects, dry Carlsbad salt was heated over a range of temperatures and the annealed material dissolved in water. It was found that the pH of the resultant solutions also increased in a similar manner to that for irradiated salt, reaching a maximum of 9.5. The measured total base in solution, however, was much lower than that measured for irradiated samples.

Based on the above BNL experiments, it was postulated that both acidic and basic brine may contact the container at different times during the repository post-closure period. If brine is present around the container during the early period of irradiation, it may become acidic due to the release of HCl, $SO_2$ and $CO_2$ from the salt. Later, brine inclusions migrating through a

colloidal sodium field would reach the waste package and their high NaOH content would begin to neutralize the acidic brine. As more inclusions arrive at the container surface, the brine would become basic.

Container/overpack materials and fuel cladding, therefore, need to be characterized with respect to a range of anticipated pH conditions. In addition hydrogen generated by colloidal sodium interactions with brine and radiolytic hydrogen need to be addressed in terms of their potential to cause embrittlement of metallic barriers.

3.2.1.5 Stress Environment

Claiborne and others (ORNL/TM-7201, 1980) calculated the pressure environment within a waste package borehole as a function of time. They considered several scenarios including (a) emplacement without packing materials, (b) emplacement with packing material with the hole sealed, and (c) the hole is sealed without packing material. Based on considerations of brine inflow rates and gas pressure buildup they showed that for the three cases the maximum pressure within the borehole occurs after 10-15 years and reaches values between 2.6 to 3.2 MPa. After 15 years, these emplacement hole stresses dropped very quickly.

Lithostatic pressures at repository depth have been calculated to be 16.2 MPa (ONWI-438, 1983) and in the long term these will determine the loads on the waste package.

3.2.2 Waste Package Environment in a Basalt Repository

3.2.2.1 Basaltic Water Chemistry

Candidate basalt repository horizons at the Hanford site are located within the Grande Ronde formation. Table 3.3 gives the nominal compositions of GR-3 and GR-4 groundwaters. Besides the components listed, GR-3 basaltic groundwater has been found to contain the following gases: 25 ppm $N_2$, 10 ppm Ar, and up to 700 ppm $CH_4$ at 25°C. The water is thought to be extremely low in oxygen because of the oxidation of $Fe^{2+}$ in the basalt mesostasis phase to $Fe^{3+}$ (DOE/RL 82-3, 1982). In fact, it has been postulated that the groundwater will be so reducing in nature that container corrosion may be inhibited (DOE/RL 82-3, 1982). A summary by BWIP of anticipated Eh/pH changes with time is given in Figure 3.2 (BWIP/DOE/NRC Workshop, 1984).

Recent work by Gause and others (BNL-NUREG-34297, 1984) investigated changes in GR-3 groundwater chemistry and pH with and without gamma irradiation. In this work, an autoclave system was designed in which an internal heater was used to impose a thermal gradient across a carbon steel sleeve (which simulated a waste container) and a 75 percent crushed basalt/25 percent (by volume) sodium bentonite packing material. The packing material was saturated with simulated Grande Ronde groundwater. In this study a non-irradiated control test has recently been completed in which the cover gas in the autoclave was methane. This gas was used to evaluate the effects of methane which has been detected in the water sampled from some BWIP boreholes.

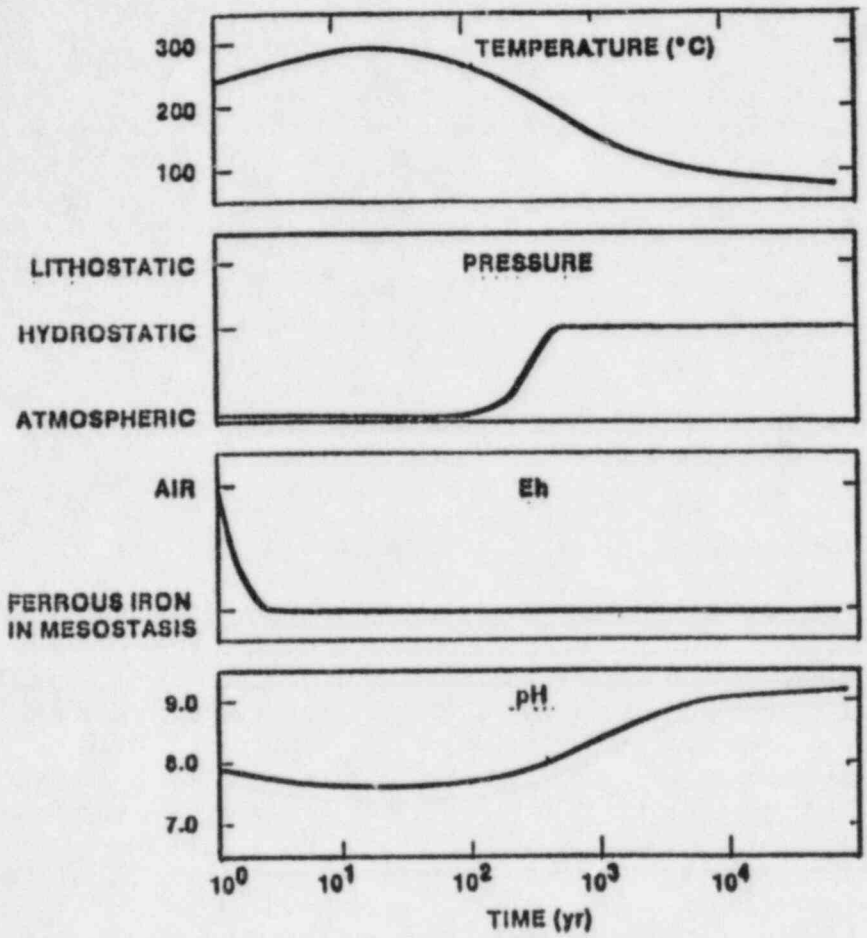


Figure 3.2. Schematic showing anticipated changes in basalt repository conditions with time (BWIP/DOE/NRC Workshop, 1984).

Analysis at room temperature of the reacted groundwater shows that $SO_4^{2-}$ levels increase, $Cl^-$ remains unchanged, and the dissolved oxygen decreases from 8.3 ppm in the starting solution to a value close to zero. The obtainment of a DO value close to zero from these unirradiated, short-term whole package tests may indicate that long-term tests may attain a reducing environment. However, under realistic conditions it should be noted that gamma radiolysis may provide an oxidizing environment near the package. More details of irradiation tests carried out in the BNL effort in whole package testing are given below in Section 3.2.2.4.

Table 3.3. Composition of synthetic Grande Ronde groundwaters.

| Chemical Species | GR-3 Nominal Composition (ppm) (RHO-BW-SA-315P, 1983) | GR-4 Nominal Composition (ppm) (SD-BWI-TP-022, 1984) |
|---|---|---|
| $Na^+$ | 358 | 334 |
| $Cl^-$ | 312 | 405 |
| $SO_4^{2-}$ | 173 | 40 |
| Si (as $SiO_2$) | 76.2 | 96.4 |
| Inorganic C (as $HCO_3^-$) | 100 | 92.0 |
| $F^-$ | 33.4 | 19.9 |
| $K^+$ | 3.4 | 13.8 |
| $Ca^{2+}$ | 2.8 | 2.2 |
| $Mg^{2+}$ | 0.032 | ---- |

In a second study at BNL (NUREG/CR-3091, Vol. 3, Appendix D, 1983), the main emphasis was to assess water migration characteristics through a basalt/bentonite packing. However, measurements of groundwater chemistry after reaction at a maximum temperature of 250°C for 30 days provided useful information. It was found that considerable changes occurred in the composition of the synthetic Grande Ronde water used in the tests, in contrast to Gause and others (BNL-NUREG-34297, 1984) who detected only small changes at 150°C. Changes in dissolved species are given in Table 3.4.

A comparison of the initial and final compositions shows that $K^+$, $Ca^{2+}$, Fe, Si and $SO_4^{2-}$ levels are significantly increased; $Na^+$, $Mg^{2+}$ and $Cl^-$ are slightly increased; and $F^-$ concentrations are significantly decreased.

From these experiments, it is clear that container/overpack and spent fuel cladding corrosion experiments should be carried out in the presence of packing material and irradiation because of the altered chemical and Eh/pH conditions that will prevail after repository closure.

Another effect that could perturb the composition of the groundwater is the likelihood that during the emplacement and early post-closure periods in the repository the groundwater in the near-field host rock may be converted to

steam leaving behind previously dissolved solids. Alteration of the basalt along the groundwater flow paths is also likely to occur at high repository temperatures. After repressurization of the repository, when steam conditions subside, it is possible that water entering the waste package emplacement holes will be considerably concentrated since it would tend to redissolve precipitated solids and alteration products. This effect has not been adequately characterized.

Table 3.4. Concentrations of selected species in samples of synthetic basaltic groundwater after reaction with basalt/bentonite packing at 250°C for 30 days (mg/L) (NUREG/CR-3091, Vol. 3, Appendix D, 1983).

| Element or Ionic Species | GR-3 Nominal Conc. | Unreacted Groundwater Solution | Liquid Inside Packing Material (3 Samples) | | |
|---|---|---|---|---|---|
| $Na^+$ | 358 | 350 | 510 | 500 | 490 |
| $K^+$ | 3.43 | 18 | 120 | 120 | 120 |
| $Ca^{2+}$ | 2.78 | 3.5 | 182 | 144 | 175 |
| $Mg^{2+}$ | 0.032 | 0.38 | 0.95 | 0.86 | 1.2 |
| Fe | 0 | <0.5 | 10.7 | 7.7 | 7.9 |
| Si | 35.3 | 69 | 300 | 310 | 240 |
| $F^-$ | 33.4 | 25.8 | 2.68 | 4.30 | 4.08 |
| $Cl^-$ | 312 | 320 | 358 | 380 | 370 |
| $SO_4^{2-}$* | 173 | 196 | 899 | 744 | 855 |

*$SO_4^{2-}$ did not increase after oxidation with $H_2O_2$. Therefore, total S is attributed to $SO_4^{2-}$.

3.2.2.2 Hydrology

The hydraulic conductivity is a measure of the ability of a particular geologic medium to transport water under a hydraulic gradient. Although its units are length per unit time, this parameter is not a velocity; it is, rather, a measure of the volume rate of flow through a unit cross sectional area. It is a property of both the geologic medium and the groundwater under the temperature and pressure conditions in the waste repository. There is considerable uncertainty in the hydraulic conductivities for Grande Ronde basalt. Flow is relatively fast in sedimentary interbeds compared to columnar material. Some estimates by the Basalt Waste Isolation Project (BWIP) for the horizontal hydraulic conductivities in the flow top and columnar zones are, respectively, $10^{-10}$ to $10^{-3}$ and $10^{-13}$ to $10^{-12}$ in/sec (DOE/RL 82-3, 1982). Actual flow paths are believed to be up vertical cracks in the basalt and through the repository and then along flow tops to the accessible environment (DOE/RL 82-3, 1982; Salter, P. F. and others, 1982; and Deju, R. A. and others, 1983). At present there do not appear to be any measured values for

vertical hydraulic conductivities, but vertical flow through the repository horizon may be relatively high because of buoyancy effects.

3.2.2.3 Thermal Environment

Figure 3.3 shows the anticipated time-temperature profile for spent fuel waste package components emplaced in basalt. The anticipated thermal loading is 1.74-2.16 kW per package. It corresponds well to the general schematic for temperature changes given in Figure 3.2. The spent fuel at the fuel centerline and the container reach a peak temperature of about 260°C, 20 years after emplacement in the presence of dry packing material. It is assumed that the cladding temperature could not exceed this maximum value. After 300 years, the temperature decreases to about 150°C. Estimations of cladding failure rates should focus, therefore, in the 150-260°C temperature range.

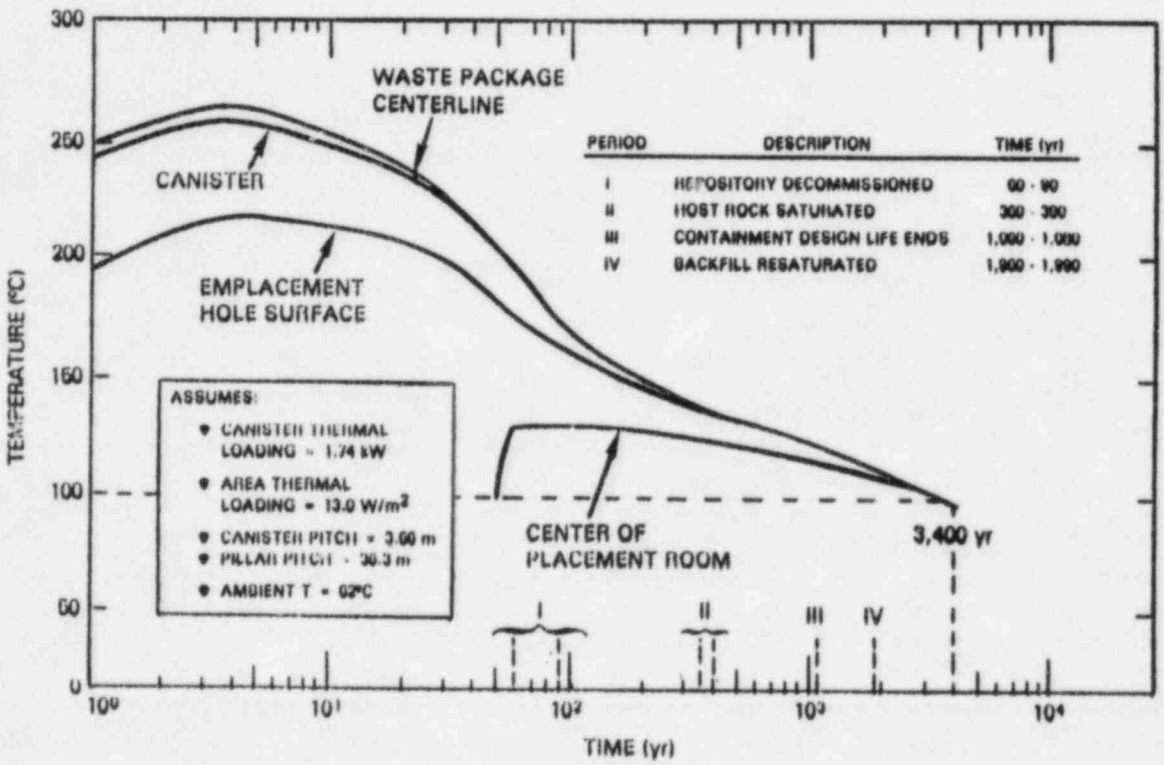


Figure 3.3. Temperature-versus-time curves for different components of a vertically-emplaced spent fuel waste package in a repository located in basalt (DOE/RL 82-3, 1982). (Note calculations performed assuming presence of dry packing material.)

It should be noted that the design maximum temperature limit for spent-fuel cladding is 300°C as stated in DOE/RL 82-3 (1982) but is 380°C as stated in RHO-BW-CR-136 (1982).

3.2.2.4 Irradiation Effects

Gamma irradiation fluxes are not available for a finalized spent fuel waste package design. However, early work estimates that the initial flux at the surface of a pressurized water reactor spent fuel package are approximately $2.9 \times 10^4$ mrem/h (AESD-TME-3142, 1982). This gives a total gamma dose over the 300-year containment period of about $10^7$-$10^8$ rads, assuming that the dose rate decreases linearly to zero during this time.

Prior BNL work has summarized gamma radiolysis effects in pure water (NUREG/CR-2482, Vol. 2, 1983). These are expected to give a good indication of the types of radiolytic specie that will be present around non-shielded waste packages emplaced in basalt. The following reaction summarizes products formed by gamma radiolysis:

$$H_2O \longrightarrow H\bullet,\ \bullet OH,\ e^-_{aq},\ H_3O^+,\ H_2,\ H_2O_2,\ OH^-,\ HO_2$$

Dissolved oxygen in the groundwater will increase the yield of $HO_2$, and $O_2^-$ may also form. The yields of altered species produced by radiolysis are usually defined in terms of the number of molecules produced per 100 eV of adsorbed irradiation; this is termed the G value. In neutral pure water typical values are:

$G(H\bullet) = 0.60$
$G(H_2) = 0.45$
$G(H_2O_2) = 0.74$
$G(H_3O^+) = G(e^-_{aq}) = G(\bullet OH) = 2.6 \pm 0.3$
$G(HO_2\bullet) = 0.02$ ($O_2$ absent).

Decomposition of $H_2O_2$ will yield $O_2$.

Some experiments have recently been completed at BNL to investigate local conditions around a waste package in a basalt repository. The work consisted of autoclave tests in which a carbon steel sleeve and a basalt/bentonite packing material were reacted in the presence of gamma irradiation ($3.8 \times 10^4$ rads/h), Grande Ronde GR-3 basaltic water, and methane. The gas was included in some of the tests since some groundwater samples from the BWIP site were found to contain methane (DOE/RL 82-3, 1982). Three separate experiments were conducted at a carbon steel temperature of 150°C:

Phase I - a two-month hydrothermal test using an inert argon cover gas under a gamma flux;
Phase II - a two-month hydrothermal test using a methane cover gas under a gamma flux;
Phase III - a two-month hydrothermal test using a methane cover gas without irradiation.

Table 3.5 summarizes analyses made for selected constituents of filtered water samples taken from the basalt/bentonite mixture after completion of the tests. Levels of $Cl^-$ remain constant and $SO_4^{2-}$ concentrations were nearly doubled. The Si level based on the Phase I study decreased and it was likely caused by the formation of an Fe-Si-Ca-Al rich colloid. For all three tests, the measured dissolved oxygen levels (DO) fell in the range 0.2 to 0.6 ppm. Based on similar values obtained with the oxygen meter on chemically reduced solutions, it is concluded that after 90 days of reaction at 150°C the water in the basalt/bentonite packing contains little dissolved oxygen. This indicates that the basalt and the carbon steel sleeve are capable of maintaining very low dissolved oxygen levels even though gamma radiolysis creates oxidizing species. Metallurgical analysis of the carbon steel sleeve, in fact, verifies that the surface reaction layer contains iron, silicon and oxygen. Nevertheless, there are apparently no data obtained for realistic waste package conditions that prove that the oxygen levels are sufficiently low to give reducing conditions.

Other work by Gray (RHO-BW-SA-315 P, 1983) shows that Grande Ronde groundwater saturated with methane and irradiated at much higher dose rates in the absence of package components forms polymeric material containing 1.0 to 2.9 weight percent oxygen. These short-term tests (three days) permitted an evaluation to be made as to the effect of an accumulated gamma dose of $\approx 10^8$ rads on the groundwater chemistry. In the BNL experiments, the simulated waste package contacting methane-saturated groundwater was irradiated to dose levels of $\approx 10^7$-$10^8$ rads and yielded a completely different type of colloidal material suspended in solution. A comparison of Gray's and BNL's work highlights the importance of performing irradiated whole package tests to determine the characteristics of the environment that the package will produce and will experience.

Table 3.5. Average water compositions after 60-day hydrothermal tests at a temperature of 150°C (BNL-NUREG-34297, 1984).*

| | Chemical Composition Measured at 24°C (ppm) | | | |
|---|---|---|---|---|
| Parameter** | Starting Value | Phase I ($\gamma$ + Ar) | Phase II ($\gamma$ + $CH_4$) | Phase III ($CH_4$) |
| $Cl^-$ | 312 | 313 | 296 | 409 |
| $SO_4^{2-}$ | 165 | 280 | 246 | 231 |
| Fe | 0 | <2 | 1 | 0.5 |
| Si (as $SiO_2$) | 79 | 34 | not meas. | not meas. |
| DO | 8.7 | 0.6*** | 0.2*** | 0.5*** |
| pH | 9.8 | 6.9 | 6.6 | 7.1 |

* This temperature is the maximum value and was maintained at the carbon steel heater sleeve. A thermal gradient was present due to heat loss at the autoclave wall.

** Other species were present but were not measured.

***These dissolved oxygen values are similar to those measured for chemically reduced water, indicating that after 60 days of testing the actual DO level is close to zero.

Measurements on the reacted water in the BNL tests showed that after 90 days the pH decreased from 9.8 to values lying in the range 6.6 to 7.1 (Table 3.5). This, again, is in general agreement with BWIP data (DOE/RL 82-3, 1982).

3.2.2.5 Stress Environment

During repository operations, the stress on the waste package will be approximately 1 atm. After repository closure, however, water ingress will raise the stress towards the hydrostatic stress level (11 MPa). If the host rock settles, the stresses in the waste package would rise to the lithostatic stress (33 MPa) as shown in Figure 3.2. It should be noted that the lithostatic stress is a vertically applied value estimated on the basis of the rock overburden at the repository horizon. No estimates appear to exist for the horizontal component of the stress on the waste packages. This is possibly an important consideration since it has been shown that the horizontal stresses at the Stripa granite mine in Sweden are up to two times as large as the lithostatic stress [ONWI-9(4), 1980]. A similar situation may be present in a basalt repository. Although some relaxation of these horizontal stresses will occur because of the presence of the package boreholes, the net stress on the waste package will be determined by the magnitudes of the lithostatic and the horizontal stress components.

3.2.3 Waste Package Environment in a Tuff Repository

3.2.3.1 Tuffaceous Water Chemistry

The current reference location of the tuff repository at the Nevada Test Site is in the Topopah Spring Member of the Paintbrush Tuff at Yucca Mountain. At the repository horizon, the tuff is in the unsaturated welded devitrified zone (UCRL-89988, 1983). The rock has a porosity of 12 percent and contains 5 percent water by volume. Water samples have not been taken at the repository horizon but the groundwater chemistry based on J-13 well water taken from below the water table is available and given in Table 3.6. The water contains 5.7 ppm of dissolved oxygen. Since the host rock is porous, water from the surface percolates past the repository horizon at an estimated flow rate of 8 mm/year (UCRL-89988, 1983).

The porous nature of the host rock creates a significant difference when compared to salt and basalt systems. Since the repository will not pressurize after sealing, water approaching the waste will boil at ≈95°C (the boiling point at the repository horizon) and steam will form and be dissipated. Presumably, dissolved salts in the water will be deposited along water flow paths and these will be redissolved, either fully or partially, by downcoming water as the repository cools. It is, therefore, highly probable that the water that eventually contacts the waste container will be considerably more concentrated than the J-13 water composition given in Table 3.6.

Some data cited by McCright (UCRL-89988, 1983) to justify high temperature corrosion tests in J-13 water are misleading. He showed that for crushed tuff/J-13 water interaction tests at 90 and 150°C the composition of the reacted water was similar to the J-13 composition, although an increase in pH

was detected. Such tests, however, do not take into account the effect of precipitated salts on the tuff which would be expected to give an increased dissolved salt level. No estimates of concentration effects are currently available.

Table 3.6. Reference groundwater composition for tuff repositories (based on composition of Jackass Flats Well J-13 at the Nevada Test Site).

| | Concentration (mg/L) |
|---|---|
| $Li^+$ | 0.05 |
| $Na^+$ | 51.0 |
| $K^+$ | 4.9 |
| $Mg^{2+}$ | 2.1 |
| $Ca^{2+}$ | 14.0 |
| $Sr^{2+}$ | 0.05 |
| $Ba^{2+}$ | 0.003 |
| Fe | 0.04 |
| $Al^{3+}$ | 0.03 |
| $SiO_2$ | 61.0 |
| $F^-$ | 2.2 |
| $Cl^-$ | 7.5 |
| $CO_3^{2-}$ | 0.0 |
| $HCO_3^-$ | 120.0 |
| $SO_4^{2-}$ | 22.0 |
| $NO_3^-$ | 5.6 |
| $PO_4^{3-}$ | 0.12 |
| pH - slightly basic (7.1) | |

Before the waste packages have cooled to the point where boiling ceases it is expected that a steam/air environment will be present. It is possible that gaseous or volatile constituents could be formed around the waste packages because of high temperature tuff/steam/air reactions but this is speculative at this time.

3.2.3.2 Hydrology

As mentioned above in Section 3.2.2.1 it is estimated that the water flow rate down to the repository horizon is about 8 mm/year (UCRL-89988, 1983).

This calculation is based on annual precipitation rates at the Nevada Test Site. For the first few hundred years, however, steam/air conditions will be present at the repository horizon. These will be superseded by liquid water/air conditions as the repository cools. Boiling of groundwater adjacent to the container will cease after about 150 years.

3.2.3.3 Thermal Conditions

The most recent assessment of thermal conditions within a spent fuel waste package is given in Figure 3.4 (UCRL-80820, 1983). Note that the calculations made for this figure do not include the presence of a packing material component. The maximum fuel temperature is 330°C and the maximum temperature of the reference Type 304L stainless steel container is about 250°C. It is, therefore, assumed that the maximum temperature of the cladding lies in the temperature range 250°C-330°C.

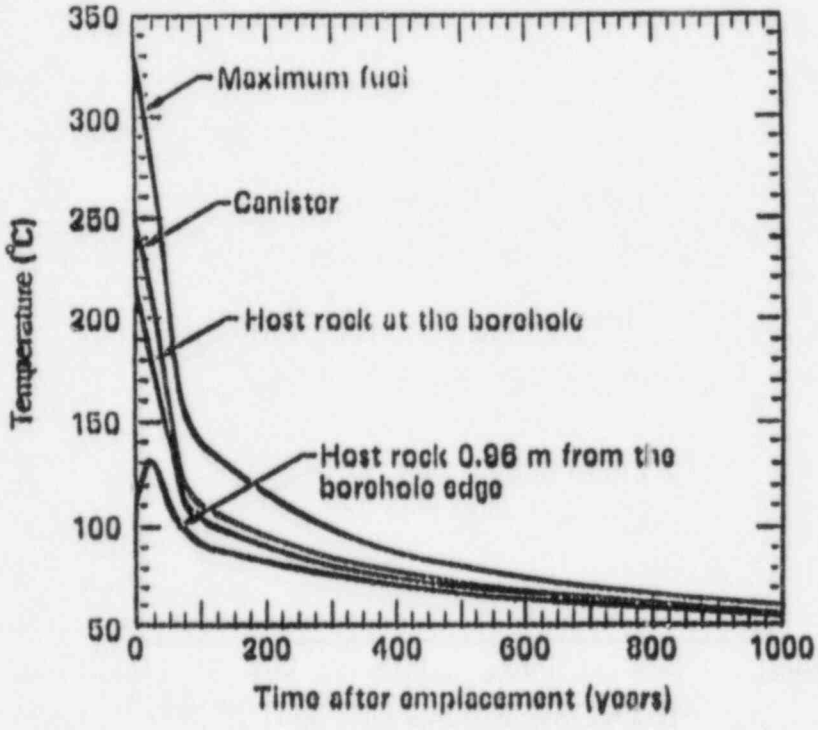


Figure 3.4. Temperature histories of waste package components and host rock for vertically emplaced BWR spent fuel in tuff (UCRL-80820, 1983). (Note that calculations do not assume the presence of packing material.)

It should be noted that the maximum package centerline and canister temperatures that will be experienced by the package will be a function of the diameter of the waste package and power output of the waste form, that is, the design. Thus, the peak temperature can be a critical factor in establishing whether a particular diameter and waste package power is acceptable. Peak centerline temperatures have been calculated by Hockman (1984) assuming six PWR fuel assemblies per container with a package power level of 3.3 kW/canister. Some centerline temperatures that were calculated were in excess of the design maximum of 350°C. Further calculations are in progress assuming four fuel assemblies per container.

3.2.3.4 Irradiation Effects

There do not appear to be any detailed calculations of gamma fluxes for the latest spent fuel waste package designs for tuff which will incorporate a stainless steel container and no metallic overpack (UCID-19926, 1983). In an earlier design study by Westinghouse (ONWI-439, 1983), an iron/steel overpack was considered and the calculated maximum gamma flux was $7.8 \times 10^{6}$ mrem/h. Over a 300-year irradiation period, this will give a total dose of approximately $10^{10}$ rads, assuming for simplicity that this dose rate over the 300-year period decreases linearly to zero.

Since steam conditions will prevail for the first 150 years (UCRL-80820, 1983), reduced radiolytic effects are likely because of efficient recombination reactions among the radiolytic species (SAND81-1677, 1981). As the repository cools, however, and moisture levels increase, there is a likelihood of nitric acid formation because of the formation of nitrogen oxides from $N_2/O_2$ mixtures. These oxides will dissolve in water to give acid. Other radiolytic species which could form are described in Section 3.2.2.4, above.

3.2.3.5 Stress Environment

The porous nature of tuff at the Nevada Test Site precludes pressurization at the repository horizon. Water and steam pressures will be close to atmospheric (UCRL-89988, 1983). Lithostatic stresses on the waste package will be present at the repository horizon if the host rock settles. Based on an average tuff density of 2.2 g/cm$^3$ the lithostatic stress at a depth of 400 m will be approximately 8.6 MPa.

3.2.4 General Listing of Anticipated Waste Package Conditions After Emplacement

Based on the above discussions it is possible to generally predict the corrosion and stress conditions around waste packages in salt, basalt and tuff repositories. These will be strongly dependent on final waste package geometries, designs, and materials selection. Tables 3.7 through 3.9 give semi-quantitative estimates of waste package conditions for the various repositories. These will be used in this effort to evaluate the integrity of spent fuel waste packages.

Table 3.7. List of estimated spent fuel waste package conditions for a salt repository.

| Parameter | Estimated Value | | | |
|---|---|---|---|---|
| | Operations Period | Thermal Period (0-300 yr) | Transition Period (300-1000 yr) | Geologic Control (>1000 yr) |
| Temperature at Centerline (Thermal Loading 12.4 $W/m^2$) | | 375°C max. | Approximately 150-110°C | <110°C |
| Total Gamma Dose (rad) | | $10^9$-$10^{10}$ | Little additional irradiation. | Little additional irradiation. |
| Brine Flow Rate | | Total of about 7 liters per borehole for 24.7 $W/m^2$ thermal loading. | Little additional brine inflow | Little additional brine inflow |
| Brine Chemistry | Brine A or Brine B chemistries depending on repository location. | Brine A or Brine B with significant NaOH levels. | Brine A or Brine B with NaOH present. | |
| pH (measured at 25°C) | Steam/air plus small amounts of $HCl/SO_2/CO_2/H_2S$. | Initially acidic brine (pH ≈3.5) due to dissolution of acid gases. Changing to alkaline brine because of dissolution of colloidal sodium by brine inclusions. pH could rise to 9.5 based on experiments with irradiated salt and deionized water. | Probably alkaline. | Probably alkaline. |
| pH (at high temperature) | | Lower than values measured at 25°C but no reliable values can be specified because of complex hydrothermal reactions and irradiation effects. | | |
| Redox Conditions | Oxic | Probably oxic due to brine radiolysis. | Approaching Anoxic | Probably anoxic. |
| Stress (MPa) | 0.1 | Initially 0.1 MPa, rising to lithostatic stress of 16.2 MPa as host rock settles. | | |

Table 3.8. List of estimated spent fuel waste package conditions for a basalt repository.

| Parameter | Estimated Value | | | |
|---|---|---|---|---|
| | Operations Period | Thermal Period (0-300 yr) | Transition Period (300-1000 yr) | Geologic Control (>1000 yr) |
| Temperature at Centerline (Thermal Loading 13.0 $W/m^2$) | 250°C | 265°C max. after ≈35 yr. | 140-125°C | <125°C |
| Total Gamma Dose (rad) | | $10^7$-$10^8$ | Little additional irradiation. | No additional irradiation. |
| Vertical Hydraulic Conductivity (m/sec.) | | Unknown, but likely to be much greater than that for horizontal flow because of buoyancy effects. | | |
| Water Chemistry | Steam/air. | Significant increases in $K^+$, $Ca^{2+}$, Fe, Si, and $SO_4^{-2}$ in the packing material water at higher temperatures. $F^-$ is reduced in concentration. | | Not known, but there should be a tendency to return to original Grande Ronde water chemistry. |
| pH (measured at 25°C) | | Initially 8.0 in packing material water, decreasing to 6.5-7.5. | Increasing to approximately 9.0. | |
| pH (at high temperatures) | | Lower than values measured at 25°C but no reliable values can be specified because of complex hydrothermal reactions and irradiation effects. | | |
| Redox Conditions | Oxic. | Probably oxic due to water radiolysis. | Approaching anoxic. | Probably anoxic. |
| Stress (MPa) | 0.1 | Initially 0.1 MPa, rising to a value between hydrostatic and lithostatic stresses (11 to 33 MPa). | | |

Table 3.9. List of estimated spent fuel waste package conditions for a tuff repository.

| Parameter | Estimated Value | | | |
|---|---|---|---|---|
| | Operations Period | Thermal Period (0-300 yr) | Transition Period (300-1000 yr) | Geologic Control (>1000 yr) |
| Temperature at Centerline[a] (Thermal Loading 12.4 $W/m^2$) | | 330°C max. to 100°C | 100-60°C | <60°C |
| Total Gamma Dose (rad) | | $\approx 10^{10}$ | Little additional irradiation. | No additional irradiation. |
| Water Flow Rate | Steam/air conditions. | Steam/air for first several hundred years followed by liquid water flowing at about 8 mm/yr. | About 8 mm/yr. | About 8 mm/yr. |
| Water Chemistry | Steam/air conditions. | Probably similar to J-13 well water after steam conditions subside. May be more concentrated than J-13 water if precipitated salts redissolve. | Probably similar to J-13 well water but could be more concentrated if precipitated salts redissolve. | |
| pH (Measured at 25°C) | | 7.1 for J-13 well water. May be acidic because of radiolysis of $N_2/O_2/H_2O$ mixtures. | ≈7.1 | ≈7.1 |
| Redox Conditions | Oxic | Oxic | Oxic | Oxic |
| Stress (MPa) | 0.1 | Initially 0.1 MPa, rising to the lithostatic stress of 8.6 MPa as host rock settles. | | |

[a]Calculations were made for waste package without packing material.

### 3.2.5 Cladding Containment Analysis

#### 3.2.5.1 Inventory of Radionuclides in Spent Fuel

In practically all light water reactors, the fuel designs utilize uranium dioxide fuel enclosed predominantly in Zircaloy cladding. (Some of the cladding materials in fuel rods is made of Types 304, 304L, 316 and 348 stainless steel.) This report will therefore emphasize Zircaloy cladding. The fuel is in the form of cylindrical pellets sintered to a high density (approximately 95% of theoretical). The cladding is a zirconium alloy, Zircaloy-2[2] for boiling water reactors (BWRs) and Zircaloy-4[3] for pressurized water reactors (PWRs). Fuel rods are arranged into assemblies by structural elements (spacer grids, tie plates and fitting devices). The projected cumulative discharge of spent fuel assemblies is shown in Figure 3.5.

In-reactor, the fuel pellets and Zircaloy cladding undergo various and complex changes due to neutron irradiation processes and due to exposure to the pressures and temperatures encountered in the reactor core. After the fuel is spent, it is destined to remain in water storage for periods ranging from several years to decades. This storage phase constitutes a change in the temperatures and pressures encountered by the fuel pellets and Zircaloy and also a change in the predominant radiation environment out-of-reactor. Following removal from storage, the spent fuel will be confined to a repository, where once again it will be subjected to a change in environmental conditions. These changing environments will impact on the ability of the Zircaloy cladding to contain the radioactivity within the rod.

Spent fuel from light water reactors contains all of the long-lived and stable nuclides that result from in-reactor operation of the fuel. See Tables 3.10 and 3.11 for an inventory of nuclides at various times from discharge. These nuclides include isotopes of the noble gases krypton and xenon and also some elements that are readily volatile or that can form readily volatile compounds in certain environments (viz., carbon, hydrogen, and iodine). See Tables 3.12 and 3.13 for an inventory of gases from discharge through the containment period. The presence of gaseous/volatile radionuclides in spent fuel is a special concern when breach of containment of cladding is being considered. Presently there is no stipulated value for the maximum acceptable leak rate from spent fuel that would still allow the cladding to "contain." Minimum values for containment need to be established perhaps based on the inventory sometime after discharge. See Table 3.14 for the proposed EPA cumulative release limits to the accessible environment for 10,000 years after disposal. The possibility of radioactivity leakage during the containment period will

---

[2]Zircaloy-2 has the nominal composition 1.5% Sn, 0.12% Fe, 0.10% Cr, 0.05% Ni, and the balance is Zr.

[3]Zircaloy-4 has the nominal composition 1.5% Sn, 0.20% Fe, 0.10% Cr, less than 0.005% Ni, and the balance is Zr.

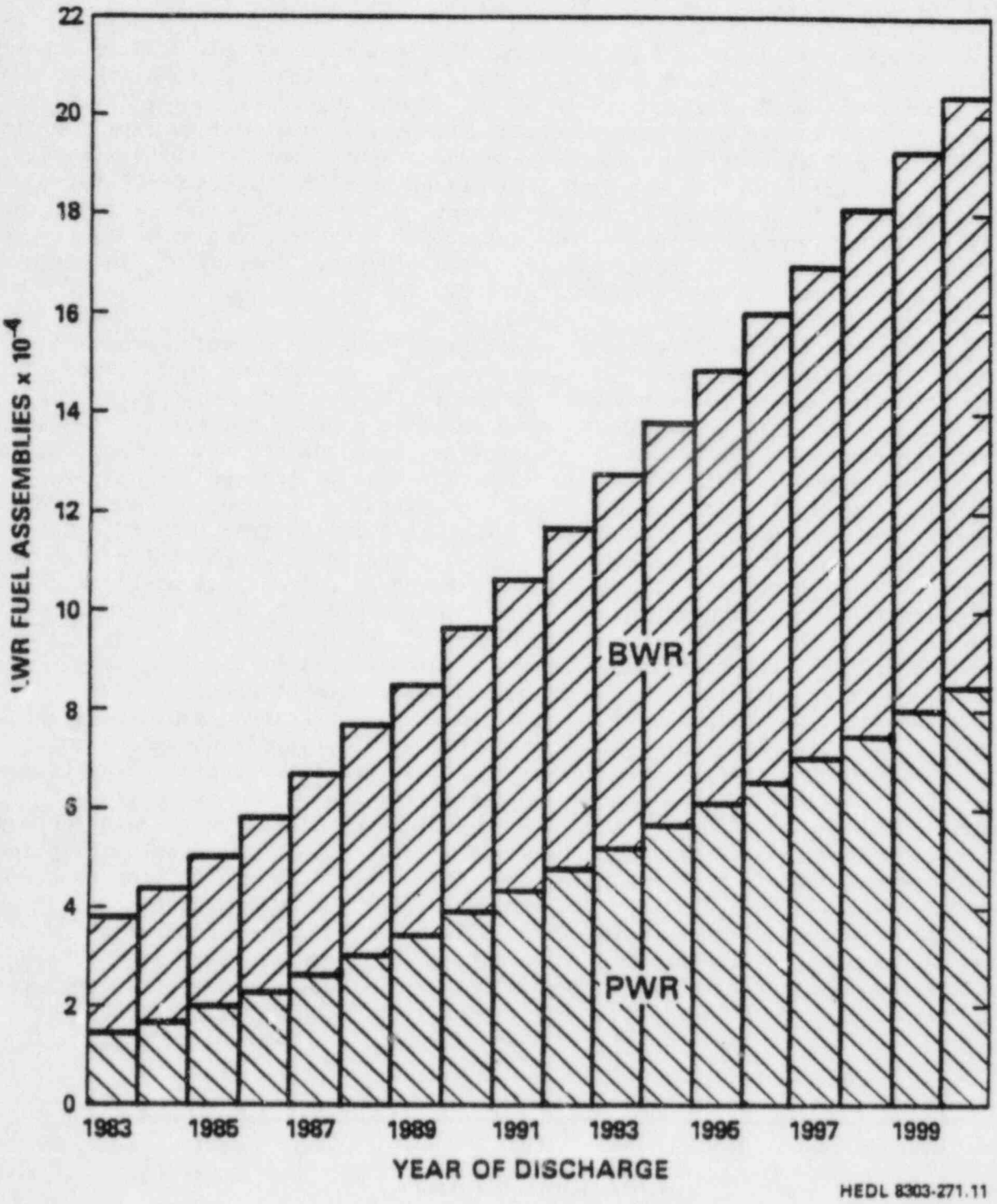


Figure 3.5. Cumulative discharges of spent LWR fuel assemblies (HEDL-TME 83-28, 1983).

## Table 3.10. Activity of radionuclides in a BWR fuel rod irradiated to an average burnup of 27,500 MWd/MTU as a function of age.[a,b]

| 10 Years From Discharge | | 300 Years From Discharge | | 1000 Years From Discharge | | | 10,000 Years From Discharge | |
|---|---|---|---|---|---|---|---|---|
| Nuclide | Activity (Ci) | Nuclide | Activity (Ci) | Nuclide | Activity (Ci) | [Weight (g) in Parentheses] | Nuclide | Activity (Ci) |
| $^{241}Pu$ | 2.013E02 | | | | | | | |
| $^{137}Ce$ | 1.989E02 | | | | | | | |
| $^{137m}Ba$ | 1.881E02 | | | | | | | |
| $^{90}Y$ | 1.419E02 | | | | | | | |
| $^{90}Sr$ | 1.419E02 | | | | | | | |
| $^{147}Pm$ | 2.435E01 | | | | | | | |
| $^{85}Kr$ | 1.177E01 | | | | | | | |
| $^{134}Cs$ | 1.117E01 | | | | | | | |
| $^{154}Eu$ | 1.082E01 | | | | | | | |
| $^{238}Pu$ | 4.732E00 | $^{241}Am$ | 7.210E00 | $^{241}Am$ | 2.351E00 | (7.252E-01) | | |
| $^{241}Am$ | 4.443E00 | $^{240}Pu$ | 1.313E00 | $^{240}Pu$ | 1.222E00 | (5.393E00) | | |
| $^{155}Eu$ | 3.683E00 | | | | | | | |
| $^{125}Sb$ | 3.405E00 | | | | | | | |
| $^{244}Cm$ | 2.051E00 | | | | | | | |
| $^{60}Co$ | 1.776E00 | | | | | | | |
| $^{240}Pu$ | 1.347E00 | | | | | | | |
| $^{106}Ru$ | 1.299E00 | | | | | | | |
| $^{106}Rh$ | 1.299E00 | | | | | | | |
| $^{3}H$ | 1.182E00 | | | | | | | |
| $^{239}Pu$ | 8.619E-01 | $^{239}Pu$ | 8.551E-01 | $^{239}Pu$ | 8.389E-01 | (1.367E01) | $^{239}Pu$ | 6.546E-01 |
| $^{151}Sm$ | 8.524E-01 | $^{238}Pu$ | 4.984E-01 | | | | $^{240}Pu$ | 4.857E-01 |
| $^{129m}Te$ | 8.316E-01 | $^{137}Ce$ | 2.502E-01 | | | | | |
| $^{144}Ce$ | 3.422E-01 | $^{137m}Ba$ | 2.367E-01 | | | | | |
| $^{144}Pr$ | 3.422E-01 | $^{90}Y$ | 1.110E-01 | | | | | |
| $^{63}Ni$ | 3.381E-01 | $^{90}Sr$ | 1.109E-01 | | | | | |
| $^{55}Fe$ | 2.375E-01 | | | | | | | |
| $^{243}Am$ | 3.568E-02 | $^{151}Sm$ | 9.803E-02 | $^{243}Am$ | 3.262E-02 | (1.761E-01) | $^{99}Tc$ | 3.149E-02 |
| $^{239}Np$ | 3.568E-02 | $^{63}Ni$ | 3.803E-02 | $^{239}Np$ | 3.262E-02 | (1.415E-07) | $^{243}Am$ | 1.443E-02 |
| $^{99}Tc$ | 3.254E-02 | $^{243}Am$ | 3.476E-02 | $^{99}Tc$ | 3.243E-02 | (1.902E00) | $^{239}Np$ | 1.443E-02 |
| $^{242}Cm$ | 1.034E-02 | $^{239}Np$ | 3.476E-02 | | | | | |
| | | $^{99}Tc$ | 3.251E-02 | | | | | |
| $^{93}Zr$ | 8.524E-03 | $^{93}Zr$ | 8.522E-03 | $^{93}Zr$ | 8.518E-03 | (3.321E00) | $^{93}Zr$ | 8.462E-03 |
| $^{242}Pu$ | 4.298E-03 | $^{93m}Nb$ | 8.096E-03 | $^{93m}Nb$ | 8.092E-03 | (2.860E-05) | $^{93m}Nb$ | 8.040E-03 |
| $^{14}C$ | 4.176E-03 | $^{234}U$ | 4.497E-03 | $^{234}U$ | 4.670E-03 | (7.543E-01) | $^{234}U$ | 4.576E-03 |
| $^{144m}Pr$ | 4.106E-03 | $^{242}Pu$ | 4.297E-03 | $^{242}Pu$ | 4.292E-03 | (1.100E00) | $^{242}Pu$ | 4.222E-03 |
| $^{93m}Nb$ | 3.948E-03 | $^{14}C$ | 4.032E-03 | $^{14}C$ | 3.705E-03 | (8.307E-04) | $^{237}Np$ | 2.978E-03 |
| $^{121m}Sn$ | 3.357E-03 | $^{242}Cm$ | 2.749E-03 | $^{237}Np$ | 2.511E-03 | (3.559E00) | $^{233}Pa$ | 2.978E-03 |
| $^{234}U$ | 2.968E-03 | $^{59}Ni$ | 2.387E-03 | $^{233}Pa$ | 2.511E-03 | (1.210E-07) | $^{59}Ni$ | 2.195E-03 |
| $^{59}Ni$ | 2.394E-03 | $^{126m}Sb$ | 1.833E-03 | $^{238}Pu$ | 2.383E-03 | (1.370E-04) | $^{126m}Sb$ | 1.714E-03 |
| $^{126m}Sb$ | 1.838E-03 | $^{126}Sn$ | 1.833E-03 | $^{59}Ni$ | 2.373E-03 | (3.130E-02) | $^{126}Sn$ | 1.714E-03 |
| $^{126}Sn$ | 1.838E-03 | $^{237}Np$ | 1.529E-03 | $^{126m}Sb$ | 1.825E-03 | (2.324E-11) | $^{14}C$ | 1.247E-03 |
| $^{119m}Sn$ | 1.150E-03 | $^{233}Pa$ | 1.529E-03 | $^{126}Sn$ | 1.825E-03 | (6.426E-02) | $^{135}Cs$ | 1.034E-03 |
| $^{135}Cs$ | 1.037E-03 | $^{135}Cs$ | 1.037E-03 | $^{135}Cs$ | 1.037E-03 | (1.174E00) | | |
| $^{79}Se$ | 9.860E-04 | $^{79}Se$ | 9.830E-04 | $^{79}Se$ | 9.757E-04 | (1.400E-02) | $^{234m}Pa$ | 9.225E-04 |
| $^{94}Nb$ | 9.344E-04 | $^{94}Nb$ | 9.251E-04 | $^{234m}Pa$ | 9.225E-04 | (1.355E-12) | $^{234}Th$ | 9.225E-04 |
| $^{234m}Pa$ | 9.225E-04 | $^{234m}Pa$ | 9.225E-04 | $^{234}Th$ | 9.225E-04 | (3.983E-08) | $^{238}U$ | 9.225E-04 |
| $^{234}Th$ | 9.225E-04 | $^{234}Th$ | 9.225E-04 | $^{238}U$ | 9.225E-04 | (2.768E03) | $^{79}Se$ | 8.863E-04 |
| $^{238}U$ | 9.225E-04 | $^{238}U$ | 9.225E-04 | $^{94}Nb$ | 9.030E-04 | (4.745E-03) | $^{235}U$ | 8.568E-04 |
| $^{237}Np$ | 7.141E-04 | $^{236}U$ | 6.230E-04 | $^{236}U$ | 6.487E-04 | (1.022E04) | $^{94}Nb$ | 6.608E-04 |
| $^{233}Pa$ | 7.141E-04 | $^{107}Pd$ | 2.760E-04 | $^{151}Sm$ | 5.295E-04 | (2.011E-05) | $^{230}Th$ | 3.822E-04 |
| $^{235}U$ | 6.117E-04 | $^{126}Sb$ | 2.567E-04 | $^{107}Pd$ | 2.760E-04 | (5.778E-01) | $^{210}Bi$ | 2.975E-04 |
| $^{107}Pd$ | 2.760E-04 | $^{241}Pu$ | 2.511E-04 | $^{126}Sb$ | 2.556E-04 | (3.082E-09) | $^{214}Bi$ | 2.975E-04 |
| $^{126}Sb$ | 2.573E-04 | | | $^{63}Ni$ | 1.948E-04 | (3.156E-06) | $^{210}Pb$ | 2.975E-04 |
| $^{153}Gd$ | 1.112E-04 | | | $^{242}Cm$ | 1.129E-04 | (3.400E-08) | $^{214}Pb$ | 2.975E-04 |
| | | | | | | | $^{210}Po$ | 2.975E-04 |
| | | | | | | | $^{214}Po$ | 2.975E-04 |
| | | | | | | | $^{218}Po$ | 2.975E-04 |
| | | | | | | | $^{226}Ra$ | 2.975E-04 |
| | | | | | | | $^{222}Rn$ | 2.975E-04 |
| | | | | | | | $^{107}Pd$ | 2.757E-04 |
| | | | | | | | $^{126}Sb$ | 2.400E-04 |
| $^{54}Mn$ | 9.205E-05 | $^{129}I$ | 7.619E-05 | $^{129}I$ | 7.619E-05 | (4.669E-01) | $^{129}I$ | 7.616E-05 |
| $^{129}I$ | 7.619E-05 | $^{121m}Sn$ | 6.014E-05 | $^{230}Th$ | 3.835E-05 | (1.972E-03) | $^{36}Cl$ | 3.054E-05 |
| $^{36}Cl$ | 3.122E-05 | $^{36}Cl$ | 3.121E-05 | $^{241}Pu$ | 3.770E-05 | (3.351E-07) | $^{241}Am$ | 1.903E-05 |
| $^{93}Mo$ | 2.270E-05 | $^{244}Cm$ | 3.083E-05 | $^{36}Cl$ | 3.116E-05 | (9.656E-04) | $^{241}Pu$ | 1.773E-05 |
| $^{65}Zn$ | 1.044E-05 | $^{93}Mo$ | 2.124E-05 | $^{93}Mo$ | 1.806E-05 | (4.695E-07) | $^{93}Mo$ | 2.257E-06 |
| $^{230}Th$ | 3.175E-07 | $^{230}Th$ | 1.035E-05 | $^{210}Bi$ | 6.990E-06 | (5.833E-11) | $^{238}Pu$ | 4.097E-22 |
| $^{123}Sn$ | 5.052E-09 | $^{214}Bi$ | 6.084E-07 | $^{214}Bi$ | 6.990E-06 | (1.568E-13) | $^{242}Cm$ | 1.698E-22 |
| $^{113m}In$ | 1.294E-09 | $^{214}Pb$ | 6.084E-07 | $^{210}Pb$ | 6.990E-06 | (8.369E-08) | | |
| $^{113}Sn$ | 1.294E-09 | $^{214}Po$ | 6.084E-07 | $^{214}Pb$ | 6.990E-06 | (2.132E-13) | TOTAL | 1.250E00 |
| $^{214}Pb$ | 8.725E-10 | $^{218}Po$ | 6.084E-07 | $^{210}Po$ | 6.990E-06 | (1.555E-09) | | |
| $^{214}Po$ | 8.725E-10 | $^{226}Ra$ | 6.084E-07 | $^{214}Po$ | 6.990E-06 | (2.175E-20) | | |
| $^{210}Po$ | 8.725E-10 | $^{222}Rn$ | 6.084E-07 | $^{218}Po$ | 6.990E-06 | (7.473E-14) | | |
| $^{226}Ra$ | 8.725E-10 | $^{210}Bi$ | 4.943E-07 | $^{226}Ra$ | 6.990E-06 | (7.073E-06) | | |
| $^{222}Rn$ | 8.725E-10 | $^{210}Pb$ | 4.943E-07 | $^{222}Rn$ | 6.990E-06 | (4.539E-11) | | |
| $^{214}Bi$ | 8.725E-10 | $^{210}Po$ | 4.943E-07 | $^{137}Cs$ | 2.497E-08 | (2.868E-10) | | |
| $^{210}Pb$ | 1.130E-10 | $^{3}H$ | 9.440E-08 | $^{137m}Ba$ | 2.362E-08 | (4.390E-17) | | |
| $^{210}Bi$ | 1.130E-10 | $^{85}Kr$ | 8.598E-08 | $^{121m}Sn$ | 3.651E-09 | (9.383E-11) | | |
| $^{210}Po$ | 1.130E-10 | $^{154}Eu$ | 7.428E-10 | $^{90}Sr$ | 3.519E-09 | (2.452E-11) | | |
| $^{95}Nb$ | 1.137E-13 | $^{60}Co$ | 4.495E-17 | $^{90}Y$ | 3.519E-09 | (6.468E-15) | | |
| $^{95}Zr$ | 5.272E-14 | $^{155}Eu$ | 2.342E-18 | $^{244}Cm$ | 7.029E-17 | (8.438E-19) | | |
| $^{160}Tb$ | 1.177E-14 | | | $^{3}H$ | 6.968E-25 | (7.186E-29) | | |
| $^{58}Co$ | 9.560E-16 | TOTAL | 1.088E01 | $^{85}Kr$ | 1.973E-27 | (5.062E-30) | | |
| $^{91}Y$ | 3.586E-16 | | | | | | | |
| $^{95m}Nb$ | 4.963E-17 | | | TOTAL | 4.562E00 | | | |
| $^{89}Sr$ | 1.130E-18 | | | | | | | |
| $^{103m}Rh$ | 5.006E-25 | | | | | | | |
| $^{103}Ru$ | 5.002E-25 | | | | | | | |
| TOTAL | 9.597E02 | | | | | | | |

[a]This table is adapted from ORIGEN-2 calculated values presented in ORNL/TM-6008 (1977) for an 8 x 8 assembly assumed to contain 63 rods.
[b]Nuclides are listed in order of decreasing activity. Activity due to $^{235}U$ is not included in this table. It is estimated to be 4.623E-05 Ci per fuel rod.

## Table 3.11. Activity of radionuclides in a PWR fuel rod irradiated to an average burnup of 33,000 MWd/MTU as a function of age.[a,b]

| 10 Years From Discharge | | 300 Years From Discharge | | 1000 Years From Discharge | | | 10,000 Years From Discharge | |
|---|---|---|---|---|---|---|---|---|
| Nuclide | Activity (Ci) | Nuclide | Activity (Ci) | Nuclide | Activity (Ci) | [Weight (g) in Parentheses] | Nuclide | Activity (Ci) |
| $^{137}$Cs | 1.863E02 | | | | | | | |
| $^{137m}$Ba | 1.763E02 | | | | | | | |
| $^{241}$Pu | 1.749E02 | | | | | | | |
| $^{90}$Y | 1.338E02 | | | | | | | |
| $^{90}$Sr | 1.338E02 | | | | | | | |
| $^{147}$Pm | 2.199E01 | | | | | | | |
| $^{134}$Cs | 1.208E01 | | | | | | | |
| $^{85}$Kr | 1.122E01 | | | | | | | |
| $^{154}$Eu | 1.073E01 | | | | | | | |
| $^{238}$Pu | 4.907E00 | $^{241}$Am | 6.221E00 | $^{241}$Am | 2.029E00 | (6.258E-01) | | |
| $^{60}$Co | 4.763E00 | $^{240}$Pu | 1.130E00 | $^{240}$Pu | 1.051E00 | (4.638E00) | | |
| $^{241}$Am | 3.794E00 | | | | | | | |
| $^{155}$Eu | 3.704E00 | | | | | | | |
| $^{125}$Sb | 2.964E00 | | | | | | | |
| $^{244}$Cm | 2.371E00 | | | | | | | |
| $^{63}$Ni | 1.392E00 | | | | | | | |
| $^{106}$Rh | 1.333E00 | | | | | | | |
| $^{106}$Ru | 1.333E00 | | | | | | | |
| $^{240}$Pu | 1.157E00 | | | | | | | |
| $^{3}$H | 1.052E00 | | | | | | | |
| $^{55}$Fe | 8.765E-01 | $^{239}$Pu | 6.926E-01 | $^{239}$Pu | 6.799E-01 | (1.108E01) | $^{239}$Pu | 5.314E-01 |
| $^{151}$Sm | 8.015E-01 | $^{238}$Pu | 5.157E-01 | | | | $^{240}$Pu | 4.179E-01 |
| $^{125m}$Te | 7.239E-01 | $^{137}$Cs | 2.345E-01 | | | | | |
| $^{239}$Pu | 6.980E-01 | $^{137m}$Ba | 2.218E-01 | | | | | |
| $^{144}$Ce | 3.719E-01 | $^{63}$Ni | 1.565E-01 | | | | | |
| $^{144}$Pr | 3.719E-01 | $^{90}$Sr | 1.048E-01 | | | | | |
| | | $^{90}$Y | 1.048E-01 | | | | | |
| $^{243}$Am | 3.738E-02 | $^{151}$Sm | 9.221E-02 | $^{243}$Am | 3.417E-02 | (1.845E-01) | $^{99}$Tc | 2.905E-02 |
| $^{239}$Np | 3.738E-02 | $^{243}$Am | 3.641E-02 | $^{239}$Np | 3.417E-02 | (1.482E-07) | $^{241}$Am | 1.512E-02 |
| $^{99}$Tc | 3.003E-02 | $^{239}$Np | 3.641E-02 | $^{99}$Tc | 2.993E-02 | (1.755E00) | $^{239}$Np | 1.512E-02 |
| $^{59}$Ni | 1.038E-02 | $^{99}$Tc | 3.000E-02 | $^{59}$Ni | 1.029E-02 | (1.357E-01) | | |
| | | $^{59}$Ni | 1.035E-02 | | | | | |
| $^{242}$Cm | 7.603E-03 | $^{93}$Zr | 7.092E-03 | $^{93}$Zr | 7.092E-03 | (2.766E00) | $^{59}$Ni | 9.520E-03 |
| $^{93}$Zr | 7.097E-03 | $^{93m}$Nb | 6.739E-03 | $^{93m}$Nb | 6.738E-03 | (2.382E-05) | $^{93}$Zr | 7.045E-03 |
| $^{144}$Pr | 4.463E-03 | $^{234}$U | 4.237E-03 | $^{234}$U | 4.416E-03 | (7.133E-01) | $^{93m}$Nb | 6.691E-03 |
| $^{242}$Pu | 4.066E-03 | $^{242}$Pu | 4.064E-03 | $^{242}$Pu | 4.059E-03 | (1.041E00) | $^{234}$U | 4.324E-03 |
| $^{14}$C | 3.355E-03 | $^{14}$C | 3.239E-03 | $^{14}$C | 2.976E-03 | (6.673E-04) | $^{242}$Pu | 3.994E-03 |
| $^{93m}$Nb | 3.237E-03 | $^{94}$Nb | 3.028E-03 | $^{94}$Nb | 2.955E-03 | (1.553E-02) | $^{237}$Np | 2.664E-03 |
| $^{94}$Nb | 3.059E-03 | $^{242}$Cm | 2.021E-03 | $^{238}$Pu | 2.386E-03 | (1.371E-04) | $^{233}$Pa | 2.664E-03 |
| $^{234}$U | 2.654E-03 | $^{126m}$Sb | 1.750E-03 | $^{237}$Np | 2.261E-03 | (3.205E00) | $^{94}$Nb | 2.163E-03 |
| $^{126m}$Sb | 1.753E-03 | $^{126}$Sn | 1.750E-03 | $^{233}$Pa | 2.261E-03 | (1.089E-07) | $^{126m}$Sb | 1.636E-03 |
| $^{126}$Sn | 1.753E-03 | $^{237}$Np | 1.413E-03 | $^{126}$Sn | 1.742E-03 | (6.134E-02) | $^{126}$Sn | 1.636E-03 |
| | | $^{233}$Pa | 1.413E-03 | $^{126m}$Sb | 1.741E-03 | (2.217E-11) | $^{14}$C | 1.002E-03 |
| $^{79}$Se | 9.255E-04 | $^{79}$Se | 9.225E-04 | $^{79}$Se | 9.157E-04 | (1.314E-02) | $^{135}$Cs | 8.377E-04 |
| $^{135}$Cs | 8.402E-04 | $^{135}$Cs | 8.402E-04 | $^{135}$Cs | 8.402E-04 | (9.510E-01) | $^{79}$Se | 8.319E-04 |
| $^{234m}$Pa | 7.113E-04 | $^{234m}$Pa | 7.113E-04 | $^{63}$Ni | 8.025E-04 | (1.300E-05) | $^{235}$U | 7.794E-04 |
| $^{234}$Th | 7.113E-04 | $^{234}$Th | 7.113E-04 | $^{234m}$Pa | 7.113E-04 | (1.045E-12) | $^{234m}$Pa | 7.113E-04 |
| $^{238}$U | 7.113E-04 | $^{238}$U | 7.113E-04 | $^{234}$Th | 7.113E-04 | (3.071E-08) | $^{234}$Th | 7.113E-04 |
| $^{237}$Np | 7.108E-04 | $^{236}$U | 5.784E-04 | $^{238}$U | 7.113E-04 | (2.134E03) | $^{238}$U | 7.113E-04 |
| $^{233}$Pa | 7.108E-04 | $^{107}$Pd | 2.540E-04 | $^{236}$U | 6.005E-04 | (9.461E00) | $^{230}$Th | 3.612E-04 |
| $^{236}$U | 5.686E-04 | $^{126}$Sl | 2.450E-04 | $^{151}$Sm | 4.985E-04 | (1.893E-05) | $^{210}$Bi | 2.810E-04 |
| $^{119m}$Sn | 4.904E-04 | $^{241}$Pu | 2.332E-04 | $^{107}$Pd | 2.539E-04 | (5.315E-01) | $^{214}$Bi | 2.810E-04 |
| $^{107}$Pd | 2.540E-04 | | | $^{126}$Sb | 2.438E-04 | (2.940E-09) | $^{210}$Pb | 2.810E-04 |
| $^{126}$Sb | 2.455E-04 | | | | | | $^{214}$Pb | 2.810E-04 |
| | | | | | | | $^{210}$Po | 2.810E-04 |
| | | | | | | | $^{218}$Po | 2.810E-04 |
| | | | | | | | $^{222}$Rn | 2.810E-04 |
| | | | | | | | $^{226}$Ra | 2.810E-04 |
| | | | | | | | $^{107}$Pd | 2.537E-04 |
| | | | | | | | $^{126}$Sb | 2.291E-04 |
| $^{129}$I | 7.078E-05 | $^{129}$I | 7.078E-05 | $^{242}$Cm | 8.304E-05 | (2.500E-08) | $^{129}$I | 7.074E-05 |
| $^{93}$Mo | 6.828E-05 | $^{93}$Mo | 6.387E-05 | $^{129}$I | 7.078E-05 | (4.337E-01) | $^{36}$Cl | 2.457E-05 |
| $^{59}$Mn | 5.225E-05 | $^{244}$Cm | 3.563E-05 | $^{93}$Mo | 5.431E-05 | (1.412E-06) | $^{241}$Am | 2.321E-05 |
| $^{36}$Cl | 2.513E-05 | $^{36}$Cl | 2.511E-05 | $^{241}$Pu | 4.698E-05 | (4.176E-07) | $^{241}$Pu | 2.208E-05 |
| $^{65}$Zn | 1.014E-05 | $^{230}$Th | 9.608E-06 | $^{230}$Th | 3.607E-05 | (1.854E-03) | $^{93}$Mo | 6.789E-06 |
| $^{230}$Th | 2.715E-07 | $^{214}$Bi | 5.598E-07 | $^{36}$Cl | 2.507E-05 | (7.769E-04) | $^{238}$Pu | 3.012E-22 |
| $^{123}$Sn | 2.198E-09 | $^{214}$Pb | 5.598E-07 | $^{210}$Bi | 6.549E-06 | (5.277E-11) | $^{242}$Cm | 1.248E-22 |
| $^{214}$Bi | 7.142E-10 | $^{214}$Po | 5.598E-07 | $^{214}$Bi | 6.549E-06 | (1.469E-13) | | |
| $^{214}$Pb | 7.142E-10 | $^{218}$Po | 5.598E-07 | $^{210}$Pb | 6.549E-06 | (7.841E-08) | TOTAL | 1.061E00 |
| $^{214}$Po | 7.142E-10 | $^{226}$Ra | 5.598E-07 | $^{214}$Pb | 6.549E-06 | (1.998E-13) | | |
| $^{218}$Po | 7.142E-10 | $^{222}$Rn | 5.598E-07 | $^{210}$Po | 6.549E-06 | (1.457E-09) | | |
| $^{226}$Ra | 7.142E-10 | $^{210}$Bi | 4.539E-07 | $^{214}$Po | 6.549E-06 | (2.038E-20) | | |
| $^{222}$Rn | 7.142E-10 | $^{210}$Pb | 4.539E-07 | $^{218}$Po | 6.549E-06 | (2.317E-14) | | |
| $^{113m}$In | 5.417E-10 | $^{210}$Po | 4.943E-07 | $^{226}$Ra | 6.549E-06 | (6.627E-06) | | |
| $^{113}$Sn | 5.412E-10 | $^{3}$H | 8.408E-08 | $^{222}$Rn | 6.549E-06 | (4.253E-11) | | |
| $^{210}$Bi | 8.779E-11 | $^{85}$Kr | 8.201E-08 | $^{137}$Cs | 2.342E-08 | (2.690E-10) | | |
| $^{210}$Pb | 8.779E-11 | $^{154}$Eu | 7.417E-10 | $^{137m}$Ba | 2.215E-08 | (4.116E-17) | | |
| $^{210}$Po | 8.779E-11 | $^{60}$Co | 1.205E-16 | $^{90}$Y | 3.325E-09 | (6.111E-15) | | |
| $^{95}$Nb | 1.190E-13 | $^{155}$Eu | 2.357E-18 | $^{90}$Sr | 3.324E-09 | (2.316E-11) | | |
| $^{95}$Zr | 5.691E-14 | | | $^{244}$Cm | 8.123E-17 | (9.749E-19) | | |
| $^{58}$Co | 5.873E-15 | TOTAL | 9.632E00 | $^{3}$H | 6.207E-25 | (6.407E-29) | | |
| $^{95}$Nb | 3.698E-15 | | | $^{85}$Kr | 1.882E-27 | (4.828E-30) | | |
| $^{91}$Y | 4.073E-16 | | | | | | | |
| $^{89}$Sr | 1.282E-18 | | | TOTAL | 3.914E00 | | | |
| $^{103m}$Rh | 5.843E-25 | | | | | | | |
| $^{103}$Ru | 5.838E-25 | | | | | | | |
| TOTAL | 8.941E02 | | | | | | | |

[a]This table is adapted from ORIGEN-2 calculated values presented in ORNL/TM-6008 (1977) for an 15 x 15 assembly assumed to contain 204 rods.
[b]Nuclides are liated in order of decreasing activity. Activity due to $^{235}$U is not included in this table. It is estimated to be ≈3.871E-05 Ci per fuel rod.

Table 3.12. Amount and activity of gases produced in a BWR fuel rod irradiated to an average burnup of 27,500 MWd/MTU as a function of age.[a]

| Gas | At Discharge | | 300 Years After Discharge | |
|---|---|---|---|---|
| | Weight (g) | Activity (Ci) | Weight (g) | Activity (Ci) |
| $H_2$ | 2.153E-04[b] | 2.076E00($^{3}$H) | 9.792E-12[b] | 9.440E-08($^{3}$H) |
| He | 7.006E-04[c] | --- | 3.133E-02[c] | --- |
| $Cl_2$ | 9.731E-04[d] | 3.124E-05($^{36}$Cl) | 9.722E-04[d] | 3.121E-05($^{36}$Cl) |
| $Br_2$ | 5.257E-02[b] | N.R.[f] | 5.259E-02[b] | N.R.[f] |
| Kr | 8.892E-01[b] | 2.244E01($^{85}$Kr) | 8.317E-01[b] | 8.598E-08($^{85}$Kr) |
| $I_2$ | 5.805E-01[b] | 7.527E-05($^{129}$I) | 5.705E-01[b] | 7.619E-05($^{129}$I) |
| Xe | 1.294E01[b] | N.R.[f] | 1.272E01[b] | N.R.[f] |
| Cs | 6.784E00[b,e] | 3.230E02($^{134}$Cs) | 3.676E00[b,e] | 7.619E-05($^{135}$Cs) |
| | | 1.035E-03($^{135}$Cs) | | 2.502E-01($^{137}$Cs) |
| | | 2.503E02($^{137}$Cs) | | |
| Rn | 3.944E-15[b] | 4.754E-11($^{222}$Rn) | 3.952E-12[b] | 6.084E-07($^{222}$Rn) |
| TOTAL | | 5.978E02[g,h] | | 2.504E-01[i] |

[a]This table is adapted from ORIGEN-2 calculated values presented in ORNL/TM-6008 (1977) for a 8 x 8 assembly assumed to contain 63 rods. All volatile materials, such as $^{125m}$Te and $^{14}$C, have not been included. For example, ≈8.0E-05 moles of $^{14}$C are produced as fission and activation products. Some of this may be present in the form of gaseous compounds.

[b]Weight shown includes weight of all isotopes present.

[c]This is the amount of He produced. It does not include He added during manufacture.

[d]$^{36}$Cl is formed as an activation product. Weight shown is only for $^{36}$Cl.

[e]Cs is a volatile fission product. The vapor pressure P (in torr) of Cs in the range 200-350°C can be calculated using the formula:

$$\log_{10} P = \frac{3833}{T(\text{in K})} + 6.949.$$

[f]N.R. indicates not reported.

[g]This activity represents ≈0.15% of the inventory at discharge.

[h]Total activity at 10 years from discharge due to these elements is 2.230E02 Ci. This represents ≈23.2% of the inventory 10 years after discharge.

[i]This activity represents ≈2.30% of the inventory 300 years after discharge.

Table 3.13. Amount and activity of gases produced in a PWR fuel rod irradiated to an average burnup of 33,000 MWd/MTU as a function of age.[a]

| Gas | At Discharge Weight (g) | At Discharge Activity (Ci) | 300 Years After Discharge Weight (g) | 300 Years After Discharge Activity (Ci) |
|---|---|---|---|---|
| $H_2$ | 1.918E-04[b] | 1.849E00($^{3}$H) | 8.722-E12[b] | 8.408E-08($^{3}$H) |
| He | 5.103E-04[c] | --- | 2.781E-02[c] | --- |
| $Cl_2$ | 7.828E-04[d] | 2.513E-05($^{36}$Cl) | 7.828E-04[d] | 2.511E-05($^{36}$Cl) |
| $Br_2$ | 4.897E-02[b] | N.R.[f] | 4.898E-02[b] | N.R.[f] |
| Kr | 8.348E-01[b] | 2.141E01($^{85}$Kr) | 7.799E-01[b] | 8.201E-08($^{85}$Kr) |
| $I_2$ | 5.422E-01[b] | 6.971E-05($^{129}$I) | 5.309E-01[b] | 7.078E-05($^{129}$I) |
| Xe | 1.199E01[b] | N.R.[f] | 1.199E01[b] | N.R.[f] |
| Cs | 6.221E00[b,e] | 3.494E02($^{134}$Cs) | 3.277E00[b,e] | --- |
| | | 8.387E-04($^{135}$Cs) | | 8.402E-04($^{135}$Cs) |
| | | 2.346E02($^{137}$Cs) | | 2.345E-01($^{137}$Cs) |
| Rn | 2.632E-15[b] | 2.879E-11($^{222}$Rn) | 3.636E-12[b] | 5.598E-07($^{222}$Rn) |
| TOTAL | | 6.073E02[g,h] | | 2.354E-01[i] |

[a]This table is adapted from ORIGEN-2 calculated values presented in ORNL/TM-6008 (1977) for a 15 x 15 assembly assumed to contain 204 rods. All volatile materials, such as $^{125m}$Te and $^{14}$C, have not been included. For example, ≈6.0E-05 moles of $^{14}$C are produced as fission and activation products. Some of this may be present in the form of gaseous compounds.

[b]Weight shown includes weight of all isotopes present.

[c]This is the amount of He produced. It does not include He added during manufacture.

[d]$^{36}$Cl is formed as an activation product. Weight shown is only for $^{36}$Cl.

[e]Cs is a volatile fission product. The vapor pressure P (in torr) of Cs in the range 200-350°C can be calculated using the formula:

$$\log_{10} P = \frac{3833}{T(\text{in K})} + 6.949.$$

[f]N.R. indicates not reported.

[g]This activity represents ≈0.13% of the inventory at discharge.

[h]Total activity at 10 years from discharge due to these elements is 2.107E02 Ci. This represents ≈23.6% of the inventory 10 years after discharge.

[i]This activity represents ≈2.44% of the inventory 300 years after discharge.

depend on several factors (1) gas tightness of the fuel rod, (2) amount of radioactive gas produced (i.e. extent of burnup) and amount released from the fuel matrix into the plenum and not reacted with other materials and (3) relative pressures of gases inside and outside the fuel rod (ORNL-5578, 1979). In the discussion that follows, corrosion mechanisms that would allow leakage of the radioactive gases or leaching of fuel pellets by water entering through cracks or pits in Zircaloy cladding are emphasized. It should be noted in the discussion on failed rods below that most of the gas in the fuel cladding gap has been released in a reactor and would not be available for release in a repository.

Table 3.14. Release limits for containment requirement of the disposal system as specified in proposed 40 CFR 191.

| Radionuclide[a] | Cumulative Release to Accessible Environment for 10,000 Years After Disposal in Ci/kg HM[b] |
|---|---|
| $^{225}Ra$ | 3E-06 |
| $^{243}Am$ | 4E-06 |
| $^{241}Am$ | 1E-05 |
| Other alpha-emitting radionuclides: | 1E-05 |
| $^{237}Np$ | 2E-05 |
| $^{126}Sn$ | 8E-05 |
| $^{90}Sr$ | 8E-05 |
| $^{239}Pu$ | 1E-04 |
| $^{240}Pu$ | 1E-04 |
| $^{242}Pu$ | 1E-04 |
| $^{14}C$ | 1E-04 |
| $^{238}Pu$ | 4E-04 |
| $^{137}Cs$ | 5E-04 |
| Other non-alpha-emitting radionuclides: | 5E-04 |
| $^{135}Cs$ | 2E-03 |
| $^{99}Tc$ | 1E-02 |

[a]Nuclides are listed in order of least to most cumulative release limit.
Releases are given in Ci/kg HM. In the proposed 40 CFR 191, they are given in Ci/MTHM.

[b]Sum of fractions rule is to be applied if a mixture of radionuclides is present in the waste.

A study by Fish and Einziger (HEDL-TME 81-3, 1981) suggested that Kr, Xe and He are the only gases released from the fuel rod in significant quantities as a result of cladding breach. Based on an estimate of $75 \times 10^3$ MTU/repository and 1% gas release from the fuel pellets, the data in Figure 3.6 indicate that if all the rods in the repository were simultaneously breached after 200 years, ≈7.5 Ci would be released.

Our calculations (see Tables 3.12 and 3.13) show that based on the content derived from the ORIGEN calculation presented in ORNL/TM-6008 (1977) the gaseous or volatile elements comprise ≈23% of the inventory 10 years after discharge and ≈2% of the inventory 300 years after discharge. Assuming 10% of these gaseous/volatile materials are available in the plenum, a very conservative assumption, this would make 2.3%-0.2% of the inventory readily available if the cladding is breached after discharge and during the containment period. If we assume that only 1% of the gas is available for release to the repository, the percentage of inventory in the plenum would range from 0.2% to 0.02%. Recent work (PNL-5109, 1984) has indicated that the release of Xe and Kr from spent PWR fuel pellets is in the range 0.2-0.3%; i.e. less than 1%. See Section 3.2.5.4.1 below for further discussion. Whether releases to the environment of this amount of activity constitute breach of containment will have to be determined.

### 3.2.5.2 Loss of Containment in Reactor

#### 3.2.5.2.1 Failure Rate of Fuel Assemblies

The integrity of the fuel rod cladding and the internal conditions of the fuel rods established during their reactor residence are of particular importance as regards disposal in a repository. If the cladding is failed in-reactor, the following will occur: (1) release of gases, mainly Kr and Xe, (2) leaching/dissolution of the fuel pellets in the presence of water, and (3) oxidation of the fuel, with resulting expansion.

In the inventory of spent LWR fuel, one can estimate that the cladding of at least one fuel rod in each $10^4$ rods (0.01%) has failed in-reactor (HEDL-TME 83-28, 1983). Earlier BWR failure rates approached 1%. Fuel failures are ultimately identified and isolated either by visual means in the case of relatively large defects or by techniques such as sipping, the detection of the activity increase outside a fuel rod due to the release of fission products. Other techniques include gamma scanning, mensural, eddy current, and ultrasonic. In the case of BWR fuel assemblies, sipping can be performed either in-core or out-of-core, whereas PWR fuel assemblies are normally sipped out-of-core. It should be noted that sipping indicates solely that a fuel assembly contains one or more failed fuel rods. The identification of individual failures can be accomplished only when individual rods can be removed from the assembly and sipped separately. This is seldom done. Values for failure fraction should be considered to be estimates and do not arise from precise determinations of the number of failed fuel rods.

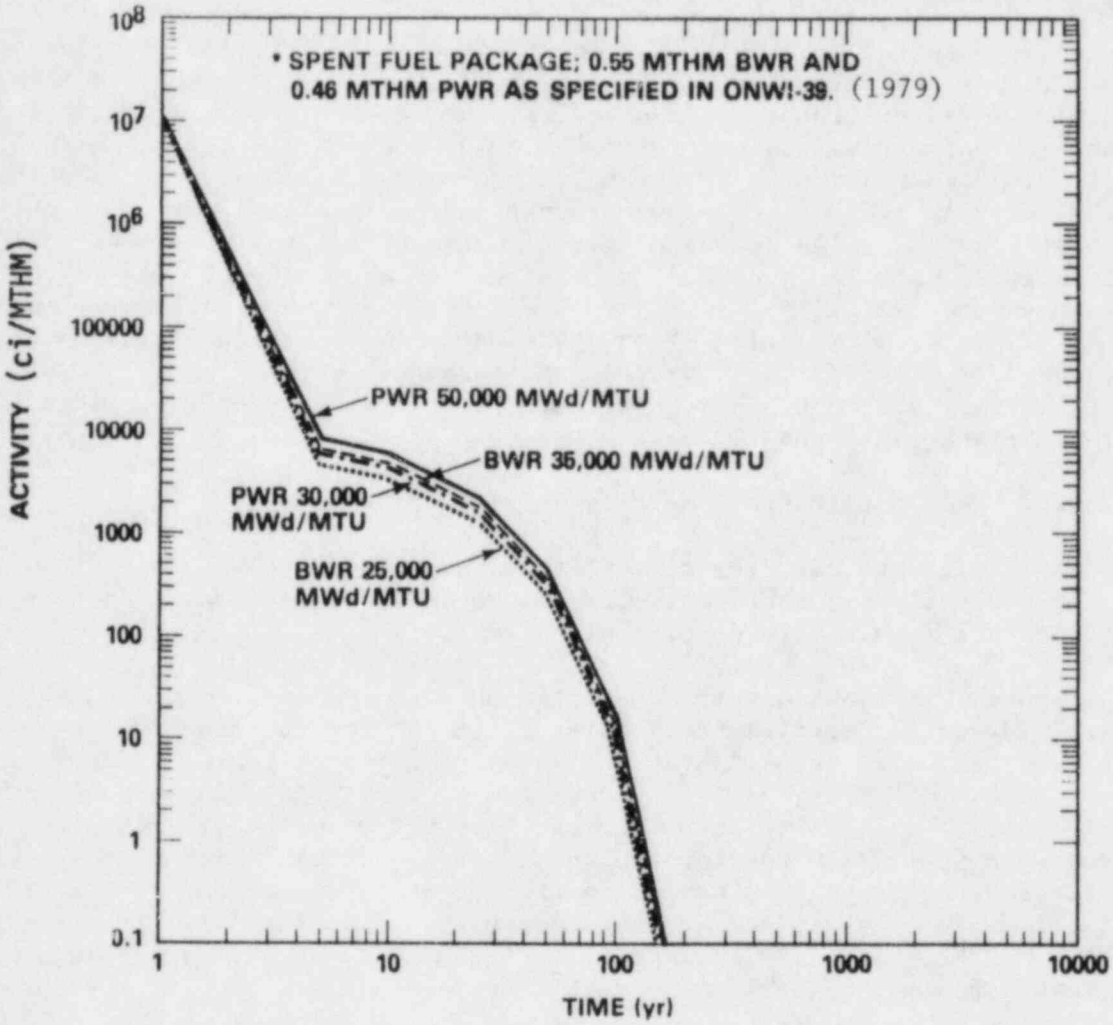


Figure 3.6. Total krypton and xenon activity as a function of time in spent fuel packages (HEDL-TME 81-3, 1981).

Mechanisms by which pre-storage cladding degradation has occurred include hydriding, pellet-cladding interaction, water-side corrosion, cladding collapse, and fretting. In those fuel rods in which cladding penetrations occur, localized hydriding leads first to blistering and then cladding cracks as a result of the lower density of the hydride. The greatest susceptibility for localized hydriding seems to be shown by welds and the surrounding heat-affected areas. The hydriding phenomenon has been eliminated by drying the $UO_2$ pellets prior to their insertion into the Zircaloy cladding. Pellet-cladding interaction is manifested by stress-corrosion cracking of the cladding starting on its inner surface. Because it requires the presence of aggressive gases, it occurs at the locations of pellet-pellet interfaces and transverse cracks through which fission products can reach the cladding. Less than 0.002% of failures have resulted from water-side corrosion. The blockage of heat flow by corrosion layers or by "crud" deposits (e.g. in early BWRs) results in higher Zircaloy temperatures and corrosion rates. See Section 3.2.5.2.2 below for a discussion of crud-induced localized corrosion (CILC). Although cladding collapse has affected a significant number of PWR fuel rods, it is reported that only a small percentage of the collapsed rods released fission product activity (see Figure 3.7). It has been totally eliminated since 1973 by pressurization of the PWR fuel rods. Fretting failures which are caused by flow-induced vibration are responsible for less than 0.01% of the failures. Graphs of average failure levels due to specific causes are shown in Figures 3.8 and 3.9.

3.2.5.2.2 Radioactive Crud Deposits on Fuel Rods

As part of the cladding containment analysis, contamination of the cladding by activation products, fission products, and transuranics was considered as a possible form of breach of containment.

Figure 3.10 shows a thin $ZrO_2$ layer on a fuel rod surface and other superficial oxide deposits (crud layers). [Post-reactor examination has shown that external cladding oxidation thickness ranges from 1.3 μm to 27.9 μm, depending on the alloy, operating conditions, and time in core (HEDL-TME 79-20, 1980).] The deposits form from circulating corrosion products that either dissolve or spall from reactor coolant system surfaces. Since the deposits are exposed to a neutron flux, a fraction of the atoms become radioactive and activation products are formed. The deposits are principally mixed oxides of Fe, Cr, and Ni, with smaller amounts of Co, Mn, Zn and W. See Table 3.15 for the most important activation product isotopes that are carried into spent fuel pools.

The second type of radioactivity found on spent fuel arises from fission products that enter the system because of fuel cladding defects. Soluble fission products circulate in the reactor coolant and some adsorb on the fuel surfaces, particularly on the crud layers. These may desorb upon contact with water. See Table 3.16 for a list of the principal fission products transported to spent fuel pools by mixing with reactor coolant or desorption from spent fuel assembly surfaces. At the time of disposal in a repository, these

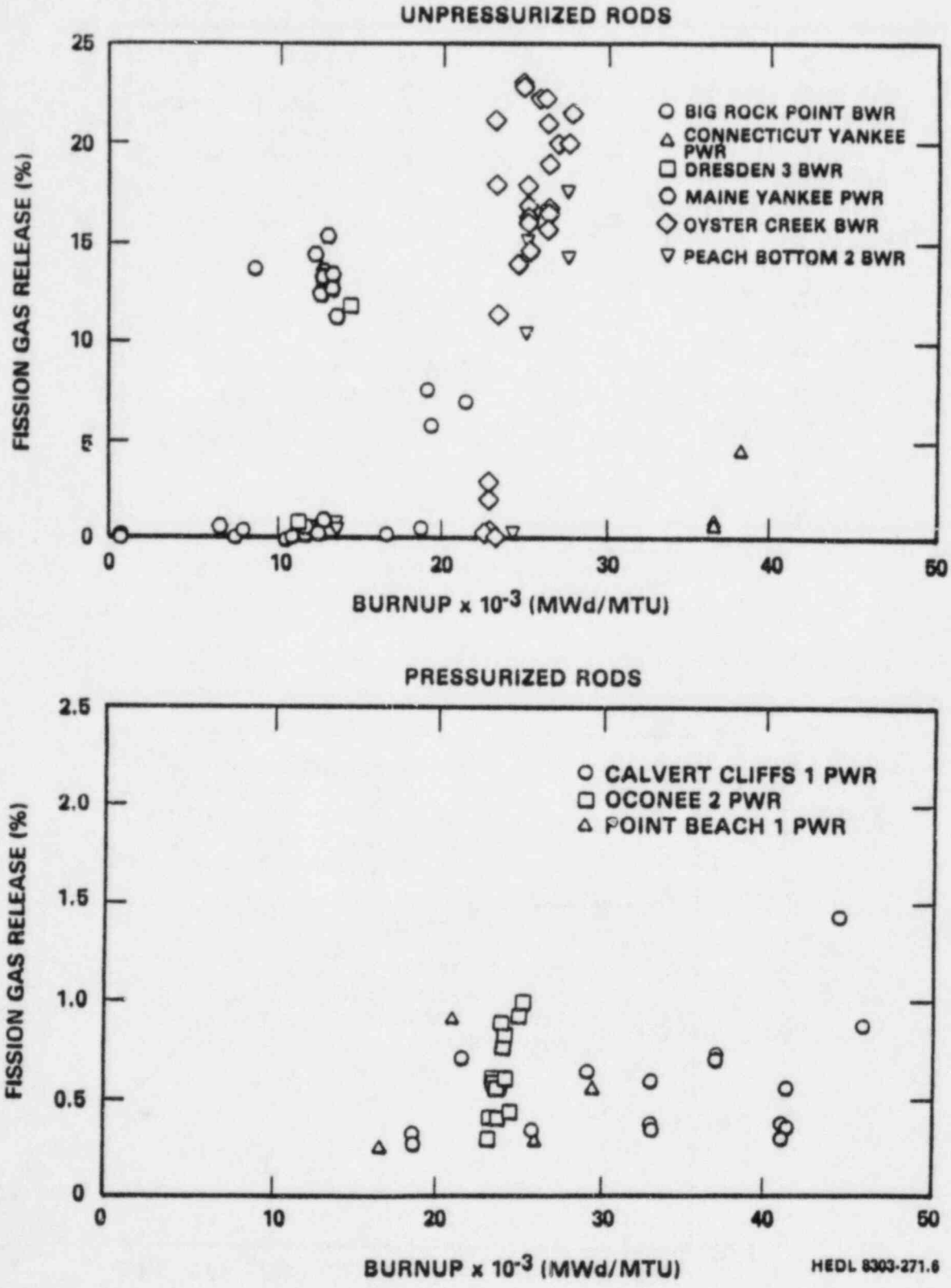


Figure 3.7. Comparison of fission gas release from unpressurized and pressurized LWR fuel rods (HEDL-TME 83-28, 1983).

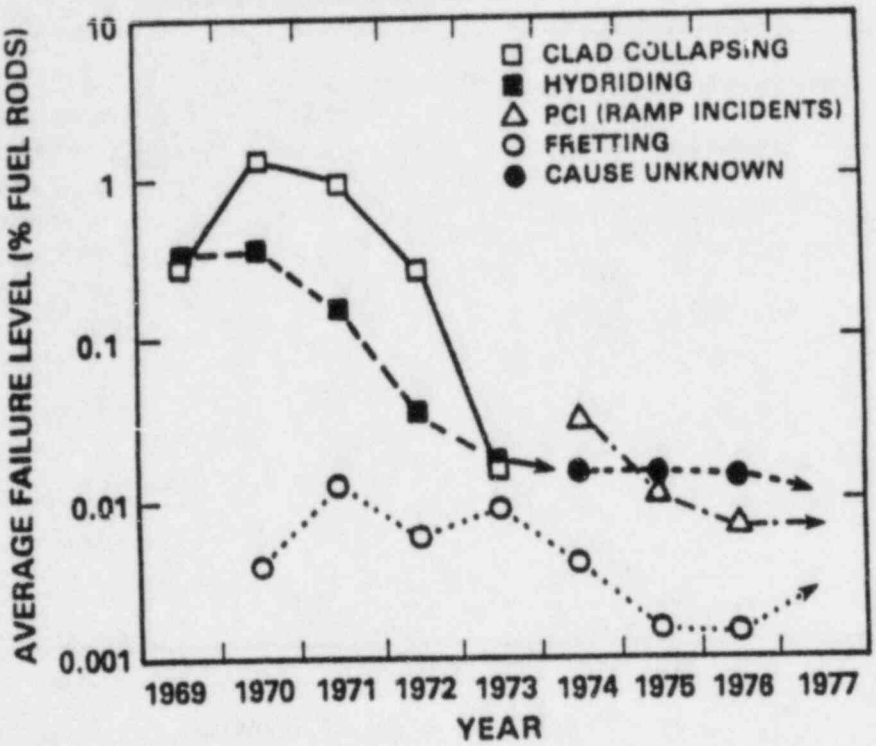


Figure 3.8. Fuel rod failures in PWR plants (Garzarolli, F., 1979).

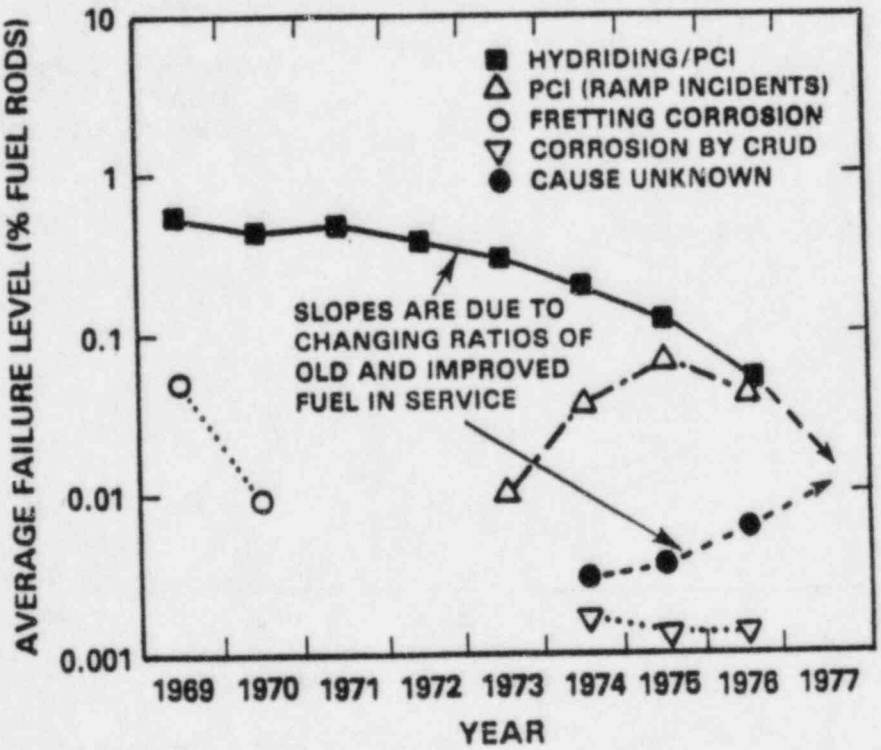


Figure 3.9. Fuel rod failures in BWR plants (Garzarolli, F., 1979).

Table 3.15. Principal activation products released from fuel assemblies during pool storage (IAEA-218, 1982).

| Nuclide | Half-life |
|---|---|
| $^{184}W$[a] | 24 hours |
| $^{65}Ni$[a] | 2.5 days |
| $^{51}Cr$ | 28 days |
| $^{59}Fe$ | 45 days |
| $^{58}Co$ | 72 days |
| $^{65}Zn$ | 243 days |
| $^{54}Mn$ | 310 days |
| $^{60}Co$ | 5.3 years |

[a]Only significant in at-reactor pools.

Table 3.16. Principal fission products released to spent fuel pool waters (IAEA-218, 1982).

| Isotope | Half-life |
|---|---|
| $^{131}I$[a] | 8.05 days |
| $^{126}Sb$[a] | 12.4 days |
| $^{124}Sb$[a] | 60.2 days |
| $^{95}Zr$-$^{95}Nb$[a] | 65-35 days |
| $^{144}Ce$ | 285 days |
| $^{106}Ru$-$^{106}Rh$[a] | 1.0 year to 2.2 hours |
| $^{134}Cs$[b] | 2.1 years |
| $^{125}Sb$ | 2.7 years |
| $^{3}H$ | 12.3 years |
| $^{90}Sr$ | 28.8 years |
| $^{137}Cs$ | 30 years |

[a]Only significant in at-reactor pools.
[b]Formed by neutron activation of $^{133}Cs$.

nuclides will have probably decayed to insignificant levels with respect to breach of containment. The third type of radioactivity is due to the production of transuranics, e.g., Np, Pu and Am. If failed cladding is discharged or handled at spent fuel pools, the concentration of these nuclides may be measurable and they may adsorb on the crud layer also. The half-lives of the TRU nuclides are long and the amounts present at time of d sposal in a repository may be significant.

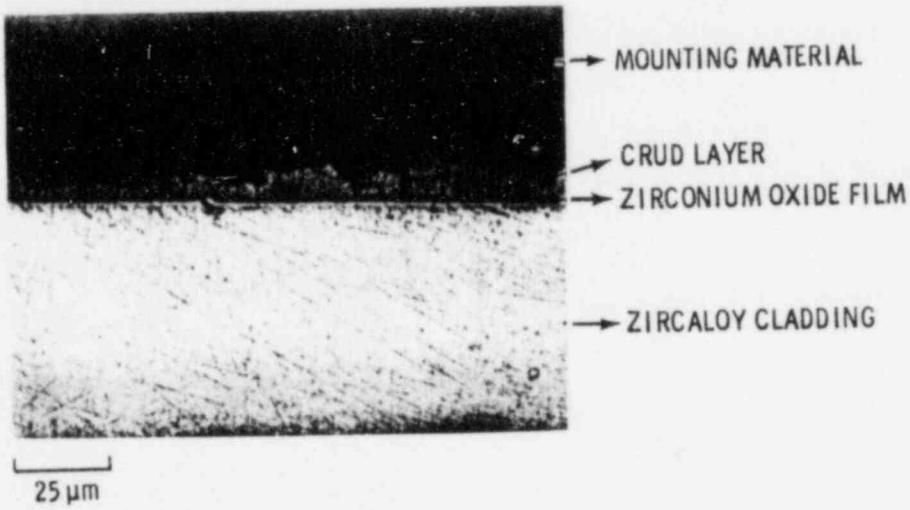


Figure 3.10. Metallographic cross-section of irradiated fuel rod from Shippingport Reactor (USA) showing relationship of crud deposit, oxide layer and Zircaloy fuel cladding (IAEA-218, 1982). (Note maximum thickness of crud layer is ≈12 µm.)

PWR deposits are dark and very adherent (IAEA-218, 1982). The BWR deposits are two-layered: an adherent inner layer and a loose red-brown outer layer of hematite. Particulates may spall during transport and handling in spent fuel pools. These types of deposits may affect the containment capability in two ways: (1) the deposits contain radioactive species and (2) the crud layer and its characteristics, such as homogeneity, cracking and uniformity, may affect the corrosion of the cladding in a repository environment, even if radioactivity has decayed to an acceptable value.

There is a type of water side corrosion, crud-induced localized corrosion (CILC), that was mentioned previously. It is responsible for failure of some rods in-reactor. Oxide nodules may form on Zircaloy-2 fuel cladding under irradiation in the oxygenated BWR coolants (GEAP-10371, 1971; Garzarolli, F., 1971; Johnson, A. B., 1977). PWR experience generally indicates an absence of oxide nodules except possibly during periods of relatively high oxygen concentration in the primary coolant. Fuel rod failures have been attributed to CILC (NUREG/CR-3602, 1984). Nodular attack in-reactor depends on nuclear flux and develops in oxygenated reactor coolants. It has been suggested that uniform concentrations of dissolved oxygen alone do not cause the large nodules which frequently develop on BWR fuel rods (Johnson, A. B., 1977).

Localized water chemistry associated with flow disturbances may be a significant factor in the nodular attack in-reactor. Out-of-reactor, a similar type of attack has been observed on Zircaloy coupons in cold-rolled or extruded conditions after autoclave treatments at 475 and 500°C in steam at 1500 to 1700 psi. It will have to be determined whether this type of attack would occur in a repository environment at lower temperatures and in the absence of a significant neutron flux.

3.2.5.2.3 Estimated Release of Inventory to an Aqueous Environment

Some data exist on the concentration of radioactive species in spent fuel pools. An examination of these data would allow an estimation of the amount of activity released to an aqueous environment at low temperatures by the presence of failed rods and crud deposits. (See Section 3.2.5.1 for the estimates of the release of gaseous nuclides to the environment.) Figure 3.11 indicates the ranges and average beta/gamma activities in $Ci/m^3$ for BWR and PWR pools. The low end of the ranges probably corresponds to periods soon after reactor startup, and the upper end corresponds to refueling periods in reactors where cladding defects have developed during the reactor exposure. Figure 3.12 indicates the percentages of the total beta/gamma activities that are accounted for by Cs isotopes. The other dominant isotopes in spent fuel pools are the cobalt activation products $^{58}Co$ and $^{60}Co$.

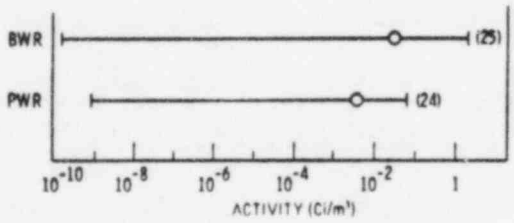


Figure 3.11. Summary of total beta/gamma activities in spent fuel pools (IAEA-218, 1982). (Figures in parentheses indicate number of pools for which data were summarized.)

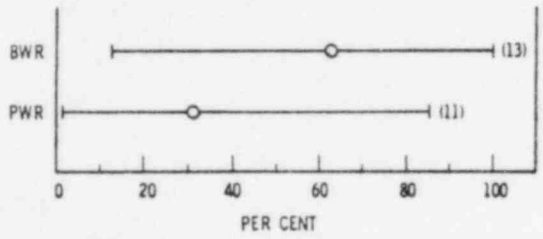


Figure 3.12. Cesium isotopes as a percentage of total beta/gamma activities in spent fuel pool waters (IAEA-218, 1982). (Figures in parentheses indicate number of pools for which data were summarized.)

Table 3.17 indicates the few alpha activity values reported for storage pools. Alpha activities generally are an order of magnitude or more below the corresponding beta/gamma activities.

Table 3.17. Alpha activity levels in the water of spent fuel pools (IAEA-218, 1982).[a]

| Reactor Type | Alpha Activity ($Ci/m^3$) |
|---|---|
| PWR | $3x10^{-7}$[b] |
| BWR | $2x10^{-7}$, $1x10^{-5}$, $1x10^{-5}$, $1x10^{-5}$ |

[a]Survey obtained very limited information for these activities.
[b]Up to $2x10^{-6}$ $Ci/m^3$ during refueling was reported by one reactor.

Using data given in IAEA-218 (1982) for the average number of fuel assemblies stored in pools, the data given in Figure 3.11 and Table 3.17 for maximum concentrations of activity in pools, and data given for the radioactive inventory at discharge for a PWR and a BWR assembly in ORNL/TM-6008 (1977), an estimation of the fractional release of the inventory was made. Pools range in size from 10-20 m in length to 7-15 m in width. The average racking is ≈5 MT heavy metal/$m^2$. It is assumed that there is 0.575 MTHM per PWR assembly and that it contains $9.25x10^7$ Ci as total inventory, excluding activity in crud deposits. It is assumed that there is 0.195 MTHM per BWR assembly and that it contains $2.56x10^7$ Ci as total inventory, excluding activity in crud deposits. For an average pool area of ≈90 $m^2$, the total activity at discharge due to the stored PWR assemblies would be $\approx 7.2x10^{10}$ Ci and the total activity at discharge due to the stored BWR assemblies would be $\approx 5.9x10^{10}$ Ci. Assuming an average activity concentration in a PWR pool to be $\approx 5x10^{-3}$ $Ci/m^3$ and the average activity in $Ci/m^3$ in a BWR pool to be $\approx 10^{-1}$ $Ci/m^3$ (see Figure 3.11), it is estimated that for an average pool volume of ≈1100 $m^3$, the fractional activity released from the inventory at discharge for the PWR assemblies is $\approx 7.6x10^{-11}$ and in the BWR assemblies is $\approx 1.9x10^{-9}$. It must be emphasized that these fractional releases do not include gases that have been released. If these are representative of the fractional release values in a repository, the question can be raised as to whether this very small amount of release constitutes "containment."

### 3.2.5.3 Effect of Storage on Loss of Containment

#### 3.2.5.3.1 Assemblies in Storage

The oldest BWR spent fuel in storage was discharged in 1969, whereas the oldest PWR spent fuel in storage was discharged in 1970 (DOE/NE-0017-1, 1982; HEDL-TME 83-28, 1983). Spent fuel discharged in prior years has been reprocessed. As of September 30, 1982, there were 31,928 LWR fuel assemblies in pool storage; 20,090 BWR fuel assemblies and 11,838 PWR fuel assemblies (DOE/RL-83-1, 1983). The fuel assemblies stored in Morris, Illinois (1212 assemblies) and West Valley, New York (750 assemblies) are not included in

these totals. On the basis of uranium weight, this amounts to a total of 8586.4 MT; 3620.7 MT from BWRs and 4965.7 MT from PWRs. It is estimated that ≈3% of the total fuel assemblies in storage contain fuel rods clad in stainless steel (HEDL-TME 79-20, 1980). See Figure 3.5 for the projected cumulative discharges of spent LWR fuel assemblies.

3.2.5.3.2 Water Pool Chemistry

The storage pool environment is considered to be much less aggressive than the reactor or repository environments. In general, spent BWR fuel is kept in deionized water pools. In a survey (IAEA-218, 1982), the maximum reported operating temperature for this type of pool was 52°C. Moreover, pools normally operate at 40°C or less. The oxygen concentration in the water at this temperature would be 4.9 ppm. The pH is nearly neutral to slightly acidic. Spent PWR fuel is generally kept in pools containing ≈13,000 ppm of boric acid (≈2000 ppm B). The water also contains lithium in the range 3 ppb to 2.2 ppm. The PWR pool pH values are mildly acidic (pH of 4.5-6) at pool temperatures. See Figure 3.13 for a summary of ranges of the above parameters along with conductivity and chlorine concentration data.

3.2.5.3.3 Effect of Pool Storage on Cladding

Based principally on visual observations and radiation monitoring of pool water, there has been little evidence that either Zircaloy or stainless steel LWR fuel rods degrade during pool storage (BNWL-2256, 1977; Johnson, A. B., 1979; NUREG/CR-0668, 1979). In the case of fuel rods with breached cladding, no progressive deterioration has been exhibited (NUREG/CR-0668, 1979).

Eight fuel rods from two bundles (0551 and 0074) of Shippingport Core 1 blanket fuel underwent extensive metallurgical examinations to assess the possible effects of extended pool storage on the integrity of Zircaloy-2-clad fuel (PNL-3921, 1981). The Shippingport Core 1 blanket fuel was clad in Zircaloy-2 rather than Zircaloy-4 and was not exposed to boric acid in the coolant as is typical for a PWR rod. Fuel rods from bundle 0551 were stored in deionized water (DIW) for nearly 21 years prior to examination in 1980. Bundle 0074 had been stored in DIW for 16 years. None of the examinations produced evidence of cladding degradation that was caused by water storage. No significant changes in the appearance of the fuel rods, cladding dimensions or mechanical properties, fission gas release fractions, hydrogen content or distribution in the cladding, or the thickness of the external oxide films were found after extended water storage. In addition, localized corrosion or hydriding was not detected.

Water was detected in some of the samples collected for fission gas analysis but was attributable to leakage into the sample vials rather than defective fuel rods. Additional support for this interpretation was obtained from the burst tests where the bursting pressures and appearance of the ruptured fuel rods were independent of the water content in the gas samples.

Small cladding defects were observed at a few locations on internal cladding surfaces. The defects were probably formed during fabrication. Some microcracks (≈50 μm deep) may have possibly formed by SCC during reactor

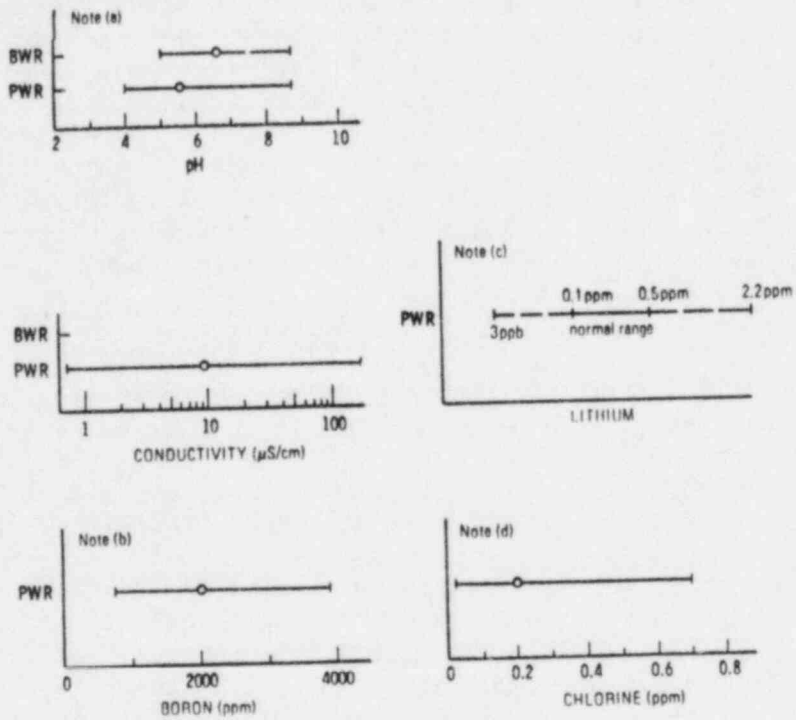


Figure 3.13. Summary of spent fuel pool chemistry data (IAEA-218, 1982). Notes: Some data reported in the survey appear to be design parameters rather than from actual experience. The average (-0-) is only of the reported actual data. The range reflects the upper and lower limits of the reported ranges. (a) Upper and lower ranges are probably specifications rather than experience data. (b) Boron is added only in PWRs. (c) The normal maximum for lithium in reactor coolant is 2.2 ppm. (d) All reactors.

operation in the highly irradiated rods (estimated average burnup was 18,000 MWd/MTU) from bundle 0074 due to cladding-fuel interaction. However, at least one mechanism by which fuel assembly degradation may occur apparently exists. It is reported that the top nozzle separated from a spent Prairie Island PWR fuel assembly during handling after a storage period somewhat less than six years (PNL-4342, 1982). The problem was attributed to SCC that developed while the assembly rested in the storage pool (HEDL-TME 83-28, 1983).

It does not appear that storage of spent fuel in aerated neutral or slightly acidic water at ≈40°C causes significant corrosion of Zircaloy or stainless steel cladding.

3.2.5.4 Potential for Loss of Containment Under Repository-Type Environments

Once the fuel rod is breached, radioactive gases can escape, water can leach/dissolve the fuel pellets, and/or the $UO_2$ fuel can be oxidized causing expansion of the fuel and rupture of the rod. The cladding can be corroded internally and externally, i.e. fuelside and waterside. [It has been estimated that the cladding contains <0.1% of the inventory (at discharge) (EUR-7671 EN, 1982; International Atomic Energy Authority, 1983.] The following discussion emphasizes Zircaloy corrosion. A brief review of stainless steel corrosion in repository-like environments is presented at the end of the discussion on Zircaloy. The main types of corrosion that could lead to breach of containment of the Zircaloy cladding are uniform, stress corrosion cracking, and hydriding. Nodular corrosion in-reactor was discussed in a previous section and is not probable as a failure mode in the repository. It should be noted that the following statements have been made:

1) Below 425°C, no cladding breach mechanism is predicted to be operative during the 1000-year thermal period (HEDL-TME 81-43, 1982) and

2) Iodine-induced SCC would not cause Zircaloy cladding breach until the temperature reached 600°C. This temperature is more conservative than that predicted by Blackburn (HEDL-TME 78-37, 1978).

3.2.5.4.1 Uniform Corrosion of Zircaloy

Corrosion Under Reactor Conditions

Waterside corrosion is responsible for <0.002% of fuel rod failures (HEDL-TME 83-28, 1983). This failure mechanism is more common in BWRs where the radiolytic production of oxygen from water is not suppressed by hydrogen addition, as it is in PWRs. Information is available on in-reactor corrosion of Zircaloy from short-term tests but little information exists on Zircaloy corrosion under the expected repository environments given in Tables 3.7 through 3.9. This is primarily due to the fact that Zircaloy is not a candidate for use as a container material. However, a comprehensive review of available aqueous corrosion data was performed by Hillner (1977) on Zircaloy-2 and Zircaloy-4 for water reactor environments. It was shown that in the temperature range 260 to 400°C the uniform corrosion rate (weight gain) initially follows a $t^{1/3}$ time dependence which, at "transition," changes to a faster

linear rate. Hillner showed that after transition the weight gain in $mg/dm^2$-day is given by the following relationship:

$$\Delta W = 1.12 \times 10^8 \exp [-12529/T(°K)] \cdot t$$

Woodley (HEDL-TME 83-28, 1983) used this equation to calculate weight increase rates for temperatures between 250 to 400°C, inclusive (Table 3.18). From these values the 300-year metal losses may be obtained assuming that the weight gain is solely from oxygen interaction to form $ZrO_2$. Note that a conversion factor (0.044) has been used to obtain an estimate of the cladding thickness (mm) corroded in 300 years from the weight gain values for Zircaloy which are normally given in units of $mg/dm^2 \cdot d$. The results in Table 3.18 show that the metal loss in 300°C water is about 0.2 mm. This may be compared to BWR and PWR cladding thicknesses of 0.85 and 0.65 mm, respectively (HEDL-TME 83-28, 1983). Under repository conditions, where the cladding would only be attacked after the metal overpack fails, the amount of uniform corrosion would be far less because of the lower temperatures involved.

Table 3.18. Summary of Zircaloy uniform corrosion data.

| Test Temp. (°C) | Test Time (d) | Environmental Conditions | Rate of Weight Increase ($mg/dm^2$-d) | Metal Loss Rate (cm/y) | 300-y Metal Loss (mm) | Reference |
|---|---|---|---|---|---|---|
| 250 | Varies | Aqueous | $4.45 \times 10^{-3}$ | | 0.02 | Woodley, (HEDL-TME- |
| 300 | " | " | $3.60 \times 10^{-2}$ | | 0.2 | 83-28, 1983) |
| 350 | " | " | $2.08 \times 10^{-1}$ | | 1.0 | |
| 400 | " | " | $9.25 \times 10^{-1}$ | | 4.4 | |
| 250 | Varies | Air or Steam | $1.75 \times 10^{-3}$ | | 0.008 | Woodley, (HEDL-TME- |
| 300 | " | " | $2.35 \times 10^{-2}$ | | 0.1 | 83-28, 1983) |
| 350 | " | " | $2.09 \times 10^{-1}$ | | 1.0 | |
| 400 | " | " | 1.34 | | 6.3 | |
| 250 | 90 | Anoxic basaltic water (pH 7.7-8.5) | 0.26 | | 1.2 | Pitman, S. G. (1981) |
| 250 | 28 | Deoxygenated WIPP Brine A (pH 6.5) | | 0.0001 | 0.3 | Braithwaite, J. W. (1980) |
| 250 | 58 | MgCl-NaCl solution (pH 9) | 0.14 | | 0.6 | Pitman, S. G. (1981) |
| ≈250 | 1134 | Air/natural salt | 0.11 | | 0.5 | Griess, (ORNL/TM-8351, 1982) |

## Corrosion Under Air and Steam Conditions

Another study by Boase and Vandergraaf (1977) evaluated data on Zircaloy-2 corrosion in dry air, laboratory air, and steam. The results were also used by Woodley (HEDL-TME 83-28, 1983) to obtain weight increase rates at 250, 300, 350 and 400°C (Table 3.18). The values obtained are quite close to those obtained for aqeuous conditions. At 300°C, the metal loss after 300 years would be 0.1 mm. This result may have some pertinence to a tuff repository environment for which air/steam conditions are present during the first few hundred years after repository closure.

## Corrosion Under Simulated Repository Conditions and In Situ Testing

The small amount of data on Zircaloy uniform corrosion for repository conditions are from early short-term screening studies carried out during the selection of reference container materials in the U.S. program. Pitman and others (1981) showed that in a 90-day test in 350°C anoxic basaltic water (pH 7.7 to 8.5) the rate of weight increase of Zircaloy-2 was 0.2 $mg/dm^2$-d. This corresponds to a metal loss of 1.2 mm in 300 years (Table 3.18). Although this indicates that the cladding would fail, the value represents a conservative estimate since the cladding will probably be much cooler than 250°C when water contact is initiated.

In a parallel experiment, Pitman and others (1981) showed that the 300-year metal loss in a 250°C MgCl-NaCl solution (pH 9) would give a metal loss of 0.6 mm (Table 3.18). Braithwaite and Molecke (1980) found that in a 28-day test in WIPP Brine A at 250°C (pH 6.5) the Zircaloy-2 corrosion rate was 0.0001 cm/y. In 300 years, a metal loss of 0.3 mm would be expected under isothermal conditions, assuming that the corrosion rate is maintained (Table 3.18).

Some data on Zircaloy-2 corrosion were reported by Griess (ORNL/TM-8351, 1982) from the Avery Island Salt Mine tests. These involved exposing a variety of metals and alloys to high temperatures in boreholes in the floor of a mined tunnel. The samples were in an air environment and spaced approximately 5 cm from the salt borehole surface. A Zircaloy-2 specimen showed a weight gain of 1.28 $mg/cm^2$ after three years exposure at about 250°C. Assuming that this gain is caused by oxygen interaction, the 300-year metal loss would be 0.6 mm, assuming isothermal conditions were maintained (Table 3.18).

## Specific Factors That Influence Corrosion Rate

The main factors which could conceivably cause an enhanced rate of uniform corrosion include the effects of specific ions with the initial and reacted groundwater composition, groundwater gamma radiolysis, and pH values which deviate significantly from the near-neutral conditions used in many corrosion tests. These factors have yet to be adequately quantified with respect to Zircaloy corrosion in a repository environment.

Effect of Silicate Ion

An ion that has specifically been implicated in the uniform corrosion of Zircaloy is silicate. The effect of this ion on the weight gain of Zircaloy has been studied (KAPL-M-6748, 1968). At a silicon concentration of 0.12 ppm, the 14-day, 400°C steam[4] weight gains of sensitized Zircaloy are ≈7.75 mg/$cm^2$-d, corresponding to a uniform corrosion thickness of ≈0.3 mm in 300 years (KAPL-M-6748, 1968). At a silicon concentration of 1.30 ppm, the cladding thickness that would be corroded in 300 years is ≈0.7 mm. In reactor-grade Zircaloy that is not sensitized, the corroded cladding thickness in 300 years is ≈0.1 mm based on 14-day data from autoclave tests using deoxygenated and deionized water having a silicon concentration of 4.70 ppm. The silicon concentrations (as $SiO_2$) in GR-3 basaltic and J-13 tuffaceous groundwaters are ≈76 ppm and ≈61 ppm, respectively. A high silicon content has been found in unfiltered samples of distilled water in contact with the nonwelded, zeolitized tuff of Calico Hills at 150°C and 325°C after one to 21 weeks of reaction (LA-9328-MS, 1982; LA-9846-PR, 1983). Concentrations were >200 ppm at 150°C and >500 ppm at 325°C. Distilled water was used because water from condensed steam -- essentially distilled water -- from the loaded repository will be a lower bound on the dissolved-solids content in water/tuff interactions. Although the test results were obtained at higher than anticipated temperatures in steam, this effect of silicate ion in large quantities on the corrosion of Zircaloy under expected repository conditions should be investigated.

Effect of Gamma Radiolysis Products and pH

From Tables 3.7 through 3.9 it may be seen that during the early thermal period in a repository, significant gamma fluxes will be present. For a salt repository, there may also be initial decreases in pH of the brine due to the thermal liberation of acid gases from the host rock. This will probably be followed by large elevations in pH as brine interacts with colloidal sodium formed by the gamma radiation of salt.

No data are apparently available for Zircaloy but preliminary information indicates that the corrosion of titanium alloy 12 in 90°C WIPP Brine A hardly increases when subjected to a gamma flux of $10^7$ R/h when compared to non-irradiation (gamma) conditions (Braithwaite, J. W., 1980). Although Braithwaite and Molecke attribute the small increase to radiolytic oxidizing species in the brine, it is interesting to note that other experiments carried out in the same study show that brine at 250°C, containing 600 ppm of dissolved oxygen

[4]The water placed in the autoclave was deoxygenated and deionized, was purged with argon, and had a pH of 6-7.

gave a corrosion rate of 0.0004 mm/yr compared to 0.003 mm/yr for deoxygenated brine. One may, therefore, infer that gamma radiation will only slightly alter the corrosion rate of Zircaloy in brine and that the irradiation may, in fact, be beneficial. Early work at Oak Ridge National Laboratory summarized by Cox (1968) shows that electron irradiation (and presumably gamma irradiation) had a negligible effect on the corrosion of Zircaloy-2 exposed to oxygenated solutions.

With respect to pH effects on Zircaloy corrosion another review by Cox (1976) shows that pH variations over the range 1-12 in sulfuric and nitric acids, and ammonium, sodium or potassium hydroxides do not significantly alter the corrosion rate.

Effect of Decreasing Temperature

A recent thermal analysis for a spent fuel waste package in a salt environment showed that the fuel rod centerline temperature will initially be about 370°C at emplacement, and will decrease to 220°C after 100 years, and to 150°C after 300 years (ONWI-438, 1983). If, for example, the overpack fails after 100 years, and the fuel pins are inundated with water, the Zircaloy cladding will be required to contain the radionuclides for the remaining 200 years to meet the NRC 300-year containment criterion. Corrosion will, therefore, take place at temperatures decreasing from 220 to 150°C, assuming that the water or crud on the rods does not alter the rate of heat transfer. If one assumes that the temperature dependence of the corrosion rates listed from Woodley's work (HEDL-TME 83-28, 1983) in Table 3.18 apply, then the rate decreases by about an order of magnitude for each 50°C decrease in temperature. Thus, the 300-year metal loss values given in Table 3.18 are likely to be one or two orders of magnitude too high since they were calculated from 250°C data. However, it should be noted that Zircaloy may exhibit memory effects in its corrosion behavior and that a decrease in temperature or oxygen level with time may not show a corresponding decrease in rate and vice versa (Bradhurst, D. H., 1972; Phadnis, S. V., 1983).

Overall Evaluation of Zircaloy Cladding Failure by Uniform Corrosion

The data in Table 3.18 give very conservative estimates of the metal losses to be expected when Zircaloy cladding is corroded after the overpack fails in a repository. The 300-year metal losses for basaltic water and brine at 250°C are, in fact, close to the cladding thicknesses. However, it is not likely that the cladding will fail by uniform corrosion during the 300-year radionuclide containment period since:

a. Significant cladding attack will only occur after the overpack has failed;
b. The temperature when attack occurs will probably be less than the 250°C values given in Table 3.18, and it will continue to decrease with time;
c. Many of the measured corrosion rates are from short-term tests during which the rate of attack is relatively fast. Corrosion rates may decrease with time as the surface oxide increases in thickness.

3.2.5.4.2 Stress Corrosion Cracking of Zircaloy (Fuelside)

Identification of Aggressive Substances

Zircaloy is subject to stress corrosion cracking (SCC) which is caused by the presence of an aggressive substance and residual and/or applied stresses in the metal. Zircaloy specimens stressed in tension may crack in the presence of iodine, metal iodides (such as $FeI_2$, $AlI_3$), and Cd at temperatures commonly found in water-cooled reactor fuel sheaths (≈300°C) (Shann, S. H., 1983; Shimada, S., 1983; Wood, J. C., 1983; Kohli, R., 1984). Fuel rods in-reactor show this type of failure mode. There does not seem to be a difference in the SCC of Zircaloy-2 and Zircaloy-4 (EPRI NP-1329, 1980). This subject has been reviewed in depth elsewhere (EPRI NP-1472, 1980; Shann, S. H., 1983).

It remains unclear what the operative mechanisms are and, even, what the responsible agents are. For example, iodine vapor has been used in simulated cladding tests to induce SCC. Minimum iodine concentrations for this to occur have been stipulated (Wood, J. C., 1972; Shann, S. H., 1983; Nishimura, S., 1984). In a study by Wood (1972), SCC did not occur after 1000 hours when the iodine available to Zircaloy surfaces was less than $2 \times 10^{-5}$ g $I_2/cm^2$ Zircaloy surface. Peehs (1979) suggested a minimum concentration of $1 \times 10^{-6}$ g/cm².[5] Shann and Olander (1983) reported a minimum $I_2$ pressure of $\approx 10^{-5}$ MPa for SCC of Zircaloy to occur[6]. Yet, iodine concentrations and pressures of this magnitude are not present inside fuel undergoing irradiation (Davies, J. H., 1979). The largest equilibrium pressure of $I_2$ inside irradiated fuel believed to be possible is $\approx 10^{-14}$ MPa at 327°C (Goetzmann, O., 1983). Malinauskas (1978) showed that very little iodine is present in volatile form in the fuel cladding gap.

Evidence exists that the SCC mechanism involves solid surface iodides on the Zircaloy and does not involve gaseous iodine/iodides (EPRI NP-1329, 1980). The details for the chemical elements found on the inner surfaces of irradiated fuel rod cladding are only known in a qualitative manner (EPRI NP-218, 1976; Cubicciotti, D., 1977, 1978). In an experimental PWR-type fuel rod, a reaction layer or duplex layer was observed between the fuel and cladding and contained the elements U, Zr, Cs, Pd, Ba and Te (Bazin, J., 1975). The following elements were observed at the fuel-to-cladding interface in PWR fuel rods of current design: large amounts of Cs and U, smaller amounts of I and Te, and lesser amounts of Cl, Mn, Fe, Ag, Si, Ba, Cu, Na and Ca (EPRI

---

[5]Using estimated surface areas for a GE BWR Zircaoly-2 rod and a Westinghouse PWR Zircaloy-4 rod of ≈1400 cm² and 1100 cm², respectively, and the production of $I_2$ from ORIGEN-2 calculations, it was determined that ≈5% of the iodine inventory would need to be available in the fuel-cladding gap to achieve this concentration.

[6]If all the iodine produced (≈0.5-0.6 g) was available in the fuel-cladding gap, the corresponding pressures of iodine would be ≈0.2 MPa at room temperature.

NP-218, 1976). In these and other studies, cesium and/or iodine have been reported to concentrate at pellet-to-pellet interfaces (NUREG/CP-0005, 1979).

At this time SCC in Zircaloy has also been induced in the laboratory by using gaseous $FeI_2$ and $AlI_3$ and Cd (Shann, S. H., 1983). The minimum pressure for $FeI_2$ and $AlI_2$ to produce $I_2$ is $\approx 10^{-5}$ MPa. The minimum pressure for Cd to produce SCC is $\approx 2.6 \times 10^{-7}$ MPa. It appears that different mechanisms with different gas pressure and stress dependencies are applicable. Cesium iodide once was believed to be an SCC agent but was shown not to be so by Shann and Olander (1983).

It should also be remembered that laboratory tests on unirradiated Zircaloy coupons may not be producing results that are valid for in-reactor Zircaloy cladding. Our concern is that SCC processes which have remained dormant during the storage period for spent fuel may become active in the repository due to the resumption of temperatures in the range 300-375°C and the corresponding increase in gas pressure inside the fuel-cladding gap. Failures in rods while in-reactor are usually associated with power ramps during which the fuel matrix reaches temperatures of ≈1400°C, with subsequent thermal expansion of the matrix, increase in release of fission products from the matrix, and the resulting gas pressure increase. Without knowledge about the identity of the specific SCC agents and their aggressive behavior and the operative mechanisms, it is not possible at this time to state whether there are sufficient aggressive substances present in the spent fuel to support SCC processes during the thermal period for spent fuel isolation.

Estimation of Gas Pressure and Average Hoop Stress in a Fuel Rod Under Repository Conditions

The minimum hoop stress required for crack initiation in iodine-induced SCC experiments has been reported to be 200-220 MPa at 400°C (Nishimura, S., 1984). This result is in good agreement with an earlier determination of 216 MPa at 300°C (Wood, J. C., 1972). The following simple analysis is an attempt to estimate the hoop stress inside a fuel rod under repository conditions. We are not considering refinements to the minimum hoop stress criterion, such as ratio of axial-to-hoop stress, effect of irradiation, or chemical/physical processes that cause a reduction in the gas which leaves the fuel matrix and pressurizes the gap. It should be noted that mechanically-induced cladding fatigue crack propagation of deep cladding flaws (i.e. on the order of 20% of the cladding wall thickness) under the anticipated applied loads in a repository is not an active degradation mechanism, as concluded by Bosi (HEDL-TME 80-84, 1981).

General Electric began using 0.3 MPa (3 atm) He prepressurization in BWR fuel pins in late 1978 (ORNL-5578, 1979). In the same time period, Westinghouse began using a helium prepressurization of 3 to 3.4 MPa (30 to 34 atm) in PWR fuel pins. Prior to this time, the prepressurization of He inside fuel pins was ≈0.1 MPa. Additional pressurization is generated by fission gas production during irradiation. Hann and Wilson (BNWL-2256, 1977) estimate that the majority of stored PWR assemblies have pressures of 1.7 to 3.7 MPa (17 to 37 atm) and occasionally 5.4 MPa (53 atm) at temperatures at the surface of the fuel pins during storage, i.e. <60°C. They also estimate a maximum

pressure in BWR assemblies during pool storage of 1.4 MPa to 2.0 MPa (14 atm to 20 atm). Jenks (ORNL-5578, 1979) has estimated maximum total pressure in a PWR fuel rod to be ≈9.2 MPa (91 atm) at 100°C and in a BWR fuel rod to be ≈3.1 MPa (31 atm) at 100°C. We have compiled two tables (3.12 and 3.13) from ORIGEN values presented in ORNL/TM-6008 (1977) to show the amount of gas present in a single BWR rod and a single PWR rod at discharge and at 300 years after discharge. From this inventory, the total number of moles of gas produced within the fuel rod was estimated to be in the range 0.10 to 0.16, varying with type (PWR or BWR) and/or inclusion of produced He and volatile Cs in the gaseous inventory. (In our calculations, it is assumed that the temperature is such that all the Cs volatilizes.) Most of this gas, however, is not present in the void volume, as will be discussed later.

Estimates of fission product inventory released to the gas plenum of fuel pins from the fuel matrix have been published (WASH-1400, 1975; NUREG/CR-0091, 1978; ORNL-5578, 1979). Fission gas release has been estimated to range from less than 0.4% (ORNL-5578, 1979; PNL-5109, 1984) to ≈10% (WASH-1400, 1975; NUREG-0418, 1978). See Table 3.19 for fission gas measurements performed on the MCC Approved Testing Material PWR spent fuel (PNL-4686, PNL-5109, 1984). In the calculations that follow, we use a very conservative estimate of ≈10% of the fission produce inventory release to the fuel-cladding gap. Therefore, the number of moles of gaseous fission products in the gap is considered to range from 0.01 to 0.016 moles. For gas pressure estimations, the moles of He introduced during prepressurization will be added to the value of 0.016 moles of fission products. If we assume He prepressurization was performed at 25°C, then the number of moles of gas necessary to achieve a pressure of 0.3 MPa in a BWR fuel-cladding gap (void volume of ≈30 mL) is $3.68 \times 10^{-3}$ moles of He. If we also assume He prepressurization to 3 MPa was performed at 25°C on a PWR fuel rod having a void volume of ≈20 mL, then the number of moles of He are calculated to be $2.45 \times 10^{-2}$ moles. In summary, we have estimated the gas pressure inside the fuel rod due to He prepressurization and due to fission product generation.

Using the Ideal Gas Law, the pressure inside a BWR fuel rod due to ≈0.02 moles of gas at 300°C is ≈3.1 MPa (31 atm) and at 100°C is ≈2.0 MPa. The pressure inside a PWR fuel rod due to ≈0.04 moles of gas at 300°C is ≈9.4 MPa (94 atm) and at 100°C is ≈6.1 MPa.

The hoop stress on the fuel rod has been identified as a determining factor in whether SCC will be initiated by iodine. The following is an estimation using the dimensions for the radius (r) and thickness (t) of a General Electric BWR rod in an 8x8 assembly (r = 6.26 mm, t = 0.864 mm) and a Westinghouse PWR rod in a 15x15 assembly (r = 5.36 mm, t = 0.617 mm) (HEDL-TME 83-28, 1983). See Table 3.20 The average stress ($\sigma$) in the hoop for a thinwalled cylinder can be calculated by use of the formula, $\sigma = pr/t$, where p = pressure, r = radius of the cylinder, and t = thickness of the cylinder wall. By use of this formula, we estimate an average hoop stress during the containment period in a BWR rod at 300°C to be ≈22.7 MPa and in a PWR rod at 300°C to be ≈82.5 MPa. These results are below the 200-220 MPa hoop stress needed to initiate SCC in the presence of iodine. However, different aggressive substances have lower stress thresholds to initiate cracks. Also, if surface defects are present in Zircaloy from fabrication, localized stress intensities may be

Table 3.19. Gas pressure, gas composition, and rod void volume for rods from MCC Approved Testing Material spent PWR fuel.

| Rod No. | Measured Void Volume $cm^3$ | Total Recovered Gas at STP $cm^3$ | Pressure[a] at 0°C MPa | Composition (Volume %) | | | | | | | | | Rod-Average Burnup[b] MWd/kgM | Estimated Fission Gas[b,c] Produced $cm^3$ | Fission Gas Released[b] Percent |
|---|---|---|---|---|---|---|---|---|---|---|---|---|---|---|---|
| | | | | He | Xe | Kr | Ar | $H_2$ | $CO_2$ | $N_2$ | $O_2$ | Organics | | | |
| C-5 | 23.9 ±1.1 | 362 ±8.7 | 1.54 ±0.07 | 98.3 ±0.2 | 0.89 ±0.015 | 0.10 ±0.044 | 0.61 ±0.01 | <0.01 -- | <0.01 -- | 0.06 ±0.004 | <0.01 -- | <0.01 -- | 28.2 | 1906 | 0.19 |
| D-10 | 22.5 ±1.1 | 369 ±8.9 | 1.66 ±0.08 | 98.2 ±0.2 | 1.03 ±0.08 | 0.12 ±0.004 | 0.61 ±0.01 | 0.02 ±0.008 | <0.01 -- | 0.05 ±0.004 | <0.01 -- | 0.02 -- | [28.4] | [1919] | [0.22] |
| G-9 | 22.2 ±1.0 | 373 ±8.9 | 1.70 ±0.08 | 98.9 ±0.2 | 0.72 ±0.012 | 0.08 ±0.003 | 0.30 ±0.005 | <0.01 -- | <0.01 -- | 0.04 ±0.004 | <0.01 -- | <0.01 -- | [28.4] | [1919] | [0.16] |
| G-13 | 20.0 ±0.9 | 357 ±8.6 | 1.81 ±0.08 | 97.9 ±0.2 | 0.98 ±0.017 | 0.11 ±0.004 | 0.91 ±0.016 | 0.02 ±0.008 | <0.01 -- | 0.05 ±0.004 | <0.01 -- | <0.02 -- | [28.4] | [1919] | [0.20] |
| J-12 | 22.8 ±1.1 | 368 ±8.8 | 1.63 ±0.08 | 98.7 ±0.2 | 0.88 ±0.015 | 0.10 ±0.004 | 0.25 ±0.005 | <0.01 -- | <0.01 -- | 0.05 ±0.004 | <0.01 -- | <0.01 -- | [28.4] | [1919] | [0.19] |
| L-8 | 22.1 ±1.0 | 364 ±8.7 | 1.67 ±0.08 | 96.7 ±0.02 | 1.42 ±0.024 | 0.16 ±0.006 | 0.76 ±0.013 | 0.03 ±0.008 | <0.01 -- | 0.74 ±0.13 | 0.12 ±0.004 | 0.02 -- | 30.0 | 2027 | 0.28 |
| N-4 | 20.1 ±0.9 | 368 ±8.8 | 1.85 ±0.09 | 98.7 ±0.2 | 0.74 ±0.013 | 0.08 ±0.00[illegible] | 0.33 ±0.006 | 0.02 ±0.008 | <0.01 -- | 0.08 ±0.004 | <0.01 -- | 0.02 -- | [28.4] | [1919] | [0.16] |

[a]Initial pressurization was estimated to be ≈1.8 MPa (17.8 atm).
[b]Values shown in brackets are preliminary pending $^{137}Cs$ gamma scan results.
[c]Calculated from fuel dimensions and density and assuming a fuel volume reduction of 1% for dishes, metal-to-oxide ratio of 0.88, and 31.0 $cm^3$ fission gas per MWd.

Table 3.20. Mechanical design parameters of typical BWR and PWR fuel assemblies (HEDL-TME 83-28, 1983).

| | General Electric BWR Rod Array 8x8 | Westinghouse PWR Rod Array 15x15 |
|---|---|---|
| Fuel Assemblies | | |
| Transverse Dimension | 14.016 cm | 21.402 cm |
| Assembly Weight | 272.16 kg | 644 kg |
| Overall Assembly Length | 434.8-452.6 cm | 409.7 cm |
| Fuel Rods | | |
| Number per Assembly | 63 | 204 |
| Rod Pitch | 1.626 cm | 1.430 cm |
| Length | 409.2 cm | 380.2 cm |
| Fueled Length | 370.8 cm | 365.8 cm |
| O.D. | 1.252 cm | 1.072 cm |
| Diametral Gap | 0.0229 cm | 0.0190 cm |
| Cladding Thickness | 0.0864 cm | 0.0617 cm |
| Cladding Material | Zircaloy-2[a] | Zircaloy-4[b] |
| Fuel Pellets | | |
| Density (% TD) | 95 | 95 |
| Diameter | 1.057 cm | 0.9294 cm |
| Length | 1.067 cm | 1.524 cm |
| Tie Plate | | |
| Material | 304-SS | 304-SS |
| Spacers | | |
| Number | 7 | 7 |
| Material | Zircaloy-4[b] | Inconel-718 |
| Springs | Inconel | Inconel-718 |
| Plenum Springs | | |
| Working Length | 26.9-30.6 cm | 17.27 cm |
| Material | Inconel | Inconel-718 |
| Compression Springs | | |
| Working Length | 2.13 cm | ---- |
| Material | Inconel | ---- |
| Guide Tubes | | |
| Number | ---- | 20 |
| Upper O.D. | ---- | 1.382 cm |
| Wall Thickness | ---- | 0.043 cm |
| Material | ---- | Zircaloy-4[b] |
| Instrument Tubes | | |
| Number | ---- | 1 |
| O.D. | ---- | 1.382 cm |
| Wall Thickness | ---- | 0.043 cm |
| Material | ---- | Zircaloy-4[b] |

[a]Zircaloy-2 has the nominal composition: 1.5% Sn, 0.12% Fe, 0.10% Cr, 0.05% Ni, and the balance is Zr.

[b]Zircaloy-4 has the nominal composition: 1.5% Sn, 0.20% Fe, 0.10% Cr, <0.005% Ni, and the balance is Zr.

sufficient to permit the occurrence of SCC. Examination of some internal cladding surfaces revealed small fabrication defects ≈50 μm in depth (PNL-3921, 1981). Further, there is good indication that crack initiation occurs at chemical inhomogeneities (EPRI NP-1329, 1980). These are described as higher-than-normal concentrations of certain alloying additives (Fe, Cr, Ni) or impurities (Al, Si, other). Iron seems to be encountered particularly frequently. In addition, hydriding may cause crack initiation (Cox, B., 1978). See section on hydride formation.

In summary, the factors influencing the potential iodine-induced SCC of Zircaloy for short periods of time at 300-400°C are weight of $I_2$ per $cm^2$ of Zircaloy surface area and the average hoop stress. Our estimates for these parameters suggest that enough iodine could be present in the fuel/cladding gap if it is not trapped in the fuel pellets or combined with other elements. However, the average hoop stress is not sufficient to initiate SCC. Also, the identity of the aggressive substances in the irradiated fuel and the corresponding threshold stresses for SCC are not known. In the absence of sufficient high average stress, localized stresses due to defects and inhomogeneities that exist in the internal cladding surface may be sufficient to cause SCC. Additionally, the mechanisms for SCC may involve the deposition of solids, which upon irradiation would give high localized concentrations. During reactor operation, sufficient solid may be deposited so that at the elevated temperature in the repository, SCC may eventually develop.

3.2.5.4.3 Hydriding of Zircaloy

SCC may be enhanced by other forms of corrosion that may be occurring, such as hydriding. Hydrogen is present in as-manufactured Zircaloy tubing to the extent of about 20 ppm, the approximate solubility level at room temperature. The largest single source of hydrogen in a reactor is from the coolant, which interacts to form a corrosion layer of $ZrO_2$ on the external surfaces of the cladding with the liberation of hydrogen. Some of the hydrogen diffuses through the oxide layer and is absorbed in the Zircaloy to a concentration of 20-40 ppm in a BWR environment, and 100-200 ppm in a PWR environment (GEAP-12205, 1971; IAEA-221, 1983). This means that the $H_2$ content reaches supersaturation in the Zircaloy. [The solubility of hydrogen in ppm by weight, $C_m$, in zirconium and Zircaloy-2 and Zircaloy-4 at temperatures ranging from 300° to 500°C is given by $C_m = 1.2 \times 10^5 \exp(-4305/T)$ where T is in Kelvin (Kearns, J. J., 1967; KFK 2677, 1978).] In light water reactors, ≈50% of the fission product tritium remains in the Zircaloy cladding (KFK-2677, 1978). Tritium is nonuniformly distributed in the cladding (GEAP-12205, 1971) in concentrations of ≈0.07 ppm (≈2 appm) (EPRI-RP-455-1, 1976). At reactor shutdown, any excess hydrogen in the cladding is precipitated as zirconium hydride platelets. The orientation of the platelets is determined by the prior mechanical working history and stress level at the time of formation. In cold-worked, stress-relief-annealed tubing the mode of orientation may be either radial or circumferential, in a recrystallized tube it tends to be random. (Radial hydride precipitation has generally been assumed to be undesirable and liable to lead to low-ductility failure.) The sources of hydrogen in the repository environment can be from the radiolysis of groundwater and galvanic reactions in which zirconium acts as the cathode and hydrogen accumulates in the metal. However, it should be noted that evidence exists that dissolved

hydrogen lowers the corrosion rate of Zircaloy irradiated in high-temperature water (Asher, R. C., 1970; Burns, W. G., 1976).

3.2.5.4.4 Stress Corrosion Cracking of Zircaloy (Waterside)

Chloride ion has been implicated in the cracking of zirconium and zirconium alloys. Stress corrosion cracking (SCC) of Zircaloy-2 is known to occur in the presence of acidic ferric chloride solutions (BM-RI-5784, 1961; Thomas, K. C., 1965). Previous studies on corrosion in neutral aerated chloride solutions of unstressed zirconium and zirconium alloys (not Zircaloy) specimens have also been performed (Maraghini, M., 1954; Hackerman, N., 1954). Zirconium and the alloys studied were readily corroded and pitted in the presence of chloride ion, even when only small anodic currents of the order of 1 $\mu A/cm^2$ were impressed. Data for stressed and unstressed specimens seem to indicate that this type of corrosion should be investigated as a possible mode for breach of containment of the Zircaloy cladding in a salt repository.

3.2.5.5 Corrosion of Stainless Steel Cladding Under Repository Conditions

Stainless steel cladding (Types 304, 304L, 348 and 316) is used in several operating PWRs and BWRs. It is estimated that ≈3% of the total fuel assemblies in storage contain fuel rods clad in stainless steel (HEDL-TME 83-28, 1983). The following is a general description of the types of corrosion that may lead to breach of containment of stainless steel cladding in a repository environment. A detailed review of stainless steel corrosion in a salt or basaltic environment was presented in NUREG/CR-2482, Vol. 3 (1983). A discussion of its corrosion in a tuff repository was provided by Pescatore and Soo (1983).

The primary modes of possible chemical failure for Type 304L-stainless steel are uniform, pitting, crevice corrosion, stress corrosion cracking and hydrogen/helium embrittlement.

3.2.5.5.1 Uniform and Pitting Corrosion

Several materials were exposed to deoxygenated brines and seawater at 250°C for 28 days (Braithwaite, J. W., 1980). The corrosion rates for Type 304L-stainless steel in WIPP Brine A, Brine B, and seawater were reported to be 18, 10, and 6 μm/yr, respectively. In 300 years time, this represents losses in thicknesses of 5.4 mm, 3 mm, and 1.8 mm, respectively. All of these values exceed the average thickness of cladding. PNL (PNL-3484, 1980) exposed 22 different metals to $MgCl_2$-NaCl brine at 250°C for up to 72 days. The descaled weight change for Type 304L-SS was reported to be -5 $mg/dm^2$ (≈0.32 μm/yr). This corresponds to a loss in thickness in 300 years of 0.096 mm, which is less than the usual cladding thickness.

The corrosion behavior of Type 304L-stainless steel was also investigated in Hanford basaltic groundwater at 250°C in 90-day tests (PNL-3484, 1980). The corrosion rate was determined to be less than 0.076 μm/yr which corresponds to a thickness loss in 300 years of less than 0.02 mm.

Data are also being obtained on the corrosion of candidate steels Type 304L, 316L and 321 under steam/air conditions that will prevail in a tuff repository during the containment period (UCRL-89404, 1983). Sensitization of this class of steels represents one of the more important potential problems since it could lead to intergranular attack.

Experimental work reported by Burns (1983) may have application to corrosion conditions in a tuff repository. Air-saturated pure water was gamma irradiated in the presence of air at a dose rate of $1.5 \times 10^5$ rad/h for 96 days at a temperature of 30°C in sealed Type 304 stainless steel containers. Hydrogen and oxygen were formed in amounts that were less than one-tenth of the maximum possible for continuous aqueous radiolysis but the increase in oxygen appearing as gas was less than that equivalent to the hydrogen formed from the water present, indicating that corrosion of the Type 304 stainless steel had occurred. From the experimental description and data provided, we estimate a weight gain of 0.079 $mg/dm^2/d$. The loss in cladding thickness over a period of 300 years at this corrosion rate would be approximately 0.1 mm. In the absence of irradiation, no change in gas composition was observed. When the air in solution and in the gas space inside the test vessel was replaced by argon or by hydrogen, radiolysis and corrosion were virtually suppressed. Irradiation-enhanced uniform corrosion should be investigated as part of cladding containment testing under tuff repository conditions.

Pitting is a form of localized attack that usually occurs in stainless steels where passivity has been destroyed. There are many environmental variables which can influence pitting behavior. Increasing the chloride concentration of a solution significantly increases the tendency for pitting. This is likely to be a consideration in a salt repository. Of the other halogen ions, bromides will also cause pitting, but fluoride and iodide solutions do not promote pitting. Among metal ions cupric, ferric, and mercuric ions in chloride solutions are particularly aggressive (Sedriks, A. J., 1979). Among anions that reduce the tendency to pit in chloride solutions, as indicated by a displacement of the pitting potential in the noble direction, are $SO_4^{2-}$, $OH^-$, $ClO_4^-$, and $NO_3^-$. Their inhibiting effects depend upon their concentrations and the concentrations of chloride ions in the solution (Leckie, H. P., 1966). There is relatively little effect of pH in the range 1.6 to approximately 10.

An increase in temperature generally results in an increased tendency for pitting. It has been observed that pitting attack may increase abruptly once some critical temperature has been exceeded. Tests by Brennert (1937) in 3N sodium chloride solution indicated a critical temperature of ≈54°C for Type 304 stainless steel. Similarly Uhlig (1941) found that with Type 304 stainless steel corrosion tended to increase sharply above 60°C and to reach a maximum at about 91°C. At higher temperatures the lower solubility of oxygen tended to reduce the intensity of pitting attack.

Pitting studies of stainless steel cladding under repository conditions are required if credit for containment is to be given. Testing under the various conditions of temperature, radiation, solutions, etc. should be performed. A characterization of the environment in and surrounding the pit

would aid in the determination of the controlling mechanisms. Statistical analyses to characterize pitting behavior are required using long-term test data.

3.2.5.5.2 Crevice Corrosion

Crevice corrosion may occur if a metal surface is shielded in such a way that areas of limited access to corrosive solutions exist. Peterson and others (1970) have reported intense crevice corrosion of Type 304 stainless steel in seawater. Ellis and LaQue (1951) have shown that for stainless steel crevices in seawater, decreasing the crevice area or increasing the area of material outside the crevice (bold area) results in an increase in crevice attack.

The maximum depth of crevice corrosion attack after a 30-day exposure to seawater at 15°C was reported to be 0.28 mm (≈3.4 mm/yr) (Sedriks, A. J., 1979). The effect of increasing temperature on crevice corrosion is not easy to predict. Transport processes and reaction kinetics would be accelerated by increasing temperature but the solubility of oxygen would be reduced.

Braithwaite and Molecke (1980) exposed welded coupons with clamped crevices made from Type 304L stainless steel to deaerated WIPP Brine B at 70°C and 200°C. Crevice corrosion problems were not reported in these deaerated solutions; however, numerous pits occurred around the welded areas at 70°C.

3.2.5.5.3 Stress Corrosion Cracking

For the austenitic steels, it is well known that failure by stress corrosion cracking can occur in chloride and caustic solutions (Truman, J. E., 1976). Failure will occur for chloride concentrations between 10-1800 ppm if the tests are of sufficient duration (Warren, D., 1960). Short-term laboratory tests, lasting for days or weeks, may be totally inadequate in the prediction of stress assisted failure. The traditional engineering viewpoint, based on practical experience (Moxie, E. C., 1977), is that chloride cracking can occur at temperatures above 60°C provided that the material is exposed for very long times.

Type 304L stainless steel has been found to catastrophically fail by SCC in dilute chloride solutions at 49°C during a two-year period of service in a feedwater deaerator system (Van Der Horst, J. M. A., 1971). The feedwater chloride content was about 160 ppm but the overall chloride level at the steel surface was probably much less. After careful analysis it was concluded that stress corrosion cracking induced by thermal gradients caused the failure. Work by Braithwaite and Molecke (1980) indicate that oxygen in water in the range of parts per billion could enhance chloride SCC.

It has been known for some time that for certain combinations of caustic concentration and temperature stainless steels can exhibit caustic cracking (Edeleanu, C., 1957; Agrawal, A. K., 1970). A recent summary of available caustic cracking data for Type 304-stainless steel indicates that there is an inherent danger of caustic cracking in strong caustic solutions when the temperature approaches 100°C (Sedriks, A. J., 1979).

Levy and others (1980) have shown that the expected radiation levels from an unshielded waste package could produce large quantities of colloidal sodium in salt. This raises the possibility of brine solutions containing large amounts of sodium hydroxide and caustic SCC occurring in a salt repository.

Pescatore and Soo (1983) have commented on the possibility of SCC of Type 304L stainless steel occurring in a tuff repository under liquid water and steam conditions in the presence of traces of $O_2$ and $Cl^-$. Extensive testing is required since this is thought to be the most likely mechanism by which early failure will occur in waste packages emplaced in tuff.

3.2.5.5.4 Hydrogen/Helium Embrittlement

The source of hydrogen in repositories is likely to be a natural consequence of aqueous corrosion, but it may also be generated by the radiolysis of water by gamma irradiation. The austenitic stainless steels are a frequent choice for immunity to hydrogen embrittlement; however, hydrogen embrittlement has been observed in Types 304 and 304L stainless steel (Holzworth, M. L., 1969; Seys, A. A., 1974).

Eliezer (1981) has studied the hydrogen embrittlement of Type 304L stainless steel by cathodic charging of thin tensile specimens. Hydrogen induced slow crack growth was observed at room temperature when the specimen was stressed while undergoing cathodic charging. Room temperature cathodic charging of unstressed specimens for 15 days resulted in intergranular attack during subsequent tensile testing in air.

The ductility loss in Type 304L stainless steel in the presence of hydrogen has been studied by Thompson (1974). The elongation of sheet specimens was measured without exposure, and after exposure for two months at 475°K (202°C) in air and also hydrogen at a pressure of 69 MPa. It was found that the Type 304L stainless steel experienced a sharp decrease in ductility of about 50%. The proposed mechanism involves dislocation transport of hydrogen and accumulation of the hydrogen at interfaces between the matrix and nonmetallic inclusion particles. Fracture then occurs by normal, though accelerated, ductile rupture processes.

The effect of hydrogen on the mechanical properties of stainless steels has usually been considered to be independent of isotope type. However, analysis of long-term exposure to tritium is complicated by the fact that it decays to helium. Some earlier studies concluded that degradation of mechanical properties due to the presence of helium in austenitic stainless steel (maximum concentration 50 appm helium) occurred only after high temperature annealing caused helium bubble formation (Louthan, M., 1975; CONF 750989-P4, p.98, 1975; Thompson, A., 1975). Our interest in helium embrittlement arises because of the high pressurization of some rods with helium and the presence of tritium in the cladding.

Louthan and others, on the basis of short-term simulation of long-term tritium decay effects, concluded that helium had little effect on the mechanical properties studied of Types 304L and 309S stainless steels exposed to more than one atmosphere pressure at 27°C for 25-50 years (CONF 750989-P4, p.98, p.117, 1975).

More recent experiments performed by West and Rawl has revealed a potential concern for helium embrittlement in tritium-processing equipment or CTR (controlled thermonuclear reactor) inner ("first") walls (CONF 800427, 1980). Austenitic stainless steel samples thermally charged with hydrogen and tritium revealed little difference in mechanical properties (usually tested are loss of ductility and yield strength change) when testing was conducted immediately after charging. However, dramatic differences were noted in aged specimens, which exhibited time dependent ductility losses. No evidence was provided that bubble formation was required to cause degradation. Additionally, evidence for ambient temperature helium degradation (280 appm $^{3}He$) in Type 304L and 21-6-9 stainless steels tested for 66 months after charging with tritium was presented when dramatic changes in both ductility and fracture mode were noted (Rawl, D, Jr., 1980).

Thomas and Sisson found that below 900K, more than 99% of introduced helium is retained in the sample, regardless of heat treatment conditions (SAND80-8628, 1980). Initially, the tensile specimens of Types 304L and 21-6-9 stainless steel were charged (500 appm $^{3}He$) at 354°C for 17 months under 47 MPa and subsequently stored for 66 months at 270K. The total room temperature exposure after aging was approximately seven months. Surprisingly, the fraction of $^{3}He$ released varied inversely with the $^{3}He$ content. Similar experiments on tritium-soaked samples of a variety of metals indicated that over 90% of the helium atoms generated during low-temperature storage were retained in the solid during subsequent thermal desorption (Thomas, G, 1979).

Donovan has reported that helium, produced by tritium decay, affects the strength and ductility of Types 304L, 309 and 21-6-9 stainless steel (CONF-800427, 1980). In general, the effects are very temperature dependent. These stainless steels fail after high temperature annealing by intergranular fracture due to helium bubble formation on grain boundaries. However, high temperature annealing was not necessary to cause helium embrittlement. Helium-charged Type 21-6-9 stainless steel was severely embrittled and failed intergranularly at room temperature. The probable reason given was that tritium was trapped at microstructural features and that decay caused high localized concentrations and subsequent embrittlement.

Bisson and Wilson have given the following explanation for the deleterious effects of small amounts of helium trapped in a metal (CONF 800427, 1980). (Helium is normally not that soluble in a metal, but tritium is and decays to helium). Helium trapped in a face-centered cubic lattice has a high binding energy for other helium atoms. Continual trapping of helium atoms by previously trapped helium atoms is energetically favored. The energy of the decay of tritium is insufficient to disrupt the crystal lattice of the metal. Although the helium does not have sufficient energy to recoil a substantial distance, it will subsequently migrate or diffuse through the metal via thermally-induced forces until it meets another helium atom. Five helium

interstitials clustered together will spontaneously drive a metal atom off its lattice site creating a self-interstitial and a vacancy containing the five helium atoms. Also, beta particles from those tritium atoms which decay near the surface of a metal will provide a reducing atmosphere, which will tend to react to some extent with any protective oxide layer, increasing uptake of additional tritium.

3.2.5.6 Cladding Containment Tests

A spent fuel testing program is under way to study and compare the release rates of radionuclides from failed/defected fuel rods, undefected fuel rods, and bare $UO_2$ fuel pellets (HEDL-TC-2353-2, 1983; UCRL-89869, 1984). The purpose of this program is to determine how much credit can be given to the cladding for containment of the radionuclides selected for the preliminary leaching studies, i.e. U, $^{239}Pu$, $^{240}Pu$, and $^{137}Cs$. The scoping portion of the experimental work consists of leaching bare fuel and 5-inch sections of PWR spent fuel rods (discharged November 1975) with defected and undefected Zircaloy cladding under static conditions in deionized water (250 mL, BNL estimated SA/V ≈0.18) at hot cell ambient temperature (25-30°C) for periods from two to six months.

Concentrations of selected radionuclides were determined in the leachate along with amounts of radionuclides deposited on quartz rods that were placed in each test vessel. In the defected-cladding specimens, the leachant completely surrounds the fuel matrix. Results showing U, $^{239}Pu$, $^{240}Pu$ and $^{137}Cs$ concentrations in solution and on the fused quartz rod samples for 180 days are shown in Figure 3.14. It is of interest to note that the analytical techniques used and the corresp[illegible] detection limits are as follows: U, fluorescence, 0.01 ppm; $^{239}Pu$ [illegible]u, alpha-spectrometry, 2 pCi/mL, 0.00003 ppm; $^{137}Cs$, gamma-spectrometry, 1000 pCi/mL, 0.00001 ppm. Absolute quantities detected in solution could be determined by selecting the appropriate concentration in Figure 3.14 and multiplying it by 10 mL, the size of the aliquot.

These data seem to indicate that:

1) static leaching in deionized water at 25-30°C of undefected cladding yields measurable activity in solution;
2) defected cladding allows release of more of these radionuclides than undefected cladding;
3) bare fuel releases more of these radionuclides than undefected and defected cladding except for $^{137}Cs$ after 100 days of leaching;
4) the presence of undefected cladding decreases the release of radionuclides to solution by two to three orders of magnitude.

It should be emphasized that (1) these results were not obtained for repository-like conditions and (2) the scoping studies do not include the nuclides that contribute the most activity during the containment period. Since this review is concerned with the containment capability of the cladding, it is noteworthy that the undefected cladding is itself a source for measurable radioactivity in the leachate. The definition of containment based on quantities allowed will determine whether the leaching of these nuclides

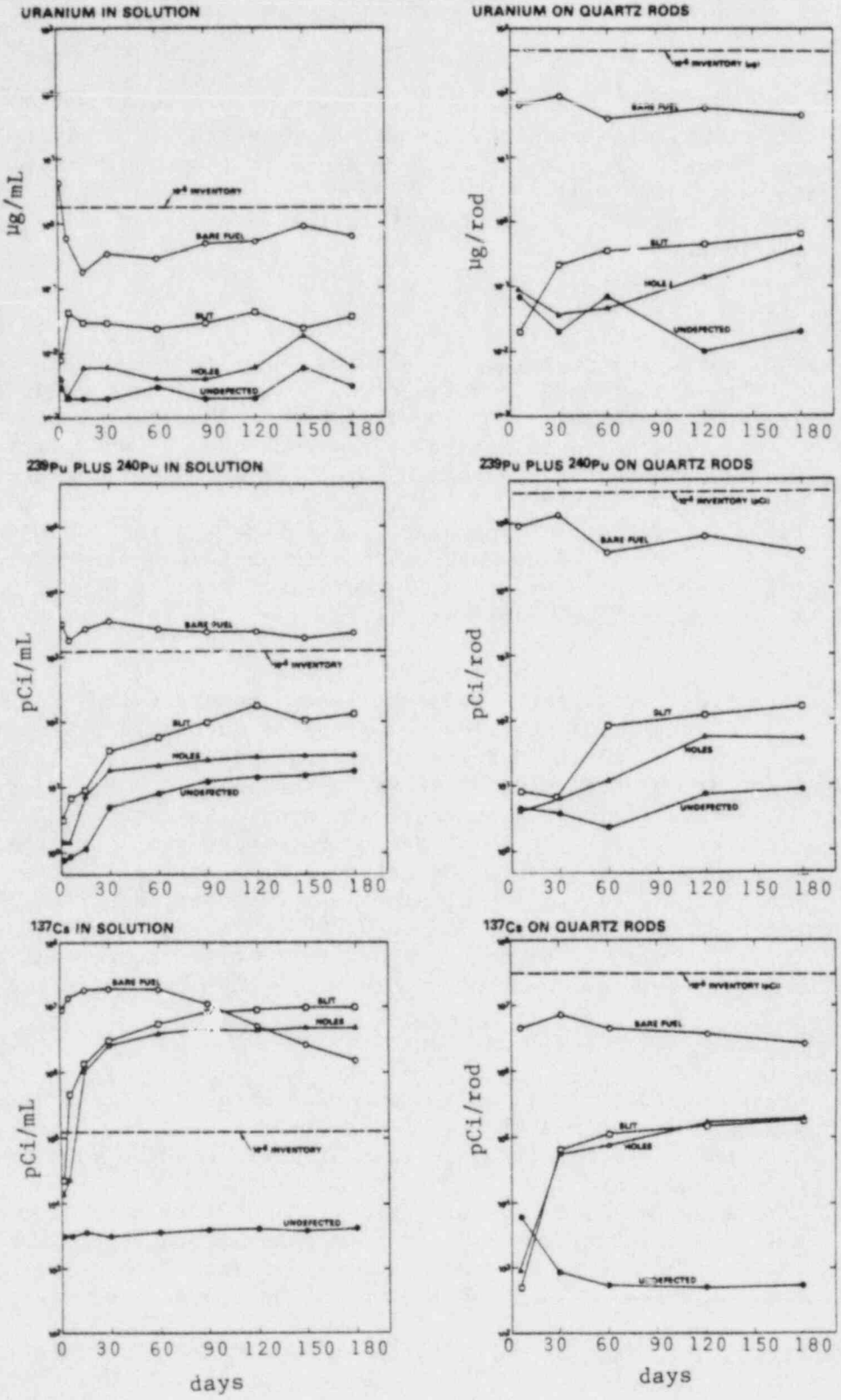


Figure 3.14. Concentrations of U (in µg/mL), $^{239}Pu$ plus $^{240}Pu$ (in pCi/mL) and $^{137}Cs$ (in pCi/mL) measured in solution and amounts on rod (µg for U, pCi for Pu and Cs) on fused quartz rod specimens during the first 180 days of cladding containment credit testing (UCRL-89869, 1984).

from the cladding under a more severe regimen condition, i.e. repository-like, will be considered as breach of containment.

### 3.2.6 Summary and Conclusions Regarding Cladding Containment Capability Under Repository Environments

The purpose of this review and evaluation was to assess the potential of spent fuel cladding (Zircaloy or stainless steel) to meet the containment criterion in 10 CFR Part 60. The major conclusion of this study is that both non-failed and failed fuel rods will release some radioactivity to the repository environment. Some rods fail in-reactor (estimated to be ≈0.01%) and release the fission gases Xe and Kr that are present in the fuel-cladding gap. Storage does not seem to degrade the cladding material significantly.

In a repository environment, the failed cladding will permit the groundwater to contact the $UO_2$ fuel. Non-failed rods that are placed in a repository, and remain unbreached, will still release radioactivity by (1) leaching of the crud deposits which contain adsorbed fission and activation products and transuranics, (2) uniform corrosion which may release nuclides to the water if the oxide layer is breached, (3) diffusion of gases through the cladding and oxide layers. Non-failed rods may be breached in the repository environment by waterside chloride-induced SCC of stainless steel and fuelside SCC of Zircaloy. If the rods are breached, they will release the fission gases and permit oxidation/expansion and dissolution/leaching of the fuel matrix.

There is a need for evaluation of the radionuclide inventory in the spent fuel as a function of time to permit the study of those nuclides that are contributing significant activity. There is also a need to determine the location and forms in which the nuclides are found in the fuel rods, i.e. inventory in the cladding, on the cladding surfaces (inside and outside), in the fuel-cladding gap, and in the fuel matrix (internally and externally). Then containment and controlled release studies should be made on those nuclides that are most predominant and that are most likely to be released.

Since some activity will be released to the repository environment by failed and non-failed fuel rods, there must be a quantitative definition of what level of radioactivity constitutes effective containment. Then, once the release rates from spent fuel in a repository environment are measured, the containment capability of the cladding can be established.

### 3.2.7 References

Agrawal, A. K. and R. W. Staehle, "Stress Corrosion Cracking of Fe-Cr-Ni Alloys in Caustic Environments," Report No. COO-2018-21(Q6), Ohio State University, Columbus, Ohio, April-July 1970.

Asher, R. C. and others, "Effects of Radiation on the Corrosion of Some Zirconium Alloys," Corrosion Science 10, 695-707, 1970.

Bazin, J., J. Jouan and N. Vignesoult, "Oxide-Cladding Reactions and Their Effect on Water Fuel Column Behavior," Trans. Am. Nucl. Soc. 20, 235, 1975.

BM-RI-5784, J. T. Dunham and H. Kato, 1961.

BMI-1571, "Zircaloy-4 Corrosion in Halide Solutions and at Crevices in High Temperature Water," W. E. Berry, E. L. White and F. W. Fink, Battelle Memorial Institute, 1962.

BNL-NUREG-34297, "Determination of the Waste Package Environment for a Basalt Repository: Phase I - Gamma Irradiation Conditions in the Absence of Methane," Draft Report, E. P. Gause and others, Brookhaven National Laboratory, May 1984.

BNWL-2256, "Behavior of Spent Nuclear Fuel in Water Pool Storage," A. B. Johnson, Jr., Pacific Northwest Laboratory, September 1977. (Appendix by C. R. Hann and C. L. Wilson.)

Boase, D. G. and T. T. Vandergraaf, "The Canadian Spent Fuel Storage Canister: Some Material Aspects," Nuclear Technology 32, 60, 1977.

Bradhurst, D. H., P. J. Shirvington and P. M. Heuer, "The Effects of Radiation and Oxygen on the Aqueous Oxidation of Zirconium and Its Alloys at 290°C," J. Nucl. Mat. 46, 53-76, 1973.

Braithwaite, J. W. and M. A. Molecke, "Nuclear Waste Canister Corrosion Studies Pertinent to Geologic Isolation," Nucl. and Chem. Waste Management 1, 37-50, 1980.

Brennert, S., "Influence of Temperature on the Occurrence of Pitting in Stainless Steels," International Association Testing Materials, London Congress, 1937, p. 44. Cited in Chromium-Nickel Stainless Steel Data, International Nickel Company, New York, 1963, Section III, Bulletin A, p. 8.

Burns, W. G. and P. B. Moore, "Water Radiolysis and Its Effect Upon In-Reactor Zircaloy Corrosion," Radiation Effects 30, 233-242, 1976.

Burns, W. G., W. R. Marsh and W. S. Walters, "The Gamma Irradiation-Enhanced Corrosion of Stainless and Mild Steels by Water in the Presence of Air, Argon and Hydrogen," Radiat. Phys. Chem. 21, 259-279, 1983.

BWI.., DOE/NRC Geochemistry Workshop, Hanford, Washington, January 1984.

CONF-750989-P4, Proceedings of the International Conference on Radiation Effects and Tritium Technology for Fusion Reactors, Gatlinburg, Tennessee, October 1-3, 1975, Editors: J. S. Watson, F. W. Wiffen.

CONF-800427, Proceedings of the Symposium on Tritium Technology in Fission, Fusion, and Isotopic Applications, Dayton, Ohio, April 29-May 1, 1980.

Cox, B., "Effects of Irradiation on the Oxidation of Zirconium Alloys in High Temperature Aqueous Environments," J. Nucl. Mat. 28, 1, 1968.

Cox, B., "Oxidation of Zirconium and Its Alloys," in Advances in Corrosion Science and Technology, Vol. 5, New York, Plenum Press, 1976, pp. 173-391.

Cox, B., "Hydride Cracks as Initiators for Stress Corrosion Cracking of Zircaloys in Zirconium in the Nuclear Industry, ASTM STP 681, 1978.

Cubicciotti, D. and J. E. Sanecki, "The Nature of Fission-Product Deposits Inside LWR Fuel Rods," presented at the ANS Topical Meeting on Water Reactor Fuel Performance, St. Charles, Illinois, May 9-11, 1977.

Cubicciotti, D. and J. E. Sanecki, "Characterization of Deposits on Inside Surfaces of LWR Cladding," J. Nucl. Mat. 78, 96-111, 1978.

Davies, J. H., F. T. Frydenbo and M. G. Adamson, J. Nucl. Mat. 80, 366, 1979.

Deju, R. A. and others, "Performance Allocation Traceable to Regulatory Criteria as Applied to Site Characterization Work at the Basalt Waste Isolation Project," in Waste Management '83, ANS, pp. 135-141, 1983.

DOE/RL 82-3, "Site Characterization Report for the Basalt Waste Isolation Project, Vol. II," 1982.

DOE/RL 83-1, "Spent Fuel Requirements," Department of Energy, January 1983.

DOE/NE-0017-1, "Spent Fuel and Radioactive Waste Inventories, Projections and Characteristics," Department of Energy, October 1982.

Edeleanu, C. and P. P. Snowden, "Stress Corrosion of Austenitic Steels in Steam and Hot-Water Systems," J. Iron St. Inst. 186, 406, 1957.

Eliezer, D., "Hydrogen Assisted Cracking in Type 304L and 316L Stainless Steel," in Hydrogen Effects in Metals, I. M. Bernstein and A. W. Thompson, Editors, Warrendale, The Met. Soc. of AIME, 1981, pp. 565-574.

Ellis, O. B. and F. L. LaQue, "Area Effects in Crevice Corrosion," Corrosion 7, 362, 1951.

EPRI NP-218, "Evaluation of Fuel Performance in Maine Yankee Core 1 - Task C," Combustion Engineering, November 1976.

EPRI NP-1329, "Stress Corrosion Cracking of Zircaloys," D. Cubicciotti, R. L. Jones and B. C. Syrett, SRI International, March 1980.

EPRI-RP-455-1, "The Nature of Fission Product Deposits Inside Light Water Reactor Fuel Rods," D. Cubbicciotti and others, Stanford Research Institute, November 1976.

EUR-7671 EN, "The Characterization of Activities Associated With Irradiated Fuel Element Claddings," I. L. Jenkins and others, AERE, Harwell, 1982.

Garzarolli, F. and others, Proceedings of the British Nuclear Energy Society Conference, London, July 1-2, 1971, p. 15.

Garzarolli, F., R. vonJan and H. Stehle, "Main Causes of Fuel Element Failure in Water-Cooled Power Reactors," Atom. Energy Rev. 17, 31, 1979.

GEAP-10371, "Zircaloy-Clad $UO_2$ Fuel Rod Evaluation Program Final Report November 1967 to June 1971," F. Megerth, C. Ruiz and U. Wolff, General Electric Company, June 1971.

GEAP-12205, "Tritium Distribution in High Power Zircaloy Fuel Elements," L. N. Grossman and J. O. Hegland, General Electric Vallecitos Nuclear Center, June 1971.

Goetzmann, O., "Thermochemical Evaluation of PCI Failures in LWR Fuel Pins," J. Nucl. Mat. 107, 185-195, 1982.

Hackerman, N. and O. B. Cecil, "The Electrochemical Polarization of Zirconium in Neutral Salt Solutions," J. Electrochem. Soc. 101, 419-425, 1954.

HEDL-TME 78-37, "Maximum Allowable Temperature for Storage of Spent Nuclear Fuel," L. D. Blackburn and others, Hanford Engineering Development Laboratory, May 1978.

HEDL-TME 79-20, "Spent Fuel Data for Waste Storage Programs," E. M. Greene, Hanford Engineering Development Laboratory, September 1980.

HEDL-TME 80-84, "An Assessment of Spent Fuel Structural Integrity Under Disposal Cycle Conditions," D. M. Bosi, Hanford Engineering Development Laboratory, July 1981.

HEDL-TME 81-3, "A Perspective on Fission Gas Release From Spent Fuel Rods During Geologic Disposal," R. L. Fish and R. E. Einziger, Hanford Engineering Development Laboratory, May 1981.

HEDL-TME 81-43, "Assessment of Spent Fuel Waste Form/Stabilizer Alternatives for Geologic Disposal," R. E. Einziger and D. A. Himes, Hanford Engineering Development Laboratory, June 1982.

HEDL-TME 83-28, "The Characteristics of Spent LWR Fuel Relevant to Its Storage in Geologic Repositories," R. E. Woodley, Hanford Engineering Development Laboratory, October 1983.

Hillner, E., "Corrosion of Zirconium-Based Alloys - An Overview," in Zirconium in the Nuclear Industry, ASTM Special Technical Publication STP 633, 1977, pp. 211-235.

Hockman, J. N. and W. C. O'Neal, "Thermal Modeling of Nuclear Waste in Tuff," paper presented at the ANS/ASME WASTE MANAGEMENT '84 Meeting, Tucson, Arizona, March 11-15, 1984.

Holzworth, M. L., "Hydrogen Embrittlement of Type 304L Stainless Steel," Corrosion 25, 107-115, 1969.

IAEA-218, Storage of Water Reactor Spent Fuel in Water Pools, Vienna, International Atomic Energy Authority, 1982.

IAEA-221, Guidebook on Quality Control of Water Reactor Fuel, Vienna, International Atomic Energy Authority, 1983.

International Atomic Energy Authority, Conditioning of Radicactive Wastes for Storage and Disposal, Vienna, IAEA, 1983.

Johnson, A. B., Jr., "Spent Fuel Storage Experience," Nucl. Tech. 43, 165, 1979.

Johnson, A. B., Jr. and R. M. Horton, "Nodular Corrosion of the Zircaloys," in Zirconium in the Nuclear Industry, ASTM 633, A. L. Lowe, Jr. and G. W. Parry, Editors, American Society for Testing and Materials, 1977, pp. 295-311.

KAPL-M-6748, "The Effects of Silica in Autoclave Test Water on the Steam Corrosion of Zircaloy," E. J. Callahan and J. F. Kabat, Knolls Atomic Power Laboratory, January 1968.

Kearns, J. J., J. Nucl. Materials 22, 292, 1967.

KFK-2677, "Behavior of Tritium in Zirconium and Zircaloy: Absorption, Diffusion, Desorption, a Literature Survey," H. Muenzel and G. U. Greger, 1978.

Kohli, R., Battelle Columbus Laboratories, "A Chemical Model for Cadmium Liquid-Metal Embrittlement of Zircaloy," paper presented at American Nuclear Society Meeting, New Orleans, Louisiana, June 4-7, 1984.

LA-9328-MS, "Summary Report on the Geochemistry of Yucca Mountain and Environs," W. R. Daniels and others, Los Alamos National Laboratory, December 1982.

LA-9846-PR, "Research and Development Related to the Nevada Nuclear Waste Storage Investigations, April 1-June 30, 1983, " A. E. Ogard, K. Wolfsberg, and D. T. Vaniman, Compilers, Los Alamos National Laboratory, December 1983.

Leckie, H. P. and H. H. Uhlig, "Environmental Factors Affecting the Critical Potential for Pitting in 18-8 Stainless Steel," J. Electrochem. Soc. 113, 1262, 1966.

Levy, P. W., and others, "Radiation Damage Studies on Synthetic NaCl Crystals and Natural Rock Salt for Radioactive Waste Disposal Applications," in The Technology of High-Level Nuclear Waste Disposal, Vol. 1, DOE, 1981, pp. 136-167.

Louthan, M. R., Jr., J. A. Donovan and G. R. Caskey, Jr., "Tritium Absorption in Type 304L Stainless Steel," Nucl. Tech 26, 192, 1975.

Maraghini, M. and others, "Studies on the Anodic Polarization of Zirconium and Zirconium Alloys," J. Electrochem. Soc. 101, 400-409, 1954.

Molecke, M. A., and others, "PNL-Sandia HLW Package Interaction Test: Phase One," in Scientific Basis for Nuclear Waste Management, Vol. 6, New York, North-Holland, 1982, pp. 337-345.

Moxie, E. C., "Some Corrosion Considerations in the Selection of Stainless Steel for Pressure Vessels and Piping," in Pressure Vessels and Piping: A Decade of Progress, Vol. 3, New York, American Society of Mechanical Engineers, 1977.

Nishimura, S., "Evaluation of Crack Growth Rate and Variation of Initiation Time for Stress Corrosion Cracking in Zircaloy-2 Cladding Tube," paper presented at American Nuclear Society Meeting, New Orleans, Louisiana, June 4-7, 1984.

NUREG-0418, "Fission Gas Release From Fuel at High Burnup," R. O. Meyer, C. E. Beyer and J. C. Voglewede, March 1978.

NUREG/CP-0005, Proceedings of the Conference on High-Level Radioactive Solid Waste Forms, L. A. Casey, Editor, 1979, pp. 561-595.

NUREG/CR-0091, "Fission Product Source Terms for the LWR Loss-of Coolant Accident: Summary Report," R. A. Lorenz, J. L. Collins and A. P. Malinauskas, Oak Ridge National Laboratory, June 1978.

NUREG/CR-0370, "Quarterly Progress Report on Fission Product Behavior in LWRs for the Period April-June 1978," A. P. Malinauskas, Oak Ridge National Laboratory, September 1978.

NUREG/CR-0668, PNL-2379, "An Evaluation of Potential Chemical/Mechanical Degradation Processes Affecting Fuel and Structural Materials Under Long-Term Water Storage," G. E. Zima, Pacific Northwest Laboratory, May 1979.

NUREG/CR-2482, Vol. 2, BNL-NUREG-51494, "Review of DOE Waste Package Program," P. Soo, Editor, Brookhaven National Laboratory, 1983.

NUREG/CR-2482, Vol. 3, BNL-NUREG-51494, "Review of DOE Waste Package Program," P. Soo, Editor, Brookhaven National Laboratory, 1983.

NUREG/CR-2482, Vol. 4, BNL-NUREG-51494, "Review of DOE Waste Package Program," P. Soo, Editor, Brookhaven National Laboratory, 1983.

NUREG/CR-2482, Vol. 6, BNL-NUREG-51494, "Review of DOE Waste Package Program," P. Soo, Editor, Brookhaven National Laboratory, 1984.

NUREG/CR-3001, PNL-4342, "Fuel Performance Annual Report for 1981," W. J. Bailey and M. Tokar, U.S. Nuclear Regulatory Commission, December 1982.

NUREG/CR-3091, Vol. 3, BNL-NUREG-51630, "Review of Waste Package Verification Tests," P. Soo, Editor, 1984.

ONWI-9(4), "Technical Progress Report for the Quarter 1 July - 30 September, 1980," Office of Nuclear Waste Isolation, 1980.

ONWI-39, Vol. 3, "An Assessment of LWR Spent Fuel Disposal Options," Office of Nuclear Waste Isolation, July 1979.

ONWI-438, "Engineered Waste Package Conceptual Design: Defense High-Level Waste (Form 1), Commercial High-Level Waste (Form 1), and Spent Fuel (Form 2) Disposal in Salt," C. R. Bolmgren and others, Westinghouse Electric Corporation, 1983.

ORNL-5578, "Effects of Gaseous Radioactive Nuclides on the Design and Operation of Repositories for Spent LWR Fuel in Rock Salt," G. H. Jenks, Oak Ridge National Laboratory, December 1979.

ORNL-TM-6008, "Projections of Spent Fuel to be Discharged by the U. S. Nuclear Power Industry," C. W. Alexander and others, Oak Ridge National Laboratory, October 1977.

ORNL/TM-7201, "Expected Environment in High Level Nuclear Waste and Spent Fuel Repositories in Salt," H. C. Claiborne and others, Oak Ridge National Laboratory, 1980.

ORNL/TM-8351, "Evaluation of Corrosion Damage to Materials After Three Years in the Avery Island Salt Mine," J. C. Griess, Oak Ridge National Laboratory, 1982.

Peehs, M., H. Stehle and E. Steinberg, "Out-of-Pile Testing of Iodine Stress Corrosion Cracking in Zircaloy Tubing Under the Aspect of the PCI-Phenomenon," in Zirconium in the Nuclear Industry, ASTM STP 681, Philadelphia, Pennsylvania, American Society for Testing Materials, 1979.

Pescatore, C. and P. Soo, Brookhaven National Laboratory, Memo to File, "NRC-NNWSI Waste Package Workshop Held in Dublin, California, October 18-19, 1983," December 1983.

Peterson, M. M., Z. I. Lennox and R. E. Groever, Materials Protection 9, 23, 1970.

Phadnis, S. V., P. K. Chauhan and H. S. Gadiyar, "Ellipsometric Evaluation of Various Pretreatments on Zircaloy-2," J. Electrochem. Soc. India 32, 41-46, 1983.

Pitman, S. G., B. Griggs and R. P. Elmore, "Evaluation of Metallic Materials for Use in Engineered Barrier Systems," in Scientific Basis for Nuclear Waste Management, Vol. 3, New York, Plenum Press, 1981, pp. 523-530.

PNL-3484, "Investigation of Metallic, Ceramic, and Polymeric Materials for Engineered Barrier Applications in Nuclear-Waste Packages," R. E. Westerman and others, Pacific Northwest Laboratory, October 1980.

PNL-3921, "Examination of Zircaloy-Clad Spent Fuel After Extended Pool Storage," E. R. Bradley and others, Pacific Northwest Laboratory, September 1981.

PNL-4686, "LWR Spent Fuel Approved Testing Materials for Radionuclide Release Studies," J. O. Barner, Pacific Northwest Laboratory, January 1984.

PNL-5109, "Characterization of LWR Spent Fuel MCC-Approved Testing Material - ATM-101," J. O. Barner, Pacific Northwest Laboratory, June 1984.

Rawl, D. E., Jr., G. R. Caskey, Jr. and J. A. Donovan, "Low Temperature Helium Embrittlement of Tritium-Charged Stainless Steel," 190th Annual AIME Meeting, Las Vegas, Nevada, February 24-28, 1980.

RHO-BW-CR-136P/AESD-TME-3142, "Waste Package Conceptual Designs for a Nuclear Repository in Basalt," Westinghouse Electric Corporation, October 1982.

RHO-BW-SA-315P, "Gamma Radolysis Effects on Grande Ronde Basalt Groundwater," W. J. Gray, Pacific Northwest Laboratory, 1983.

RHO-BW-ST-21P, "Evaluation of Sodium Bentonite and Crushed Basalt as Waste Package Backfill Materials," M. I. Wood, G. D. Aden and D. L. Lane, Rockwell Hanford Operations, October 1982.

Roedder, E., and H. E. Belkin, "Thermal Gradient Migration of Fluid Inclusions in Single Crystals of Salt From the Waste Isolation Pilot Plant Site (WIPP)," in Scientific Basis for Nuclear Waste Management, Vol. 2, New York, Plenum Press, 1978, pp. 453-464.

Salter, P. F. and others, "Application of Systems Analysis to the Development of Engineered System Performance Requirements for a Hard Rock Nuclear Waste Repository," in Waste Management '82, ANS, 1982, pp. 97-112.

SAND80-8628, "Tritium and Helium-3 Release From 304L and 21-6-9 Stainless Steels," G. J. Thomas and R. Sisson, Sandia National Laboratories, June 1980.

SAND81-1677, "Effects of Radiation in the Chemical Environment Surrounding Waste Canisters in Proposed Repository Sites and Possible Effects on the Corrosion Process," R. S. Glass, Sandia National Laboratories, 1981.

SAND83-0516, "A Comparison of Brines Relevant to Nuclear Waste Experimentation," M. A. Molecke, Sandia National Laboratories, 1983.

Schweitzer, P. A., Corrosion Resistance Tables, New York, Marcel Dekker, Inc., 1976.

SD-BWI-TP-022, "Barrier Materials Test Plan," Rockwell Hanford Operations, March 1984.

Sedriks, A. J., Corrosion of Stainless Steels, New York, John Wiley and Sons, 1979.

Seys, A. A., M. J. Brabers and A. A. Van Haute, "Analysis of the Influence of Hydrogen on Pitting Corrosion and Stress Corrosion of Austenitic Stainless Steel in Chloride Environment," Corrosion 30, 47-52, 1974.

Shann, S. H. and D. R. Olander, "Stress Corrosion Cracking of Zircaloy by Cadmium, Iodine and Metal Iodides," J. Nucl. Mat. 113, 234-248, 1983.

Shimada, S., T. Matsuura and M. Nagai, "Stress Corrosion Cracking of Zircaloy-2 by Metal Iodides," J. Nucl. Sci. Tech. 20, 593-602, 1983.

Thomas, G. J., W. A. Swansiger and M. I. Baches, "Low Temperature Helium Release in Nickel" J. Appl. Phys. 50, 6942-6947, 1979.

Thomas, K. C. and R. J. Allio, "The Failure of Stressed Zircaloy in Aqueous Chloride Solutions," Nucl. Appl. 1, 252-258, 1965.

Thompson, A. W., "Ductility Losses in Austenitic Stainless Steels," in Hydrogen in Metals, I. M. Bernstein and A. W. Thompson, Editors, Metals Park, Ohio, American Society for Metals, 1974, pp. 91-105.

Thompson, A. W., "Mechanical Behavior of Face-Centered Metals Containing Helium," Mat. Sci. Eng. 21, 41, 1975.

Truman, J. E., "Stainless Steels," in Corrosion, Vol. 1, L. L. Shreir, Editor, Boston, Newnes-Butterworth, 1976, pp. 3:31-3:63.

UCID-19926, "Initial Specifications for Nuclear Waste Package External Dimensions and Materials," D. W. Gregg and W. C. O'Neil, Lawrence Livermore National Laboratory, 1983.

UCRL-80820, "Thermal Modeling of Nuclear Waste Package Designs for Disposal of Tuff," J. N. Hockman and W. C. O'Neil, Lawrence Livermore National Laboratory, 1983.

UCRL-89404, "Selection of Barrier Metals for a Waste Package in Tuff," E. W. Russell, R. D. McCright and W. C. O'Neal, Lawrence Livermore National Laboratory, September 1983.

UCRL-89869, "Spent Fuel Cladding Containment Credit Tests," C. N. Wilson and V. M. Oversby, Lawrence Livermore National Laboratory, February, 1984.

UCRL-89988, "Selection of Candidate Canister Materials for High-Level Nuclear Waste Containment in a Tuff Repository," R. D. McCright and others, Lawrence Livermore National Laboratory, 1983.

Uerpmann, P., and A. Jockwer, "Salt as a Host Rock for Radioactive Waste Disposal," in Geochemical Processes, Nuclear Energy Agency, OECD, Paris, 1982, p. 93.

Uhlig, H. H. and M. C. Morrill, "Corrosion of 18-8 Stainless Steel in Sodium Chloride Solutions," Ind. Eng. Chem. 33, 875, 1941.

USGS-OFR-82-1131, "A Critique of 'Brine Migration in Salt and Its Implications in the Geologic Disposal of Nuclear Waste,' Oak Ridge National Laboratory Report 5818, by G. H. Jenks and H. C. Claiborne," E. Roedder and I. M. Chou, U. S. Geologic Survey, 1982.

Van Der Horst, J. M. A., "Corrosion Cracking of Stainless Steels by Thermal Gradient Stresses," Corrosion Science 11, 885-887, 1971.

Warren, D., "Chloride Bearing Cooling Water and the Stress Corrosion Cracking of Austenitic Stainless Steel," in Proceedings of the 15th Industrial Waste Conference, Purdue University, May 1960, pp. 420-438.

WASH-1400, Appendix VII, "Reactor Safety Study - An Assessment of Accident Risks in U. S. Commercial Nuclear Power Plants," U.S. Nuclear Regulatory Commission, October 1975.

Wood, J. C., "Factors Affecting Stress Corrosion Cracking of Zircaloy in Iodine Vapor," J. Nucl. Mat. 45, 105-122, 1972/73.

Wood, J. C. and J. R. Kelm, "Effects of Irradiation on the Iodine-Induced Stress Corrosion Cracking of CANDU Zircaloy Fuel Cladding," Res Mechanica 8, 127-161, 1983.

## 4. CONTAINER SYSTEM FAILURE AND DEGRADATION MODES

Prior BNL Biannual Reports have addressed container failure/degradation modes for basaltic and salt repository conditions. Materials evaluated include carbon steel, stainless steel and titanium-based alloys (NUREG/CR-2482, Vol. 2, 1983; NUREG/CR-2482, Vol. 3, 1983; NUREG/CR-2482, Vol. 4, 1983; NUREG/CR-2482, Vol. 5, 1984).

## 5. PACKING MATERIAL FAILURE AND DEGRADATION MODES

### 5.1 Basalt-, Zeolite- and Bentonite-Containing Packing Materials

Earlier BNL Biannual Reports have addressed the subject materials mainly with respect to the basalt repository program (NUREG/CR-2482, Vol. 3, 1983; NUREG/CR-2482, Vol. 4, 1983).

### 5.2 Crushed Tuff Packing Materials

This part of the program has been completed and is reported in a prior BNL Biannual Report (NUREG/CR-2482, Vol. 5, 1984).

### 5.3 Crushed Salt Packing Materials

This part of the program has been completed and is reported in a prior BNL Biannual Report (NUREG/CR-2482, Vol. 6, 1984).

*U.S. GOVERNMENT PRINTING OFFICE: 1985-461-721:20016

NRC FORM 335 (11 81)

U.S. NUCLEAR REGULATORY COMMISSION

**BIBLIOGRAPHIC DATA SHEET**

1. REPORT NUMBER (Assigned by DDC)
NUREG/CR-2482, Vol. 7
BNL-NUREG-51494

4. TITLE AND SUBTITLE (Add Volume No., if appropriate)
Review of DOE Waste Package Program
Subtask 1.1 - National Waste Package Program
April 1984 - September 1984

2. (Leave blank)

3. RECIPIENT'S ACCESSION NO.

7. AUTHOR(S)
P. Soo, Editor

6. DATE REPORT COMPLETED
MONTH: September | YEAR: 1984

DATE REPORT ISSUED
MONTH: March | YEAR: 1985

9. PERFORMING ORGANIZATION NAME AND MAILING ADDRESS (Include Zip Code)
Department of Nuclear Energy
Brookhaven National Laboratory
Upton, NY 11973

8. (Leave blank)

12. SPONSORING ORGANIZATION NAME AND MAILING ADDRESS (Include Zip Code)
Division of Waste Management
Office of Nuclear Material Safety and Safeguards
U. S. Nuclear Regulatory Commission
Washington, DC 20555

10. PROJECT/TASK/WORK UNIT NO.
Subtask 1.1

11. FIN NO.
A-3164

13. TYPE OF REPORT
Final Report

PERIOD COVERED (Inclusive dates)
April 1984 - September 1984

15. SUPPLEMENTARY NOTES

14. (Leave blank)

16. ABSTRACT (200 words or less)

The present effort is part of an ongoing task to review the national high level waste package effort. It includes evaluations of reference waste form, container, and packing material components with respect to determining how they may contribute to the containment and controlled release of radionuclides after waste packages have been emplaced in salt, basalt, tuff, and granite repositories. In the current Biannual Report a review was carried out to determine the ability of spent fuel cladding to provide additional radionuclide containment capability should the container/overpack system fail prematurely.

17. KEY WORDS AND DOCUMENT ANALYSIS

17a. DESCRIPTORS

waste package

17b. IDENTIFIERS/OPEN-ENDED TERMS

18. AVAILABILITY STATEMENT
Unlimited

19. SECURITY CLASS (This report)
Unclassified

21. NO. OF PAGES

20. SECURITY CLASS (This page)
Unclassified

22. PRICE
$

NRC FORM 335 (11 81)

UNITED STATES
NUCLEAR REGULATORY COMMISSION
WASHINGTON, D.C. 20555

OFFICIAL BUSINESS
PENALTY FOR PRIVATE USE, $300

FOURTH CLASS MAIL
POSTAGE & FEES PAID
USNRC
WASH. D.C.
PERMIT No. G-67